Advanced Plasmonics Enabled by DNA Nanostructures

Timon Funck

München 2018

Advanced Plasmonics Enabled by DNA Nanostructures

Timon Funck

Dissertation
an der Fakultät für Physik
der Ludwig–Maximilians–Universität
München

vorgelegt von
Timon Funck
aus München

München, den 8. August 2018

Erstgutachter: Prof. Dr. Tim Liedl
Zweitgutachter: Prof. Dr. Jan Lipfert
Tag der mündlichen Prüfung: 23. Oktober 2018

ZUSAMMENFASSUNG

Die Untersuchung von Interaktionen zwischen elektromagnetischer Strahlung und Nanostrukturen bietet viel Potential für Anwendungen und Technologien. Optimale Absorption für Solarzellen, plasmonische Wellenleiter oder Metamaterialien sind nur einige Beispiele. Die Herausforderung dabei ist die hohe Präzision in der geometrischen Anordnung, die dafür benötigt wird. Ein Ansatz dafür ist, die Nanopartikel mit Hilfe von DNA und DNA-Strukturen zu verbinden. Mit der DNA Origami Technik wurden in dieser Abeit drei verschiedene Aspekte von Nanopartikelgeometrien untersucht.

Nanostrukturen können so gebaut werden, dass sie mit elektromagnetischer Strahlung im sichtbaren Spektrum interagieren. Mit einer DNA-Gold-Struktur, die einen chiralen und einen nicht-chiralen Zustand hat, wurde ein optischer RNA Sensor entwickelt. Dabei löst eine RNA Sequenz aus dem Hepatitis C Genom ein Umschalten der Struktur aus, was in einer Änderung des CD Spektrums resultiert. Es konnte eine Sensitivität von 100 pM erreicht werden. Auch Stabilität des Sensors in Blutserum konnte gezeigt werden.

Die Chiralität einer Goldnanopartikelhelix hängt von der Anzahl der beteiligten Partikel ab. In unserer Untersuchung konnten wir zeigen, dass nicht nur die Interaktion der benachbarten Partikel eine Rolle spielt, sondern auch Partikel entlang der Helix interagieren und so das CD Signal beeinflussen.

Mit Dimeren von Nanopartikeln ist es möglich, elektromagnetische Felder im Spalt zwischen den Partikeln zu verstärken. Um die Energieeffizienz noch zu erhöhen, kann man destruktive Interferenzen des Fano Effekts ausnutzen. Dazu musste eine Struktur konzipiert werden, bei der ein kleines Nanostäbchen zwischen zwei großen Partikeln plaziert wird. Durch diese spezielle Geometrie wird es möglich, Wärme in einem nanometergroßen Bereich zu erzeugen.

ABSTRACT

The investigation of interactions between electromagnetic radiation and nanostructures offers many potential technology advances. Optimal absorption of solar cells, plasmonic waveguides or metamaterials are just a few examples. The challenge here is the required precision in a geometrical arrangement. One approach is to use DNA and DNA structures to connect and arrange nanoparticles. Using the DNA origami method, this thesis investigates three aspects of geometries of nanoparticles.

Nanostructures can be built to interact with electromagnetic radiation in the visible spectrum. I developed an optical RNA sensor consisting of a DNA-gold hybrid structure with a chiral and a non-chiral state. A specific RNA sequence from a hepatitis C virus genome triggers the switching from one state to the other resulting in a change in the CD spectrum. Within the scope of this thesis, the detection of an RNA at a concentration of 100 pM is possible. By injecting the sensor into blood serum, the sensor's functional stability could be confirmed.

The chirality of a gold particle helix depends on the number of particles involved. However, my studies show that not only interaction between neighboring particles is important but also the interaction of particles along the helix in z-direction changing the CD spectrum in non-trivial ways.

Using nanoparticle dimers, it is possible to enhance electric fields in the gap between the particles. The third project was about positioning a small nanorod in the gap between two large particles to get destructive interference of the Fano effect. This special geometry could be used to achieve high heat generation in the gap.

"I do not pretend that [the experiments] are of great value in their present state, but they are very suggestive, and they may save much trouble to any experimentalists inclined to pursue and extend this line of investigation."

—Michael Faraday about his studies of gold nanoparticles[1]—

What makes it difficult is that research is immersion in the unknown. We just don't know what we're doing. We can't be sure whether we're asking the right question or doing the right experiment until we get the answer or the result.

— Martin A. Schwartz [2]—

ACKNOWLEDGMENTS

Tim
Vielen Dank, dass du mich seit vielen Jahren (BIOMOD 2011) in der Forschung begleitet und unterstützt hast. Vielen Dank für die Betreuung meiner Doktorarbeit. Du hast mir bei meinen Projekten große Freiheit gelassen und immer wieder mit guten Anregungen weitergeholfen.

Die Gruppe
Vielen Dank an alle ehemaligen und aktuellen Mitglieder der AG Liedl. Durch euch wurde meine Doktorarbeit erst möglich.

Das Büro
Vielen Dank an die Kollegen im Büro die mich über diverse Schreibetappen ertragen mussten. Vielen Dank an Rafal, Anton, Janina, Luisa und Alexandra für Hilfe und Antwort bei vielen kleinen und großen Problemen.

Der Lehrstuhl
Vielen Dank an alle Kollegen vom Lehrstuhl Rädler. Danke für alle Wandertage, Weihnachtsfeiern, Kaffeepausen und Fahrten nach Antholz.

Die Physiker
Vielen Dank an alle anderen, die mich durch mein Studium und bis zur Doktorarbeit begleitet haben. Danke Linda, Magnus, Steff, Michel, Lorenz und Patrick für alle Freundschaft, alle Hilfe und allen Spass.

Macht's gut und danke für den Fisch.

CONTENTS

Part I

Background and Literature

1

INTRODUCTION

Billions of nanosized machines get injected into a human body. AFter entering the bood stream, they form an artificail eye with each nanomachine serving a pixel on the artifical retina. The nanomachines are able to coordinate and swim through the blood vessels to take live images of various processes in the body. These nanomachines ae part of the book PREY by Michael Crichton. Unfortunately, advanced technology like that has not yet been developed. However, the concept to design such nanomachines for tasks on the nanoscale e. g. medical treatment of single (tumor) cells has been around for a long time. The various systems that need to be developed to that end are complex in structure and material. Efficient energy sources like solar cells, propulsion systems on the nanoscale and nano-computer chips are only a few examples. In the search for suitable materials to build in the nanoworld, DNA was introduced as a useful tool to construct and organize nanosystems. It is chemically well understood, versatile and biocompatible. One widespread technique is DNA origami. In this method, the single-stranded genome of a bacteriophage is folded into a desired shape by hundreds of short oligonucleotides. With computer-aided design tools, any shape is possible. Additionally, multiple switching mechanisms with different input signals like DNA, RNA or a change in pH have been introduced. One area of nanotechnology research, called nanoplasmonics, investigates the interaction of light and metal nanoparticles. Light excites oszillations of all electrons in the particles because the particles are much smaller than the wavelength of the light. Excited particles can interact. Here the spatial arrangement plays a considerable role in the achieved effects and efficiencies. DNA origami turned out to be a reliable tool to arrange nanoparticles in various geometries. The aim of nanoplasmonic research includes tailored optical effects, metamaterial, and medical applications. This work investigates the effects and application of nanoparticle geometries on DNA origami structures in three different projects.

RNA Detection: The first project is about detecting viral RNA with a nanoplasmonic switch. Chirally arranged nanoparticles exhibit a

different absorption of left and right-handed polarized light (Circular dichroism, CD). We used a DNA-gold hybrid structure that can switch between a chiral and a non-chiral state to detect a specific RNA sequence. The structure consists of a cross-like DNA structure with a gold nanorod on each arm. The trigger RNA locks the structure in a chiral state and the change in CD can be measured. Since the plasmonic properties of the nanorods enable absorption in the visible spectrum, this sensor can potentially be used as a lab-free diagnostic tool.

Switching Helix Chirality: The effects of a different number of particles a gold helix were investigated in the second project. With an increased number of particles, the CD is predicted to become stronger. However, with particles forming more than one turn, more effects than just next neighbor interaction start playing a role. Theoretical models show a switch in chirality for helices with more than one turn.

Gold Nanoparticle Assembly for Producing Fano Resonances: Plasmonic nanostructures can be designed in a way to generate heat on surfaces or in cavities. To maximize the heat generation and confine it in a nanometer space, we aimed to design a structure that utilizes the Fano effect of interference between the modes of two large particles and a small nanorod. The challenge, in this case, is to build a DNA structure suitable for arranging the nanorod linear into the gap between the particles.

2

STRAIGHTFORWARD SUMMARY FOR THE GENERAL PUBLIC IN GERMAN

In this section I attempt to explain the content of my thesis in simple terms for the general public.

Erinnerst du dich an das Schwert, das Frodo in DER HERR DER RINGE bei sich trägt? Normalerweise sieht es aus wie ein normales Schwert, aber sobald Orks in der Nähe sind, leuchtet es in einem hellen Blau. Es besteht also aus einem Material, das seine optischen Eigenschaften ändert, wenn es Orks bemerkt. Was wäre, wenn wir auch solche Materialien herstellen könnten, die ihre optischen Eigenschaften ändern, wenn sie Gefahr bemerken. So eine Gefahr könnten z.B. gefährliche Viren oder andere Krankheitserreger sein. In meiner Doktorarbeit habe ich an einem System gearbeitet, das so etwas können soll. Dazu braucht das Material zwei Eigenschaften: Zum einen muss es zwei mögliche Zustände haben, zwischen denen es umschalten kann. Zum Anderen muss es optische Eigenschaften haben, die man mit bloßem Auge sehen kann. Da Viren nanometerklein sind, muss unser Mechanismus zum Umschalten auch so klein sein. Um das alles umzusetzten habe ich mich zweier Konzepte aus der Nanotechnologie bedient, die zusammen alle Vorraussetzungen erfüllen: Für die Schaltung habe ich eine Struktur aus DNA benutzt und für den optischen Teil Nanopartikel aus Gold.

DNA kennt man eigentlich aus der Genetik als das Molekül, das alle unsere Erbinformationen trägt. DNA eignet sich aber auch wunderbar als Baumaterial für sehr kleine Strukturen oder Maschinen. Mit einer Technik, die man DNA Origami nennt, kann die schnurförmige DNA in jede beliebige Form gefaltet werden. Dabei wird ein langer DNA Strang durch viele kurze DNA Stücke, die an verschiedenen Stellen an den Langen binden, in eine bestimmte Form gebracht. Die Form, die das ganze annehmen soll, muss man sich vorher überlegen und die kurzen Stücke dementsprechend konzipieren. Wir machen das ganze mit einem Computerprogramm, das uns hilft darzustellen, an welchen Stellen die DNA binden kann.

In (Abbildung 2.1) ist das Prinzip von DNA Origami veranschaulicht. Der lange DNA Strang, den wir Scaffold nennen, besitzt ver-

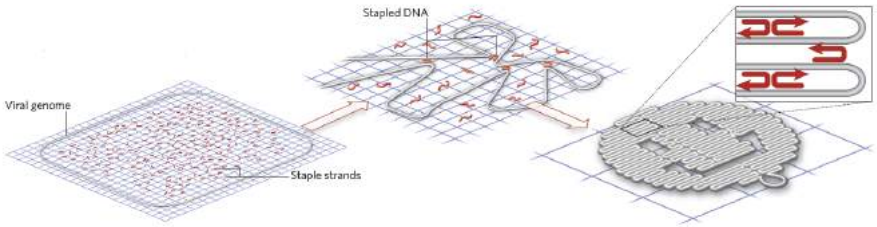

Abbildung 2.1: Grundprinzip von DNA Origami: Ein langer DNA-Einzelstrang wird durch viele kurze DNA-Einzelstränge in die gewünschte Form gefaltet, hier ein Smiley. Welche Form die DNA annimmt hängt von den kurzen Strängen ab. Die muss man je nach gewünschter Form speziell zusammenstellen. Reprinted from [3] with permission from Springer Nature

schiedene Positionen, an denen komplementäre DNA binden kann. Dabei verbinden sich die beiden DNA Stränge zu einem Doppelstrang. Die beiden Stränge können nur aneinander binden, wenn sie komplementär sind, also chemisch genau zueinander passen. Wenn man jetzt einen DNA Strang herstellt, der komplementäre Sequenzen zu verschiedenen Regionen enthält, zieht er den Scaffold an diesen Regionen zusammen. Wenn man das mit verschiedenen kurzen DNA Stücken am ganzen Scaffold macht, erhält man zum Beispiel einen Smiley. Zur einfacheren Darstellung werden die DNA-Doppelstränge meistens als einfache Zylinder dargestellt. Die Pläne für die Strukturen die ich gebaut habe finden sich im Anhang. Dabei ist der Scaffold immer in blau dargestellt. Ein besonderer Vorteil von DNA als Baumaterial sind die vielen DNA-Schalter. DNA kann ihre Form oder Zusammensetzung ändern, wenn man geeignete Sequenzen und Signale verwendet. Eine große Stärke dieser Technik ist, dass man an die DNA alle möglichen Moleküle anbringen kann. So kann man Moleküle , z.B. Proteine, Goldpartikel oder Fluoreszenzfarbstoffe, in verschiedenen Konstellationen zusammenpuzzlen (siehe Abbildung 2.2) und die dabei entstehenden Effekte untersuchen. In der Arbeitsgruppe von Prof. Tim Liedl arbeiten wir mit vielen verschiedenen Molekülen, und es kommen regelmäßig neue dazu.

Für meine Arbeit besonders interessant war das Anordnen von Goldnanopartikeln. Da diese Partikel viel kleiner sind als die Wellenlänge von sichtbarem Licht ergeben sich viele spezielle optische Eigenschaften, die man sonst nicht beobachten kann. Ein Beispiel kann man im nächsten Bild sehen. Zu sehen sind zwei Aufnahmen derselben Probe. Das kleine Gefäß enthält Milliarden kleine Goldkugeln (100 nm Durchmesser), die in Wasser schwimmen. Der deutliche Far-

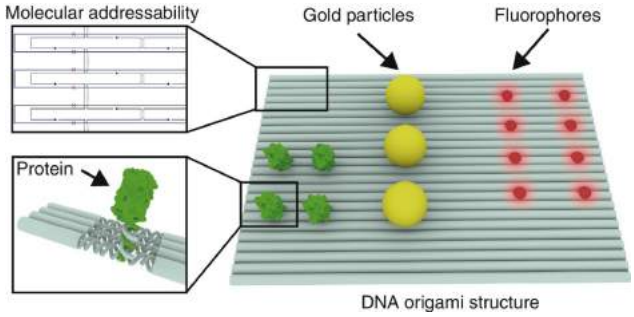

Abbildung 2.2: DNA Strukturen eignen sich sehr gut um verschiedene Moleküle und Partikel darauf anzuordnen. Reprinted from [4], with permission from Elsevier

bunterschied zwischen den beiden Aufnahmen hängt allein davon ab, von woher die Flüssigkeit beleuchtet wird. Im linken Bild kam das meiste Licht von vorne, im rechten das Licht von hinten. Der Unterschied entsteht dadurch, dass bei Partikeln dieser Größe die Lichtstreuung ähnlich stark ist wie die Lichtabsorption. Ein weiteres Beispiel für diesen Effekt ist der römische Lykurgus-Kelch aus dem 4. Jahrhundert. Bei diesem Kelch ist dem Glas kleine Mengen Gold und Silber beigefügt. Das führt dazu, dass der Kelch rot erscheint, wenn er von hinten beleuchtet wird und grün, wenn er von vorne beleuchtet wird. Diese Beispiele zeigten, dass die Eigenschaften von Goldnanopartikeln im richtigen Kontext mit bloßem Auge beobachtet werden können. Deswegen eignen sie sich besonders gut für den geplanten Virendetektor.

Ein Grundgedanke für meinen Virendetektor war es, einen weiteren optischen Effekt auszunutzen, den Cirkulardichroismus. Lichtwellen können sich bei ihrer Fortbewegung um die eigene Achse drehen. Man unterscheidet dabei ob sich das Licht links-oder rechtsherum dreht. Man nennt das Licht dann rechtshändig bzw. linkshändig polarisiert. Rechts- und linkshändiges Licht wird je nach Geometrie von Molekülen unterschiedlich absorbiert. Den Unterschied in der Absorption nennt man Circulardichroismus (CD). Mit Goldpartikeln kann man künstliche Geometrien konstruieren, die CD mit sichtbaren Licht aufweisen. Mit geeigneten Filtern kann man CD auch für das bloße Auge sichtbar machen. Deswegen war das Ziel, eine Struktur zu konstruieren, die ihr CD Signal ändert, wenn sie einen Virus detektiert. Um genauer zu sein reicht es schon, wenn nur die RNA detektiert wird, also die genetische Information des Virus. Das Ziel des gesamten Projekts war also, eine Struktur aus DNA und Gold zu bauen, die ihre Geometrie und damit ihr CD Signal ändert, wenn sie

Abbildung 2.3: Links: Zwei Aufnahmen derselben Probe. Das kleine Gefäß enthält Milliarden kleine Goldkugeln (100 nm Durchmesser), die in Wasser schwimmen. Der deutliche Farbunterschied zwischen den beiden Aufnahmen hängt allein davon ab, von wo die Flüssigkeit beleuchtet wird. Im linken Bild kam das meiste Licht von vorne , im rechten das Licht von hinten. Der Unterschied entsteht dadurch, dass bei Partikeln dieser Größe die Lichtstreuung ähnlich stark ist wie die Lichtabsorption. Rechts: Der Lykurgus Becher aus dem 4. Jahrhundert, bei dem man den gleichen Effekt sieht. (British Museum, London published under CC BY-NC-SA 4.0)

eine bestimmte RNA Sequenz detektiert. In Abbildung 2.4 sieht man ein Modell der Struktur. Zwei Balken aus DNA sind locker durch zwei DNA-Stränge verbunden und tragen jeweils ein Goldstäbchen. Stehen die beiden Arme im Winkel von 90° zueinander, bilden also ein Plus-Zeichen, liefern sie kein CD Signal. Drehen sich die Arme in die Form eines Andreaskreuzes, sieht man ein Signal. Das Umschalten funktioniert dadurch, dass der gesuchte RNA-Strang einen Mechanismus auslöst, der es den Armen erlaubt sich in die nichtrechtwinklige Geometrie zu verbinden. Ich konnte zeigen, dass dieser Virendetektor RNA in sehr kleinen Konzentrationen nachweisen kann, allerdings im Moment noch nicht mit bloßem Auge, sondern mit einem speziellen Gerät, dass CD Signale messen kann. Zusätzlich konnte ich zeigen, dass der Sensor auch RNA in einer Blutprobe nachweisen kann. Die Details zu den Messungen kann man in Kapitel 6 nachlesen.

Ich konnte also zeigen, dass es theoretisch möglich ist so etwas wie Frodos Schwert herzustellen. Dazu muss der hier vorgestellte Virendetektor noch stark verbessert werden. Es ist aber ein kleiner Schritt in Richtung der praktischen Anwendung von Nanotechnologie.

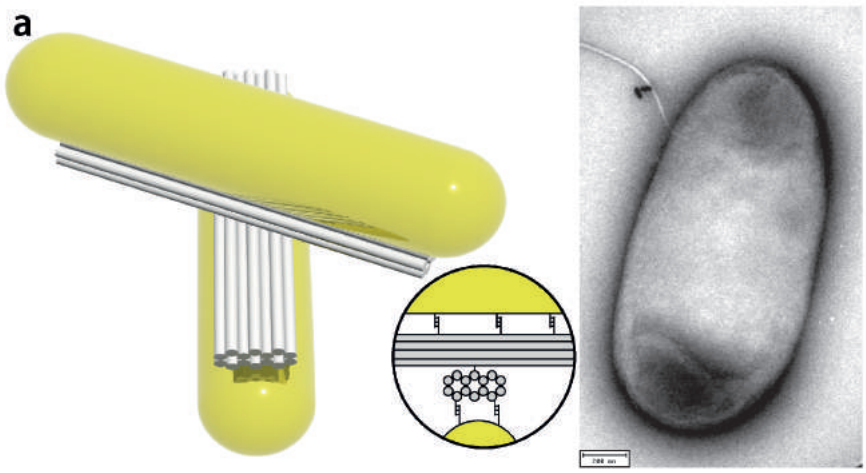

Abbildung 2.4: Links: Eine 3D Animation des Virendetektors. Die weißen Zylinder sind DNA-Stränge. Auf den Armen ist jeweils ein Goldstäbchen befestigt. Rechts: Bild von einem Elektronenmikroskop. Das große ovale Objekt ist ein Bakterium mit einer Länge von 1.7 μm. Oben links kann man die beiden Goldstäbchen (schwarz) des Virendetektors erkennen.

3

DNA NANOTECHNOLOGY

3.1 FUNDAMENTS OF DNA NANOTECHNOLOGY

Everyone has heard of DNA. Some people know it stands for Deoxyribonucleic Acid. Many people know that it has to do something with genomics and somehow dictates how our bodies work. However, in this thesis, the function of DNA as the carrier for all the information that makes life possible is not essential. The primary focus of this section is to understand the molecule itself, all its several chemical, mechanical ,and optical properties and how they can be modified or exploited. The general idea of DNA nanotechnology is to use DNA for designing and constructing useful tools to solve problems in the nanoworld.

A SHORT HISTORY OF DNA: In 1869 the swiss physician Friedrich Miescher discovered a substance he could extract from cells using acid, which he called nuclein [5]. During the next years, the chemical components of this nuclein, like the four bases, were discovered [6]. In 1943 it became clear that bacteria pass on information by sharing DNA [7, 8]. However, the chemical structure of the molecule remained a mystery. The race to solve this mystery included several players. Among them Linus Pauling at the California Institute of Technology, Maurice Wilkins and Rosalind Franklin at King's College London and James Watson and Francis Crick at the Cavendish Laboratory at Cambridge University. Pauling proposed a three-stranded helix which turned out to be wrong [9]. The actual data to solve this problem was taken by Rosalind Franklin by X-Rax scattering (Figure 3.1). After seeing Franklin's scattering data, Watson and Crick figured out the structure by building possible models and finally proposed a double helical structure (Figure 3.2) in their famous article "Molecular Structure of Nucleic Acids: A Structure for Deoxyribose Nucleic Acid" in 1953 [10]. A commented version of the article can be found on the website of the Exploratorium in San Francisco [11]. Wilkins and Franklin, who were working independently on their X-ray data, came to similar conclusions. In agreement with everyone,

all three articles were published in the same issue of NATURE [10, 12, 13].

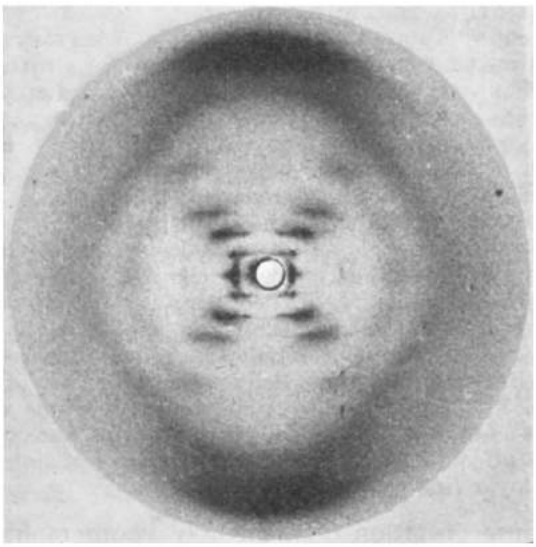

Figure 3.1: X-Ray scattering pattern taken by Rosalind Franklind, that brought Watson and Crick on the right track towards developing the idea of the double helix. Reprinted from [12], with permission from Springer Nature

PROPERTIES OF DNA: Figure 3.3 shows the chemical structure of the bases and the geometry of the double helix. The building blocks of DNA are called nucleotides. Each nucleotide consists of three components: phosphate, the sugar deoxyribose, and a nucleobase. Deoxyribose and phosphate are the same in each nucleotide and form the backbone of the double helix. The hydrophilic phosphate gives the DNA an overall negative charge in solution. There are four different bases in DNA: The purines adenine and guanine and the pyrimidines thymine and cytosine. The nucleotides are usually abbreviated with the first letter of their base: A, T, G, and C. The five carbon atoms of the deoxyribose are numbered from 1′ to 5′.The 1′ is connected to the base, the 2′ to a hydrogen atom, the 3′ to an OH-group that can bind to the phosphate group of the next nucleotide and the 5′ to the phosphate. Nucleotides are connected between 3′ and 5′ over phosphodiester bonds. These give every single strand a directionality, a 3′-end and a 5′-end. DNA polymerases, the proteins that synthesize new DNA in cells, add new nucleotides usually on the 3′-end. Two single strands of DNA form a double helix when each base connects to its counterpart on the other strand. Adenine always pairs with thymine over two hydrogen bonds, and guanine always pairs

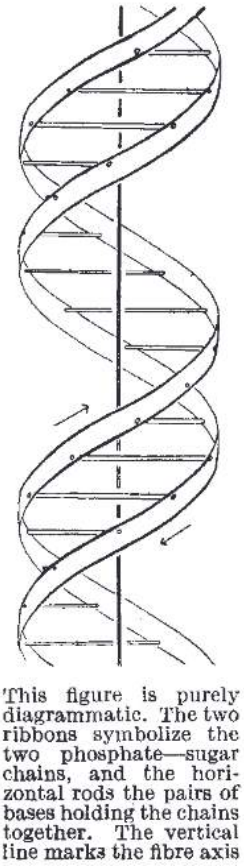

This figure is purely diagrammatic. The two ribbons symbolize the two phosphate—sugar chains, and the horizontal rods the pairs of bases holding the chains together. The vertical line marks the fibre axis

Figure 3.2: Illustration of the double helix from the original publication of Watson and Crick in 1953 "MOLECULAR STRUCTURE OF NUCLEIC ACIDS: A STRUCTURE FOR DEOXYRIBOSE NUCLEIC ACID" drawn by Crick's wife. Reprinted from [10], with permission from Springer Nature

with cytosine over three hydrogen bonds. The double helix is stabilized mainly by the stacking interaction of the consecutive bases and not, as widely thought, the base pairing by the hydrogen bonds. As the two strands are not located symmetrical to each other, there are two differently sized grooves on the double helix, called major (2.2 nm) and minor groove (1.2 nm). Those are the main binding points for other molecules like proteins or dyes. The diameter of the double helix is 2.2 to 2.6 nm depending on the solution, and one nucleotide unit is 0.33 nm long [14]. With a pitch of 3.4 nm, the helix takes two turns after 21 base pairs, an essential fact for the later explained DNA origami technique Section 3.2.

One of the fundamental concepts used in DNA nanotechnology, the Holliday Junction, was proposed 1964 by Robin Holliday [16]. It consists of four connected double-stranded DNA arms. Biologically,

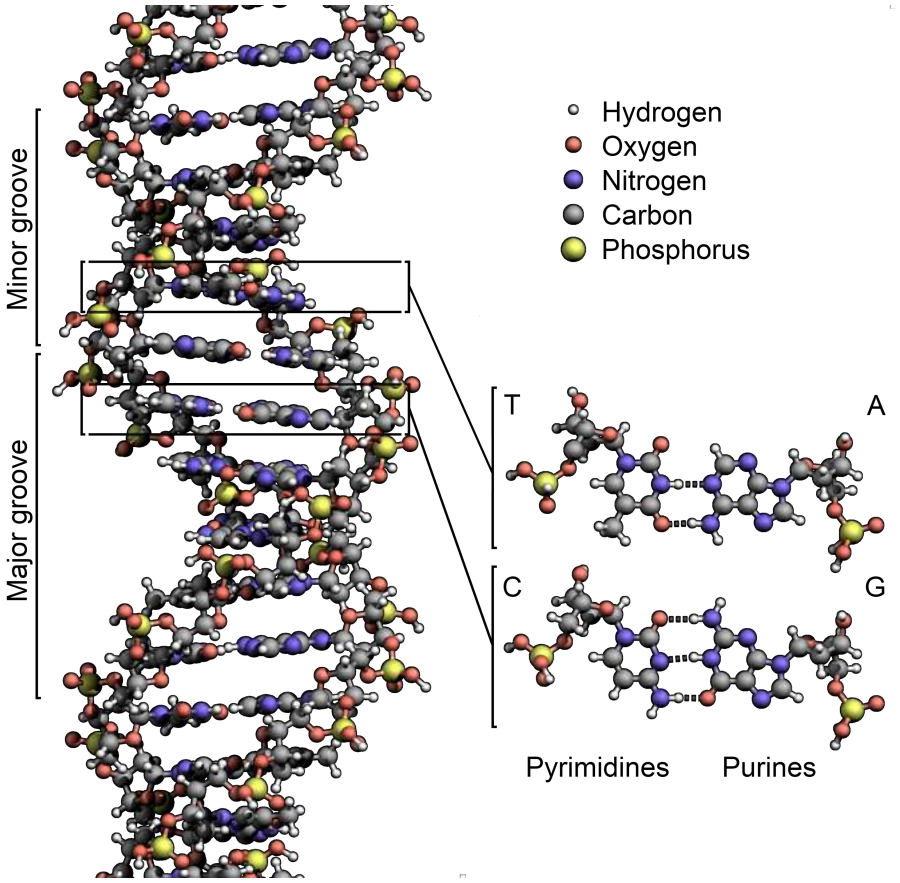

Figure 3.3: Chemical structure of the bases and geometry of the double helix. Illustration by (Zephyris (Richard Wheeler)), distributed under CC BY-SA 3.0 at [15]

this junction occurs in the process of genetic recombination during meiosis of cells. The first non-biological use of the Holliday Junction was proposed in 1982 by Ned Seeman [17] and built in 1983 [18]. The next step was the construction of a 3D cube by connecting three-arm junctions with single strands switching from one double helix to another and thus connecting those two helices. Soon, 2D lattices of Holliday Junctions containing sticky ends - often called DNA tiles - were assembled. The first "DNA machine" was presented in 1999 [19]. This construct of four single strands was able to switch between two conformations reversibly, which could be detected by two attached fluorescent molecules. The fast growth of the DNA nanotechnology field would not have been possible without the parallel discoveries and improvements of the solid-state synthesis of DNA. Faster access to any sequence of oligonucleotides increased the possibilities of sequences that could be tested and reduced the cost significantly.

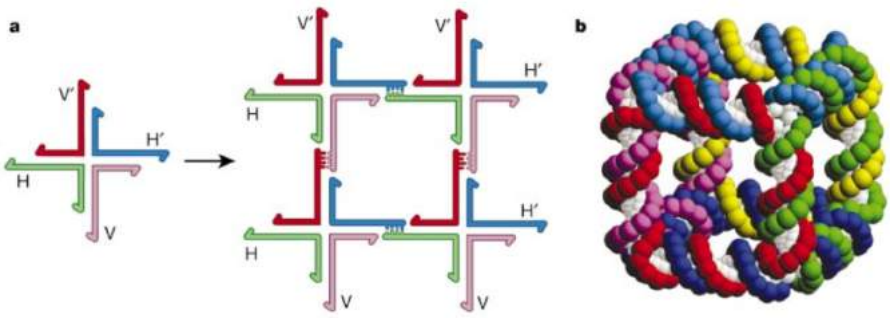

Figure 3.4: DNA cube assembled by connecting Holliday junctions. Reprinted from [20], with permission from Springer Nature

DNA-FUELED SWITCHING: Increasing interest in DNA as a material also arose because of its chemical and dynamical possibilities. In 2000 Yuke et al. showed a DNA machine that could switch between two states in an isothermal reaction by the addition of specific "fuel" DNA strands [21]. This DNA "tweezer" is closed by addition of a DNA strand and opened by another different DNA strand. The change in states could be measured by fluorescence energy transfer between two dyes (Figure 3.5). The reaction starts with the fuel strand binding to an unpaired part of the structure, the "toehold". If the toehold is long enough (usually eight base pairs), the fuel strand will start replacing the original complement and finally remove it. Many DNA switches and machines now rely on that mechanism.

PROTON-FUELED SWITCHING In 1993 Gueron *et al.* found that four sequences of multiple cytosines can form a particular tetrameric structure which they called "i-motif"[23]. Two parallel duplexes of cytosine strands intercalate with each other in antiparallel orientation. The C-C pairs are only made possible by an additional hydrogen ion in acidic conditions. I-motifs are possible with one, two or four strands as shown in. The i-motif can be used to assemble large structures in 1D [24] or 3D [25]. The i-motif can not only be used structural but also as a dynamic component, switching from i-motif in acidic conditions to B-DNA at neutral pH [26, 27]. The i-motif has been shown to produce a force output [28] and can be used for controlled cargo release [29, 30].

LIGHT-FUELED SWITCHING Azobenzene is a molecule that can switch between a cis- and a trans-state at light exposure [31, 32]. Chemically modified DNA with azobenzene between the bases can form duplexes with azobenzene in the trans-state. However, when

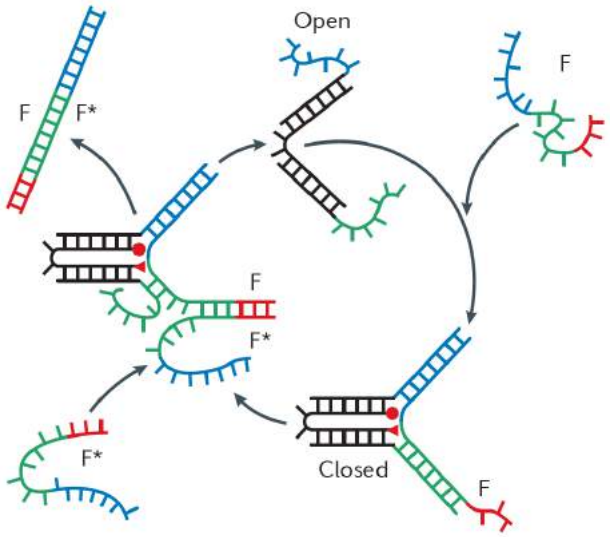

Figure 3.5: DNA "tweezer" is closed by addition of a DNA strand and opened by another different DNA strand. The change in states can be measured by fluorescence energy transfer between two dyes (Figure 3.5). The reaction starts with the fuel strand binding to an unpaired part of the structure, the "toehold". The fuel strand will start replacing the original complement and finally remove it. Reprinted from [21, 22], with permission from Springer Nature

switched to the cis-state, steric hindrance of the azobenzene prevents forming of DNA double helices. Thus, DNA can be switched between bound and unbound state using light [33].

3.2 THE EARLY PHASE OF DNA ORIGAMI

The field of DNA nanotechnology took a big step in 2006 when then Caltech postdoc Paul Rothemund published a method he called DNA Origami [34]. He showed that a long viral single strand of DNA (scaffold strand) could be folded onto itself by adding multiple specially designed oligonucleotides (staple strands) that would connect selected parts of the scaffold to fold it into the desired shape. An iconic structure of this work is the 2D DNA smiley, or as he calls it: disk with three holes. The principle of designing and folding of the smiley is shown in Figure 3.6. It enabled the construction of DNA structures with many possible shapes and addressable sites. The easy assembly method with unpurified synthetic staple strands made it a versatile tool.

Rothemund used the single-stranded circular genome of the M13 mp18 bacteriophage as a scaffold. This scaffold then has to be laid

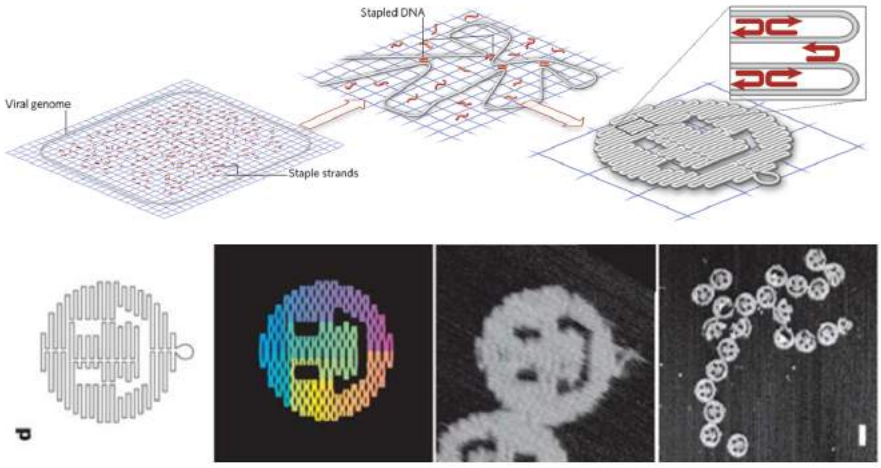

Figure 3.6: Top: Folding principle of the DNA smiley from the first DNA origami publication. Bottom left to right: scaffold path, design with connections, AFM image of single smiley and AFM zoom-out. Reprinted from [3] and [34] with permission from Springer Nature

out into the desired shape. Staple strands are designed accordingly, so the scaffold and the staples form an array of antiparallel double helices in the desired shape. Staple strands connect the double helices by crossing over multiple helices. DNA origami went from 2D to 3D in 2009 with the work of Douglas *et al.*[35]. 3D origami can be thought of as a folded up version of the 2D array with more interconnections (Figure 3.7). To connect neighboring double helices, the geometry of DNA has to be taken into account. With a pitch of 3.4 nm and a base height of 3.3 nm, each 7 base pairs, the double helix turns 240°. With this property, a honeycomb lattice is the first choice. When using a square lattice design, the geometry of the double helix does not match the crossovers perfectly, which induces a twisting force that has to be balanced by intentionally relaxing the strain or can even be used as a desired feature for twisted structures. For the easier design of new structures, a software tool was created that helped in finding the correct scaffold path and staple crossovers: the caDNAno software [36]. A scheme of the whole DNA origami design process is shown in Figure 3.8. With more and more shapes and styles being designed, it became important to predict the final shape of a DNA nanostructure. Kim *et al.* developed a computational model that can predict structures from caDNAno files [37, 38] Another approach for constructing 3D DNA structure was to combine multiple 2D sheets [39]. 6 of those sheets can be connected to form a box with

a flexible lid (Figure 3.9). The lid was connected only to one other site as a hinge. On the opposite side, it was connected with double-stranded connections, similar to the tweezer in Figure 3.5. With this mechanism, the lid of the box could be opened *via* a single-stranded signal strand by strand displacement. The opening and closing could be confirmed by energy transfer between two fluorophores at the lid and the box.

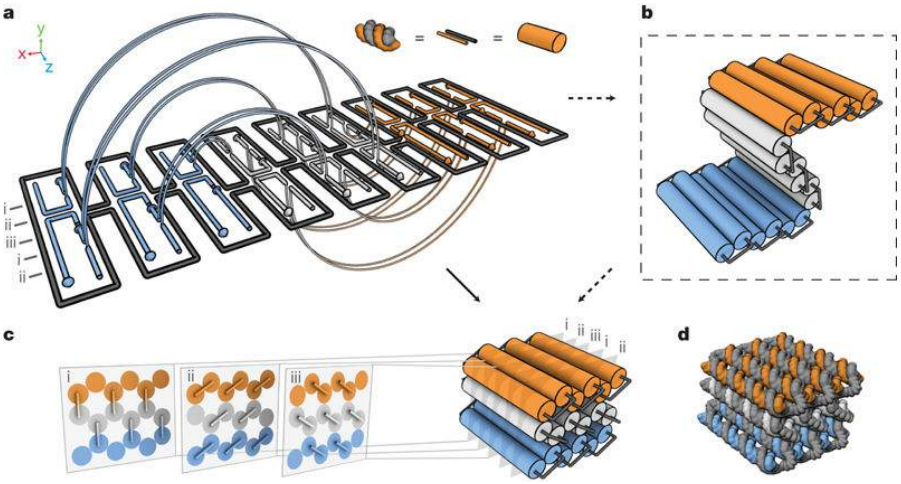

Figure 3.7: Principle for folding 3D structures. The scaffold is folded up into the desired shape with multiple interconnectionss. Reprinted from [35], with permission from Springer Nature

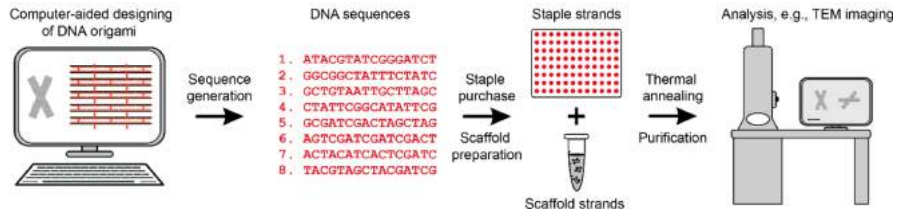

Figure 3.8: DNA origami structures are designed with caDNAno software. The software generates sequences of the staples. Staples are usually purchased in multiwell plates from commercial vendors. The scaffold is mixed with staple strands (with a large excess), and the origami structures are assembled through thermal annealing. The structures are usually purified before being used as templates for further assembly. Transmission electron microscopy (TEM) is often used to characterize origami structures. Reprinted with permission from [40]. Copyright (2018) American Chemical Society.

DESIGN STRATEGIES WITHOUT SCAFFOLD STRAND: Another powerful method for building 2D and 3D DNA structures that does not need a scaffold strand was developed by Yin *et al.*. The method uses a predesigned DNA sheet (2D) [41] or DNA block (3D) [42] made of

different connected single strands as a canvas. Each strand works as pixel/voxel that can be left out to create any shape out of the canvas. Each brick can be removed individually, allowing geometrically finer structures than DNA Origami (Figure 3.9).

TENSEGRITY Because of its flexibility, DNA can be bent or put under tension. This can be exploited to construct bent DNA origamis or stabilize structures by tension. In a standard DNA helix bundle designed with caDNAno, all helices are the same length. To create a bent shape, the helices on one side of the bundle are designed a little bit shorter to create a strain on the whole bundle and bend it [43]. When different subsets of helices are shortened throughout the structure, also twisted bundles are possible. The concept of stabilizing structures with a combination of tension and integrity (tensegrity) is well known in architecture and can also be found in biological systems like cells. First DNA nanostructures applying the tensegrity principle have been shown in 2004 [44], with a DNA triangle. This principle can also be applied to DNA origami structures. A simple double strand can serve as the tension element and helix bundles as the integrity parts. With this method three dimensional prestressed structures were built [45] (Figure 3.9).

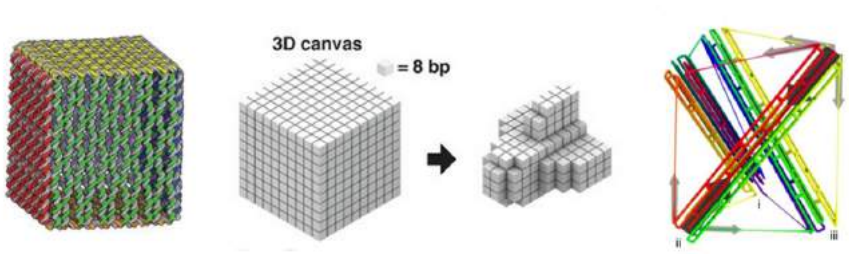

Figure 3.9: Left: 3D DNA cube made from 6 sheets with switchable lid. Reprinted from[39], by permission from Springer Nature. Middle: DNA canvas, where individual DNA stands can be left out like voxels to create any shape. Reprinted from[42], by permission from AAAS. Right: Tensegrity DNA structure with single DNA strands as tension elements and helix bundles as the integrity parts. Reprinted from[45], by permission from Springer Nature.

3.3 ORIGAMI ADVANCED

Research in DNA Origami in the recent years can roughly be divided into four areas [46].

1. ORIGAMI RESEARCH: Improving assembly methods, quantity, yield and design space
2. INTERACTING WITH BIOLOGICAL SYSTEMS: Interaction with proteins, lipids, and cells
3. MACHINES, SWITCHES AND SENSORS: Flexible, moving structures with input and/or output
4. OPTICAL EFFECTS AND MATERIALS: Combining DNA with optically active materials like gold nanoparticles or fluorescent dyes

Many projects can have connections to multiple areas, but they have been categorized by the area they had the most impact. The following description is by no means conclusive and complete but tries to give an overview of the current state-of-the-art and possibilities of DNA origami technology.

3.3.1 *Origami Research*

Much effort has been put into exploring the possibilities of DNA structures, to improve design strategies and scale up the size and quantity of the structures. This covers topics from better software tools [47] to specialized bioreactors for mass production [48]. DNA structures usually are connected by DNA base pairing. Single strands crossing from one structure to another connect the structures by binding to a complementary sequence on each side (sticky ends). In the double helix, a more significant force than the base-base interaction by hydrogen bonds is the stacking of the base pairs on top of each other. This force is the main contributor to the stability of the double helix. It can be used to connect DNA structures by designing geometrically complementary connecting sites [49]. This method can not only be used to create large structures and lattices, but also dynamically reconfigurable devices. By controlling the positive ion concentration in the solution, the strength of the DNA stacking can be controlled and consequently, connections can be opened and closed. This switching happens on the timescale of milliseconds [50], if the structures are built to ensure proximity of the binding sites. Multimerisation of different structures takes minutes to hours. With this approach, large structures in the gigadalton scale could be produced [51].

DNA origami can be used to form DNA filaments into cholesteric liquid crystals, one-dimensional supramolecular twisted ribbons, and

two-dimensional colloidal membranes [52]. By controlling the properties of the individual DNA structure, like the twist, the macroscopic properties of the system like the cholesteric pitch can be controlled. While in this system DNA structures form the liquid crystal, in another system inorganic liquid crystals have been used to align optical active DNA-gold structures [53].

To expand DNA structure design from the caDNAno honeycomb and square lattice method, Benson *et al.* developed a computational tool to create structures from any 3D mesh design from conventional CAD tools [47]. The software optimizes the scaffold path through the structure along the polyhedral mesh. By this method, various forms with finer structures than the ones in the honeycomb lattice can be achieved. However, the more detailed finer structure makes them less stable and rigid.

One big problem for people working with DNA origami has been the assembly yield and sample amount. For the most possible application of DNA nanomachines, large amounts of structures are needed. To address this need, Praetorius *et al.* developed a system, where scaffold and staples are mass produced in a one-pot reaction bioreactor [48]. Consequently, staples and scaffold are spliced out of one plasmid by self-cutting DNAzymes embedded in the plasmid.

Although highly versatile and functional, DNA as a building material has its limitations. Proteins, on the other hand, could add a lot of functionalities and possibilities to artificial nanostructures. A successful connection of proteins and DNA to form nanostructures was shown in 2017 [54]. Multiple proteins with two recognition sites each connect two specific sequences of double helices. Two dsDNA strands could be folded in various shapes with this method. Furthermore, the whole assembly can be started from DNA when the plasmids encoding the proteins and the template DNA are incubated in an expression one-pot mixture with polymerases and cofactors.

The assembly of DNA origami structures is usually done in a temperature ramp over up to 24 hours. It was discovered in [55] that most of the assembly happens at a very small temperature range of 1-2°C specific to each structure design. One can find the specific assembly temperature for a structure by either systematic testing or folding over a temperature ramp mixed with intercalating dye and observing the change in fluorescence. This reduces the time needed to assemble a structure drastically because now the sample is heated up to dena-

ture all sequences entirely and then kept at the assembly temperature for only one hour.

The most important factor for successful DNA origami assembly is the incorporation of the staple strands at the correct position. The super-resolution technique DNA-PAINT [56] (Section 3.3.4) enabled the investigation of individual oligonucleotides in DNA structures [57]. It was shown that the excess of staple strands in the assembly mixture plays a crucial role in the incorporation efficiency from 72% (10x excess) to 84% (500x excess). The staple strands also show different incorporation yields depending on the position in the structure with noticeable lower incorporation at the outside of the structure.

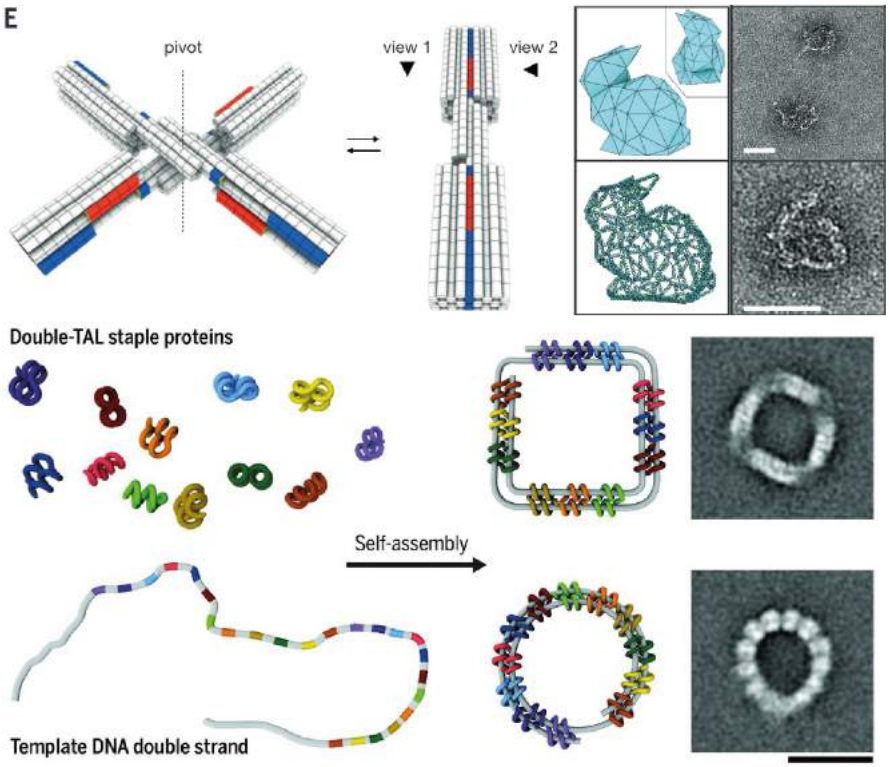

Figure 3.10: Top left: DNA structures with geometrically complementary connecting sites can be used to create dynamically reconfigurable devices. Top right: A software optimizes the scaffold path through the structure along the polyhedral mesh. By this method, various forms with finer structures than the ones in the honeycomb lattice can be achieved. Bottom: Multiple proteins with two recognition sites each connect two specific sequences of double helices. Two dsDNA strands could be folded in various shapes with this method. Republished from [47, 49, 54] with permission by AAAS and Springer Nature

3.3.2 *Interacting with Biological Systems*

It seems rather obvious to use a fully controllable biomolecule as a tool to control and investigate other biological systems. Combining DNA origami with proteins, lipids or even cells each offer their challenge as each molecule has different requirements to an artificial environment. Understanding and utilizing enzymatic pathways has always been a big part in biotechnology. DNA origami offers a promising route to organize and arrange biomolecules. Zhao *et al.* showed a method to encapsulate enzymes in a DNA nanocage for improved efficiency and stability [58]. First experiments combining two cooperating enzymes in one cage showed improved efficiency. However, the enzymes already showed improved activity with just being bound to half the nanocage without the other enzyme in close proximity. The environmental effects of a DNA origami close by seem to be enough for enhanced activity. The negative charge of the DNA structure is believed to create a highly ordered hydration layer which has been shown to increase enzyme productivity. The DNA nanocage also showed a protective effect against trypsin digestion.

Another example for encapsulated enzymes is the nanorobot by Douglas *et al.* [59]. A clamp-like shell protects a payload of active proteins. Closed by a system similar to the DNA box [39], the nanorobot can be opened by recognition of specific molecules. In this case, the lock mechanism uses two different aptamer sequences, so the lock functions as an AND logic gate for protein recognition. Upon opening, the active enzymes from the inside are free to bind to their target cell.

The high spatial control of DNA origami allows the construction of small channels. This has been shown for the first time by Bell *et al.* [60]. Attached to a lipid layer or vesicle by hydrophobic modifications on the structure, this channels can form a pore in the membrane and be used for particle transport through the membrane [61]. Translocation of dsDNA and dye molecules could be shown. Changes in electric flux through the nanopore change with the influx of particles. This can potentially be used for single-molecule detection or even DNA sequencing.

The attachment of lipid layers to DNA origami structures can also be utilized to create a virus-like protective shell. By wrapping a spherical DNA structure in a lipid bilayer, Perrault *et al.* could improve the stability against nucleases and increase the bioavailability in mice

[62]. After 120 min labeled oligonucleotides and unwrapped structures were accumulated entirely in the bladder. The structure with the lipid shell, however, could be detected throughout the whole body.

A lipid bilayer can even be utilized to facilitate DNA structure lattice formation [63]. By using the diffusion of single structures on the membrane and blunt end or sticky end interactions, lattices of multiple hundred nm could be achieved. Structures shaped like a cross, triangle or hexagon could also be assembled to a closely packed layer.

To mimic the hydrophobic effect in protein folding, Edwardson *et al.* attached hydrophobic alkyl-DNA conjugates to DNA cubes. With four of the amphiphiles on each cube, two cubes connect to form a dimer. When eight amphiphiles were attached to one cube, they form an artificial micelle inside the cube. Hydrophobic molecules can be trapped inside that micelle and released upon DNA recognition [64].

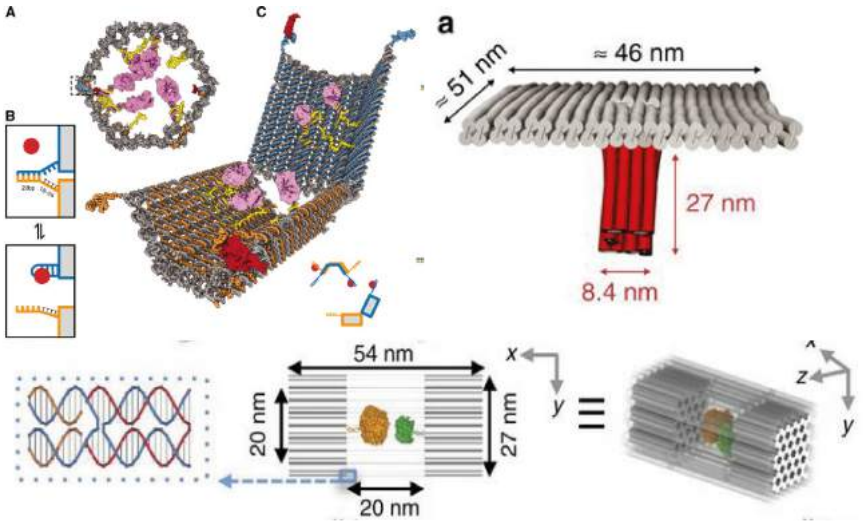

Figure 3.11: Top left: A clamp-like shell protects a payload of active proteins. The nanorobot can be opened by recognition of specific molecules. Top right: Artificial DNA nanopore. Bottom: Encapulated enzymes in a DNA nanocage for improved efficiency and stability. Republished from [58] with permission by AAAS, [59, 61] under Creative Common Licence

3.3.3 *Machines, switches, and Sensors*

With DNA being highly flexible and changeable by a variety of inputs (DNA, RNA, light, pH), DNA Origami offers an excellent opportunity to create switches and other changeable devices. To build mechanical flexible devices, moving joints are necessary. Marras *et al.* showed the combination of a hinge and a cylindrical slider to a slider-crank link-

age [65]. Defined angular and linear motion can be used to define the final degrees of freedom of a structure. Furthermore, they realized a Bennett linkage with DNA origami that can be switched between two states by adding DNA recognition strands. Also, mechanical rotation can be implemented in DNA structures [66]. Kopperger *et al.* constructed a freely rotating long arm of 25 nm that could be extended to 400 nm on a 55x55 nm sheet. The orientation was controlled externally by switching electrical fields. FRET experiments demonstrated the switching in milliseconds. The arm can be used to transport cargo or to study DNA duplex melting. With changes in pH as a trigger, DNA structures can be switched with the use of specific pH-sensitive sequences. With changes in pH, reconfiguration and structural isomerization of origami structures were shown 2016 [67]. Additional to the famous pH-sensitive i-motif sequence (**??**) they used a C-G-C triplex motif for low pH and a T-A-T triplex motif at neutral pH. Not only pH but also light can be used to trigger multimerization [68]. Implementing an azobenzene modified DNA sequence in DNA structures makes it possible to activate and deactivate the hybridization of these strands. This photoregulatory system can be used to trigger assembly remotely. Thubagere *et al.* [69] showed a cargo sorting robot 2017. It consists of a base surface made of DNA origami with binding sites for the robot. The robot consists of a foot domain for walking and an arm domain for grabbing and delivering cargo. The robot performs a random walk on the base transporting the cargo from an to specifically designed binding sites. Multiple robots can perform tasks simultaneously. DNA structures can be used as a force sensor in the piconewton regime [70]. With a force clamp structure, molecular force spectroscopy on a Holliday junction and binding of a TATA-binding protein was done. The structure can be adjusted to a specific force and the response of the attached molecules is measured by FRET. The advantage of this system over conventional AFM force spectroscopy is the massive amount of parallel measurements at once and the independence of a physical connection to the detection system. Combining a structure with mechanical hinge, fluorophores and DNA recognition leads to a sensing platform.[71] Consisting of two sheets with 60 donors and receptors respectively, it can be triggered to close leading to FRET signals from the fluorophores. Down to a concentration of 10 pM DNA could be measured using a system with the structures immobilized on a surface. In conclusion, DNA origami

structures can show changes in multiple signals after being triggered by a variety of input signals like DNA, RNA, light, pH.

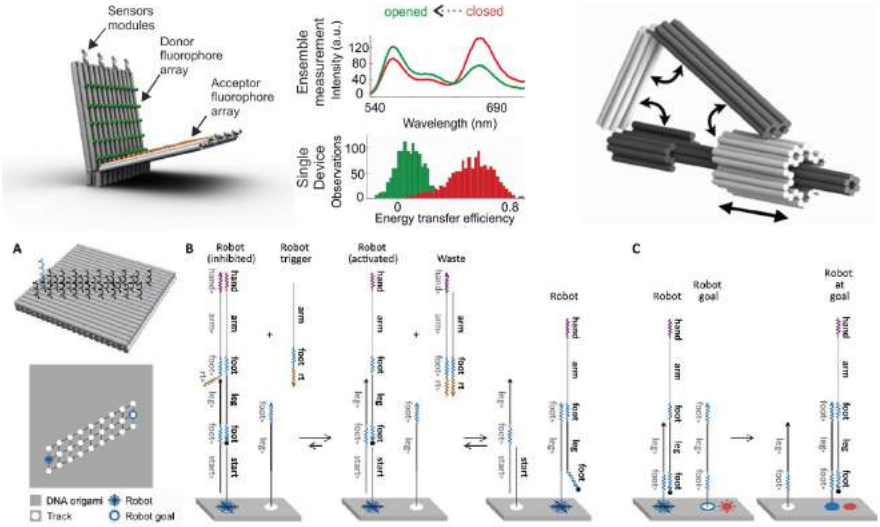

Figure 3.12: Top left: Combining a structure with mechanical hinge, fluorophores and DNA recognition leads to a sensing platform. Top right: combination of a hinge and a cylindrical slider to a slider-crank linkage. Bottom: A cargo sorting robot. Top right and bottom image republished from [65], [69] with permission from AAAS. Top left image reprinted with permission from [71]. Copyright (2018) American Chemical Society.

3.3.4 *Optical Effects and Materials*

For nano-optics, where the geometrical arrangement is as important as the included building blocks, DNA origami opened a route of precise arrangement of optical components. Arranged fluorescent dyes on a DNA nanopillar can serve as a standard for 3D superresolution microscopy [72]. Using STORM, the two dyes on the pillar can be detected individually, and thus the orientation and angle of the structure can be determined. This can be used as a size and direction standard for microscopy sample and as a measure for magnification by refraction index mismatch at sample surface interface. DNA nanotechnology offers a promising route for superresolution probes. In a modified version of the PAINT method, a DNA structure serves as a carrier for DNA binding spots. With fluorescently labeled DNA oligos binding to the spots, resolution of 1 nm can be reached [56]. A DNA structure modified with a pattern of binding sites can be used as a barcode for 124 different configurations of binding site patterns. With PAINT those patterns can be resolved. When the DNA struc-

tures are functionalized with different recognition sites, they can be used as probes for multiple targets at once [73]. Fluorescent dyes on a DNA structure can be used to realize energy transfer pathways by building a line of different dyes [74]. Transport efficiencies and distances of light energy transport can be controlled and evaluated with this system. This could eventually lead to the development of new artificial light-harvesting systems. With an effective method to functionalize metal nanoparticles with DNA [75], it was an obvious step to use DNA origami to arrange particle in specific geometries. This is especially useful to construct optically active assemblies, by utilizing plasmonic effects in metal nanoparticles. One useful effect of nanoparticles is the enhanced electric fields in the area between two particles called "hot spot". With a dimer of gold nanoparticles connected by a DNA origami structure, the hot spot can be used to enhance the signal of a fluorescent dye [76]. Fluorescent dyes attached to the structure in the hot spot showed an enhanced Raman signal. Multiple particles arranged in a helical structure can show circular dichroism (CD). Contrary to natural molecules that show a CD in the UV spectrum, artificial chiral arrangements can be tuned for a CD in the visible spectrum opening up opportunities for new optical materials [77]. Those CD signals have been theoretically predicted with an approach of interacting dipoles. Another chiral structure can be constructed with two nanorods [78]. Plasmonic nanostructures and plasmonic chirality will be discussed in the next chapter.

3.4 HOW DOES THIS THESIS RELATE TO THE RESEARCH AREAS?

The research of this thesis covers multiple areas of DNA nanotechnology. The project covering the broadest range is described in Chapter 6. Using the structure of [78], consisting of a plasmonic switch triggered by strand displacement, a sensor for viral RNA was designed and tested. Additionally, the stability of the sensor in serum as a potential test substance was investigated. Chapter 6 thus covers areas 2-4. Chapter 7 and Chapter 8 both fall into the area of optical and plasmonics effects. Chapter 7 investigates the effect of different nanoparticle arrangements in helical structures on the plasmonic CD spectrum. Chapter 8 describes the first steps towards a system of nanoparticles to produce and measure the Fano effect. Basic plasmonic theory, plasmonic circular dichroism and the Fano effect will be covered in the next chapter.

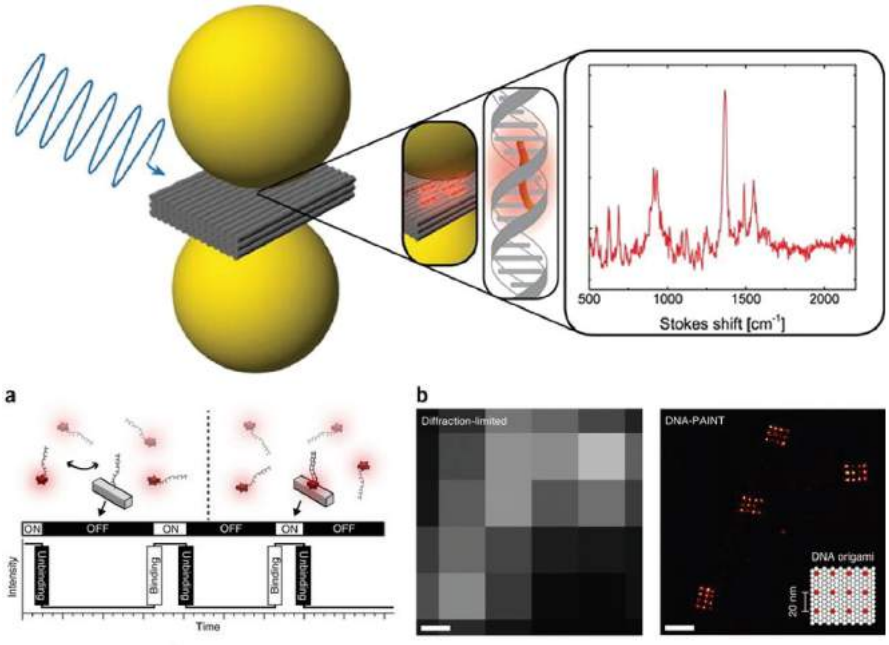

Figure 3.13: Top: With a dimer of gold nanoparticles connected by a DNA origami structure, the hot spot can be used to enhance the signal of a fluorescent dye. Fluorescent dyes attached to the structure in the hot spot showed an enhanced Raman signal. Reprinted with permission from [76]. Copyright (2014) American Chemical Society. Bottom: Modified version of the PAINT method, a DNA structure serves as a carrier for DNA binding spots. With fluorescently labeled DNA oligos binding to the spots, resolution of 1 nm can be reached Reprinted from [56] with permission from Springer Nature

4

PLASMONICS

4.1 DRUDE MODEL FOR METALS

In classical electrodynamics, electromagnetic waves are synchronized oscillations of an electric and a magnetic field that propagate at the speed of light. They can be characterized by their frequency or wavelength. The oscillation planes of the electric and the magnetic field lie perpendicular to each other and to the direction of propagation.

James Clerk Maxwell theoretically derived electromagnetic waves. Their behavior is governed by the Maxwell equations:

$$\begin{aligned}
\vec{\nabla} \cdot \vec{E} &= \frac{\rho}{\epsilon_0} \\
\vec{\nabla} \cdot \vec{B} &= 0 \\
\vec{\nabla} \times \vec{E} &= -\frac{\partial \vec{B}}{\partial t} \\
\vec{\nabla} \times \vec{B} &= \mu_0 (\vec{j} + \epsilon_0 \frac{\partial \vec{E}}{\partial t})
\end{aligned}$$

Here, $\vec{E}$ is the electric field, $\vec{B}$ is the magnetic field, $\vec{\nabla}$ is the three-dimensional gradient operator, ρ is the electric charge density, ϵ_0 is the dielectric constant, μ_0 is the permeability of free space, $\vec{j}$ the electric current density, and t is time.

The solution to Maxwell's equations can be written as a superposition of monochromatic waves to take into account the finite response time of the medium to the wave. With a constant ϵ in the Maxwell equations we assume an instantaneous response. In the superposition solution, ϵ has to be a function of the wavelength ω. The frequency dependent dielectric function gives a complete description of the optical response of a material in the classical picture. For a working model for metal nanoparticles, we need a model for the dielectric function.

The simplest model for the dielectric function in metals is given by the Drude free-electron model. The electrons of the metal are considered as a gas of free, non-interacting electrons moving against a back-

ground of positive ions. This allows to leave all quantum mechanics behind and describe the electron gas in a lattice gas

$$m\frac{d^2x}{dt^2} = -\frac{m\gamma dx}{dt} - qE_{tot}(t)$$

where m is the effective electron mass, q is the charge of the electron, γ is the collision frequency to account for electron scattering, and $E_{tot}(t)$ is the total electric field, containing the external field and internal fields generated by electron motion. The resulting dielectric function [79] is

$$\epsilon(\omega) = 1 - \frac{\omega_p^2}{\omega^2 + i\gamma\omega}$$

with the plasma frequency of the free electron gas ω_p. The dielectric function can be divided into real and imaginary component $\epsilon(\omega) = Re(\epsilon(\omega)) + iIm(\epsilon(\omega))$

4.2 NANOPLASMONICS

Nanoplasmonics is an area of solid state physics describing optical phenomena on the nanoscale of metal nanosystems. The following chapter gives a brief description of the theory behind the nanosystems in this thesis. In-depth explanations can be found in [80], [81] and [79]. The concentration of electromagnetic energy is limited by the wavelength. Even in an ideal Fabry-Perot resonator with perfect mirrors, the light cannot be confined in a length smaller than $\lambda/2$ or a total volume of $\lambda^3/8$. To achieve confinement of optical energy in the nanoscale two assumptions of optical energy have to be abandoned: (i) optical energy is electromagnetic energy and (ii) best confinement is achieved by ideal mirrors.

The skin depth, a measure how deep an electric field can penetrate a substrate, is given by

$$l_S = \lambda_V \left[\left(\frac{-\epsilon_m^2}{\epsilon_m + \epsilon_d} \right)^{1/2} \right]^{-1}$$

with the reduced vacuum wavelength $\lambda_v = \lambda/2\pi = \omega/c$. For silver and gold the skin depth is $\approx 25nm$. For a nanosystem with $a \leq l_S$ the electric field penetrates the whole system and drives oscillations of the electrons. This is called the "quasi-static approach", where retardation effects are ignored, so the incident field can be approximated by a constant field. For a spherical particle the Maxwell equations can

be solved. With an electric potential Φ, the electric field is $\mathbf{E} = -\nabla\Phi$. With a driving field in z-direction $\Phi = -Ez = -Er\cos\phi$. The potentials inside and outside of the particle can be written as

$$\Phi_{in}(r,\phi) = \sum_{l=1}^{\infty} A_l r^l P_l(cos\phi)$$

$$\Phi_{out}(r,\phi) = \sum_{l=1}^{\infty} B_l r^{l+1} P_l(cos\phi) - Er(cos\phi)$$

Applying the boundary condition that the potential are continuous at r=a:

$$\begin{aligned} &l = 0 : A_0 = B_0 = 0 \\ &l = 1 : A_1 = \frac{-3\epsilon_{out}E}{\epsilon_{in} + 2\epsilon_{out}}, B_1 = \frac{(\epsilon_{in} - \epsilon_{out})Ea^3}{\epsilon_{in} + 2\epsilon_{out}} \\ &l > 1 : -\frac{\epsilon_{out}(l+1)}{\epsilon_{in} l} = 1, A_l = \frac{B_l}{a^{2l+1}} \end{aligned}$$

The fact that there is no constant term ($l = 0$) represents the fact that there is no net charge. A response for every frequency is obtained for l=1. For $l > 1$ the response is independent of E, so higher modes cannot be exited by a constant field [81]. Through the potential of the particle dipole with dipole moment μ is $\Phi = \mu z/\epsilon_{out} r^3$ we obtain the polarizability of the particle

$$\alpha = \frac{(\epsilon_{in} - \epsilon_{out})\epsilon_{out} a^3}{\epsilon_{in} + 2\epsilon_{out}}$$

with $\alpha = \mu/E$. The polarizability shows resonant enhancement when $|\epsilon_{in} + 2\epsilon_{out}|$ is minimal, which for small or slowly varying $Im(\epsilon)$ simplifies to

$$Re(\epsilon(\omega)) = -2\epsilon_{out}$$

This is called the Fröhlich condition and the related mode the dipole surface plasmon of the particle. It emphasizes the importance of the dielectric environment to the resonance frequency. An increasing ϵ_{out} leads to a redshift of the resonance, a fact that can be exploited for optical sensing of small changes in the particle environment [82].

To measure the interaction of the particle with light one can use the absorption and scattering cross-section. The cross-section can be calculated from the absorbed/scattered light energy divided by the

incident optical flux. Using the polarizability they can be expressed as

$$\delta_{abs} = \frac{4\pi k}{\epsilon_{out}} Im(\alpha) = 4\pi k a^3 Im\left[\frac{(\epsilon_{in} - \epsilon_{out})}{\epsilon_{in} + 2\epsilon_{out}}\right]$$

$$\delta_{scat} = \frac{8\pi\omega^4}{3c^4}|\alpha|^2 = \frac{8}{3}\pi k^4 a^6 \left|\frac{(\epsilon_{in} - \epsilon_{out})}{\epsilon_{in} + 2\epsilon_{out}}\right|^2$$

This equations show the size dependecies of scattering and absorption. The absorption cross-section scales with $a^3 = V$, while the scattering cross-section scales with $a^6 = V^2$. For small particles the absorption is much stronger than scattering but with increasing size scattering becomes more and more dominant. That is why a solution of 10 nm particles appears red from all angles while a solution with 100 nm particles appears orange with light from the front and purple with light from behind. Figure 2.3 shows a sample of 100 nm particles (absorption resonance at ≈580 nm) with light from front (left) and back (right).

Beyond the quasistatic approach

Particles with radius $a > l_S$ cannot be considered with the quasistatic approach as retardation effects have to be taken into account. Expansion of the first TM mode of Mie theory for the polarizability of a sphere gives the expression:

$$\alpha_{sphere} = \frac{1 - \frac{1}{10}(\epsilon + \epsilon_m)x^2 + O(x^4)}{\left(\frac{1}{3} + \frac{\epsilon_m}{\epsilon - \epsilon_m}\right) - \frac{1}{30}(\epsilon + 10\epsilon_m)x^2 - i\frac{4\pi^2\epsilon_m^{3/2}V}{3\lambda_0^3} + O(x^4)} V$$

with volume V and $x = \frac{\pi a}{\lambda_0}$. A number of additional terms appear showing the physical differences for bigger particles [83]. The quadratic term in the numerator accounts for retardation effects leading to a shift of the plasmon resonance with increasing volume. The quadratic term in the denominator also leads to a resonance shift due to retardation of the depolarization field inside the particle. The overall shift for gold particles with increasing size is towards higher wavelengths (red shift). With a larger particle volume, the distance between the charges increases, lowering the restoring force and thus decreasing the resonance frequency. The third term in the denominator is completely imaginary and accounts for radiation damping. It is caused by the decay of electron oscillations into photons and is the main contribution for weaker dipole resonances as particle size increases. The

quadratic term in the denominator also accounts for intrinsic losses due to interband transitions. This effect becomes dominant for very small particles ($a < 5$ nm). One strategy to overcome the high losses in big particles is to utilize the Fano effect, where losses are suppressed by destructive interference at certain wavelengths. The Fano effect will be explained in Section 8.2.

Interacting particles

To this point, only single particles have been considered. When two particles are in close proximity and their plasmon resonance overlap spectrally, the resonances can couple to each other, which leads to new modes and can enhance the electric field even further. The coupling can happen in the far-field and the near-field. Far-field coupling involves distances longer than the optical wavelengths and occurs through scattered fields. In this thesis, I only deal with near-field coupling. At particle separation comparable to the evanescent field on the particle surface, Coulomb interaction of the surface charges can be observed. With this, large, strong charge dipoles can be created along the two particles, so the local fields in the gap can be enhanced greatly compared to the sum of the local fields of individual particles. The smaller the gap, the stronger the coupling. The location of high electric fields in the gap is often referred to as "hot spot". It provides strong coupling of the electric field to any molecule placed in the gap.

The simples model for coupling between plasmons treats each particle as a simple dipole. Using the plasmon-hybridization model [81] for two spherical particles, two solutions for the coupling modes can be found

$$\omega_{\pm} = \omega_1^2 \pm \frac{|U_{1m,1m}|}{2}$$

with dipole frequency ω_1 and the interaction energy U. The indices of U come from the indices of the spherical harmonics Y_{lm}. If we only consider $l = 1$, four modes evolve. For hybridized longitudinal modes (m=0), the lower frequency solution corresponds to the two dipoles being in phase, while for the higher frequency solution they are out of phase (Figure 4.1). In phase coupling can be excited by incident light and is thus called bright or bonding mode. The antibonding or dark mode cannot be excited by light. For the coupling of two transverse modes, also a bonding and an antibonding mode exist.

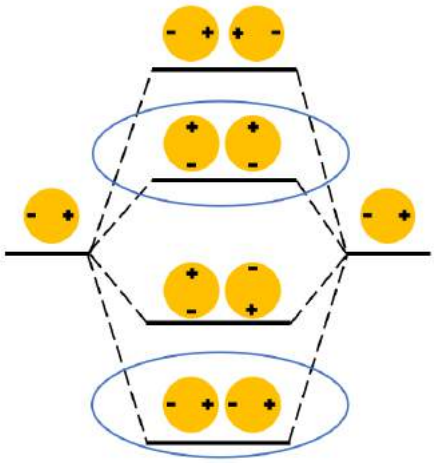

Figure 4.1: Hybridization model of two plasmonic particles in the quasi-static approximation. The circled states are the bright modes because they can be excited by an incident electric field. The other modes are dark modes, requiring special circumstances to be excited

For a symmetric pair of particles, bonding and antibonding modes do not couple. However, for two particles of different sizes, the two particle dipoles never cancel out, making all hybridization modes bright modes. Even for symmetric particles, dipole cancellation is never perfect. Dark modes can be excited by the Fano effect. The linewidths of dark modes are significantly narrower than the bright modes, which under certain conditions can give rise to Fano resonances by interference between dark and bright modes (see Section 8.2). Other ways to excite dark modes are incident fields that vary rapidly in space, like highly focused laser beams, the evanescent field produced by total internal reflection, radiation from local emitters or the field produced by a beam of high energy electrons.

4.3 PLASMONIC CIRCULAR DICHROISM

Geometries that cannot be superimposed with their mirror image are called chiral. Chirality is an important part of life. Molecules and their mirror image are called enantiomers. Interestingly, many important biomolecules only exist in one handedness, e. g. all amino acids are left-handed, hinting to some evolutionary selection for chirality [84]. Chiral differences in geometry influence the optical properties. Chiral molecules can rotate the oscillation plane. Those molecules are called optical active.

Chiral differences in the structure of molecules influences not only their biological but also their optical properties. Samples of chiral molecules can rotate the oscillation plane of linear polarized light. Electromagnetic waves consist of an electric and a magnetic field which oscillate in planes orthogonal to each other. If the oscillating plane rests, it is called linear polarized light; if the planes rotate, it is called circularly polarized light. Different absorption of left and right-handed polarized light is called circular dichroism (CD). The interaction between light and chiral molecules can be described by the optical rotational strength. It measures how much incoming linear polarized light is rotated by the molecules. The formulation of the rotational strength R was derived by Rosenfeld in 1928 [85].

$$R = -Im(\mu^{if} \cdot m^{if})$$

where μ^{if} and m^{if} are the electrical and magnetic transition dipole moments from initial to final state. The Rosenfeld formula gives two pieces of information:

1. Because the charge density and with that the transition moment depend on the molecular structure, the rotational strength depends directly on the geometrical structure.

2. Because of the scalar product, the rotational strength not only has a value but also has a sign. So the value of R not only depends on the transition moments but also on the angle between them.

Those dependencies are, what gives CD spectroscopy its great sensitivity to small changes in molecular structures [86].

To measure a CD spectrum, the sample is illuminated with left and right-handed light at the same wavelength. The difference in absorption is the CD value. Measuring this for multiple wavelengths results in a spectrum specific to the sample. CD is measured as $\Delta A = (A_L - A_R)$ as the difference between the absorbed left (A_L) and right-handed (A_R) light. CD can also be measured in ellipticity θ as follows:

$$\theta = 32980 \cdot \Delta A = 32980 \cdot (A_L - A_R))$$

The constant prefactor $32980 = \frac{\ln 10}{4} \cdot \frac{180}{\pi}$ is derived by a series expansion of the rotational strength around $\Delta T = 0$. Sometimes instead of ellipticity, molar circular dichroism ϵ is used: $\epsilon = \frac{\Delta A}{concentration \cdot optical pathlengt}$.

For a non-zero CD signal of a high number of randomly oriented microscopic objects a high homogeneity is necessary. While biomolecules of the same species and chirality offer this homogeneity, artificial nanostructures need to be carefully designed and selected. Coulomb interaction of chiral assemblies of metallic nanoparticles leads to plasmonic circular dichroism. It has to be distinguished from the excitonic circular dichroism exhibited by e.g. chiral biomolecules.

The overall plasmonic CD signal of nanostructures includes [87]:

1. CD effects of chiral molecules at the surface of nanoparticles, a metal cluster with a chiral atomic structure or a chiral environment around a cluster
2. Coulomb interaction between a metal nanoparticle and a chiral molecule
3. Plasmon-plasmon interaction between non-chiral nanoparticles arranged in a chiral geometry

While 1) relies on the chiral atomic structure of molecules, 2) and 3) are based on the idea of building chiral optical active structures from chiral and non-chiral building blocks. It is hard to control or change the atomic structure of molecules, but chiral geometries can be achieved with various methods, e. g. lithography [88, 89] or DNA nanotechnology [77, 78].

4.4 DNA PLASMONICS

DNA plasmonics describes the area of research where plasmonic structures are constructed using all the tools from DNA nanotechnology [40, 90, 91]. The great advantage over lithography is the complete freedom for spatial arrangement in 3D. Plasmonic DNA structures are used to investigate various effects like plasmonic CD [77, 91], fluorescent enhancement [76, 92], and energy transfer [93].

Multiple particles arranged in a helical structure can show circular dichroism. Contrary to natural molecules that show a CD in the UV spectrum, artificial chiral arrangements can be tuned for a CD in the visible spectrum opening up opportunities for new optical materials [77]. Those CD signals have been theoretically predicted with an approach of interacting dipoles. A pattern of two lines of particles on a rectangular DNA sheet can be rolled up to form a helix, resulting in the same CD spectrum [94]. While helices are chiral due to their asymmetric pattern (configuration), another group of chiral objects can be

constructed by arranging asymmetric building blocks in a symmetric pattern (constitution) [91]. One example is a pyramid consisting of four non-identical particles [95]. The pyramid shows a CD spectrum and can even be used to detect DNA [96]. Another concept for chiral nanostructures is stacked nanorods. Two rods are already enough to give strong CD signal in the visible spectrum. Depending on the position of the rods, left- and righthanded CD can be created [97]. Even stronger signals can be achieved by chiral stacks of multiple nanorods connected by DNA sheets [98]. Active plasmonic systems are shown by two rods with switchable position either with a rod walking on a sheet [99] or as gold modified DNA switch [78].

Assemblies of nanoparticles can be used to place target molecules in hot spots, thus significantly increasing fluorescent signals. A dimer of two 40 nm gold particles was used to enhance Raman signal of fluorescent dyes in the hotspot [76]. The fluorescent enhancement was also used to detect RNA of the ZIKA virus [92]. Finally, DNA has been used to create plasmonic waveguides by assembling a row of nanoparticles [93].

5

METHODS

5.1 TRANSMISSION ELECTRON MICROSCOPY

"Als Elektronenmikroskop bezeichnen wir eine elektronenoptische Anordnung, die zur Untersuchung emittierender oder bestrahlter Objekte durch vergrößerte Abbildung dieser Objekte dient, wobei mindestens die erste Stufe der Abbildung durch Elektronenstrahlen erfolgt." [100]
Ernst Ruska describes the electron microscope he invented as an electron-optical arrangement to investigate objects by enlarged imaging, where at least the first step in imaging is done by electron beams. To overcome the resolution limit of classical light microscopy [101], an electron beam with a much smaller wavelength than light is used.

The theoretical maximum distance d between two points under a light microscope is limited by the wavelength of the incident light λ, refractive index n and the numerical aperture of the system NA (Rayleigh-criterion)[102].

$$d = \frac{0.61\lambda}{n \sin \alpha} = \frac{0.61\lambda}{NA}$$

Using the wave characteristics of electrons, a beam of electrons can behave like light. With the de Broglie equation, the wavelength of electrons can be calculated. Additional relativistic corrections have to be added, as electrons approach the speed of light in an electron microscope.

$$\lambda_e = \frac{hc}{\sqrt{2E_0E + E^2)}} \approx 3.7 \cdot U_b^{-0.6}$$

With acceleration voltage $U_b^{-0.6}$. Electron microscopes with voltages of 100-300keV give a resolution of 0,2-0,3 nm. With higher voltages, resolution down to atomic scale is possible. Electrons interact the stronger with the atoms of the sample, the higher the atomic number. Biological samples are therefore stained with heavy metal atoms for better contrast. Typical stains are solutions with heavy metal salts derived from uranium, molybdenum or tungsten. The salt attaches to the biomolecules, so the outline and cavities become visible. This negative staining can give a resolution down to 1.5 nm.

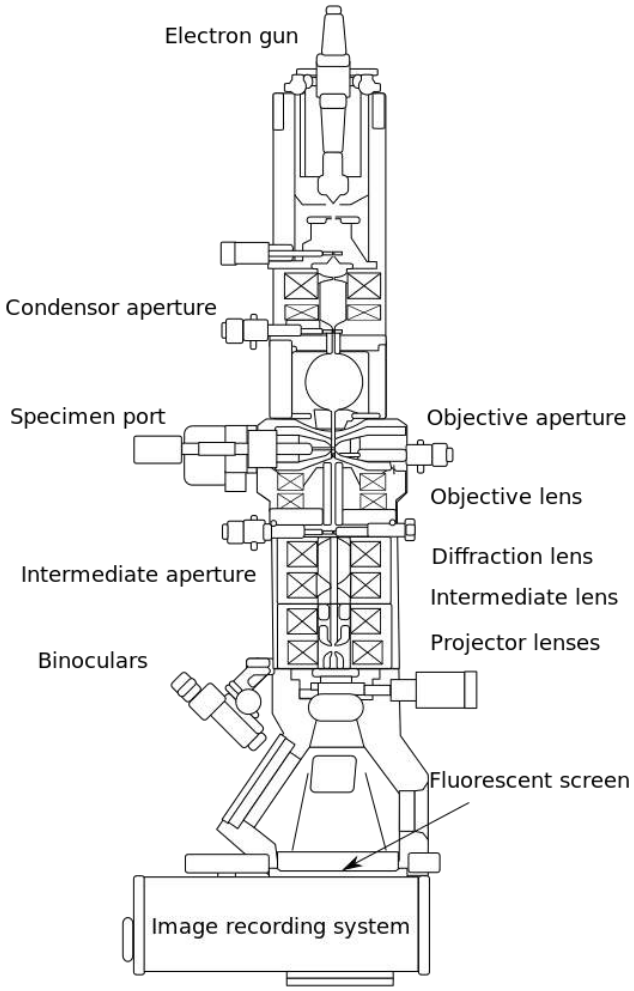

Figure 5.1: Layout of optical components in a basic TEM. Republished from [15] under Creative Commons License

5.2 NANOPARTICLE DNA FUNCTIONALISATION

In 1996, thiol-modified short ssDNA was used to functionalize gold nanoparticles by Mirkin *et al.* [103] and Alivisatos *et al.* [104] who published in the same issue of NATURE. While Alivisatos and colleagues focused on binding a single strand to each nanoparticle, Mirkin *et al.* covered the particles with multiple strands.

As DNA structures need high salt concentrations to be stable, particles need to be protected from the ions to prevent clustering. Complete coverage of the particles with DNA is the better choice. Methods to cover nanoparticles with as much ssDNA as possible have been improved a lot since then [75, 105]. High loading protects the ssDNA against degradation by nucleases and stabilizes the particles against salt-induced clustering. With the high amount of $MgCl_2$ needed for

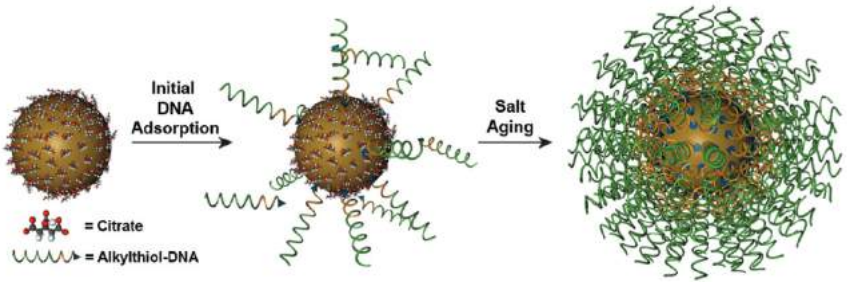

Figure 5.2: DNA coverage of a gold nanoparticle by salt aging: Slow increasing the salt concentration to counteract the negative charge of the DNA leads to a higher packing of DNA on the nanoparticles. Reprinted with permission from [105] . Copyright (2012) American Chemical Society.

DNA origami solutions, a very high DNA loading is needed. Especially as bigger particles (100 nm) are more sensitive to the effects of positive ions. To maximize the loading, the salt concentration in the solution was slowly increased to counteract the repulsion of the negatively charged DNA (Figure 5.2). Additional sonication also improves the loading density [75]. From the originally proposed 40 hours incubation, over "fast salt aging" with 10 hours [106], I finally used a "super fast salt aging" for all particles used in this thesis. Over 1 hour the NaCl concentration in the sample is raised from 0 to 600 mM. The detailed steps can be found in Table 5.1. After each step from 100 to 600 mM NaCl, the sample was sonicated for 30 seconds to prevent particle clusters and improve loading density. Surfactants like SDS can be used to stabilize particles during the process even more. For spherical particles, the stability decreases with size. On a curved surface, each adsorbed molecule occupies a conical volume. The higher the curvature (the smaller the particles), the bigger this conical volume gets. So for smaller particles, lateral electrostatic interaction by between the DNA strands becomes less, thus enabling denser loading. Additionally, a higher curvature may result in a higher number of adsorbed molecules per metal surface atom, up to roughly one thiol per two gold surface atoms on 2 nm particles [107].

While most available protocols for DNA functionalization are variations of the salt aging method, two other methods should be mentioned: the low pH and the freezing method. I tested both, but they seemed not very reliable for large particles. The low pH methods, as the name implies, uses low pH to counteract the negative charges of the DNA. After mixing the particles with thiolated DNA, the solution is brought to a pH of 3-4 for a few minutes. After neutralizing, small

STEP	ADD EVERY 5 MIN	FINAL CONCENTRATION
1	1 mL AuNR/AuNP	1 OD
2	50 μl reduced thiol-DNA (100 μM)	~4,7 μM
3	1,7 μl 20% SDS	0,03 %
4	100 μl 10xTAE+0,03% SDS	~1x TAE
	1 M NaCl+1xTAE+0,03% SDS [μl]	final concentration in mM
5	14,68	12,5
6	14,86	25
7	30,5	50
8	31,2	75
9	32	100
10	67,6	150
11	71	200
12	158	300
	5 M NaCl [μl]	final concentration in mM
13	32,2	400
14	32,8	500
15	33,5	600

Table 5.1: Protocol for functionalizing gold nanoparticles with DNA used in this thesis. NaCl concentration is slowly increased to 600 mM

particles (5-10 nm) are stable enough for usual origami applications [108]. For larger particles, the loading was not enough to stabilize them in high salt concentrations. The freezing method uses the exclusion effect in the freezing process to press the particles and the DNA together to overcome the repulsion of DNA by pure force [109].

5.3 DARK FIELD MICROSCOPY

The first description of dark field microscopy was done by Joseph Bancroft Reade in 1837 [110]. He discovered that by placing a candle at certain angles next to the microscope, he could achieve brilliant colors in his samples without the candle flame in the field of view, thus removing the bright background. To this day the basic principle has not changed. Illuminating a sample with light at a certain angle and construct a microscope in a way that only scattered light enters the objective makes it possible to see otherwise undetectable features and properties of samples. Figure 5.3 shows the basic principle of a

microscope objective specifically designed for dark-field microscopy. The illuminating light (1) is reflected in the outer ring of the objective (3) by a mirror (2). The sample is hit by the light at an angle ensuring that only light scattered at the sample enters the objective. [108]

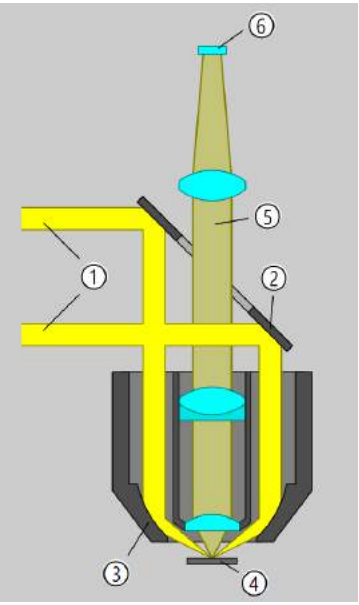

Figure 5.3: Basic principle of a microscope objective specifically designed for dark-field microscopy. The illuminating light (1) is reflected in the outer ring of the objective (3) by a mirror (2). The sample is hit by the light at an angle ensuring that only light scattered at the sample enters the objective. [15]

One advantage of the dark-field microscope is a possible high contrast without prestaining of the sample. Another advantage is that also objects below the limit of resolution create signals if the background is dark enough and illumination is bright enough. An application is the characterization of single or clustered nanoparticles. Strong scattering of light on plasmonic particles leads to bright spots that can be observed, so this method is limited to big particles (>50 nm) or clusters and assemblies. The first person to use dark field microscopy to investigate the properties of gold nanoparticles was Richard Zsigmondy, who got the noble prize in chemistry in 1925 [111] for his work with colloidal gold. On an appropriately diluted sample, one can identify individual particles as distinct colored spots with dimensions determined by the diffraction limit. The color depends on the plasmon resonance and thus on size and shape of each particle. To record the spectrum of an individual particle the scattered light can be spectrally resolved by a grating and recorded with a spectrograph including a charge coupled device (CCD) camera. The same

CCD camera can be used to take a real picture of the particle by using the zero order reflection of the grating. A particle is singled out by using an entrance on the spectrograph, isolating the signal of a single particle.

Although dark-field microscopy ensures a minimal background, the final signal still has to be corrected for weak scattering from the substrate and fluctuations of lamp intensities over all wavelengths [112]. The real spectrum can be obtained by

$$I = \frac{I_S - I_{BG}}{I_{STD} - I_{DC}} \tag{5.1}$$

with

I_S	recorded spectrum of the particle
I_{BG}	the background spectrum
I_{STD}	spectrum of a white light standard
I_{DC}	detector dark counts when the lamp is switched off

For further investigation, polarized light can be used to excite only longitudinal or transversal modes. To correlate the recorded spectrum with the actual particle size and shape, electron microscopy can be used on the sample to take pictures of the actual particles. To this end, some reference has to be placed on the used substrate to triangulate the particle positions.

Part II

Tuning optical properties of advanced plasmonic DNA structures

6

RNA DETECTION

6.1 INTRODUCTION

This chapter is based on the research presented in [113]. Figures and text reused with permission by John Wiley and Sons.

RNA plays many different roles in biology by serving as an information carrier for protein expression and a catalytic agent in gene regulation. It is also involved in amino acid transportation and forms the fast mutating genome in many viruses, including the Zika virus, the human immunodeficiency virus (HIV) and hepatitis C virus (HCV). Thus being able to detect low (picomolar) amounts of specific RNA sequences in a diagnostic process can greatly aid in the identification of certain diseases or virus infections. Current state-of-the-art detection methods for short RNA sequences such as quantitative Real-Time PCR (qRT-PCR) or DNA microarrays [114] are often time-consuming, require pre-amplification of the target and / or rely on specialized equipment. Therefore, the development of a single-step, robust system capable of detecting low concentrations of short RNA sequences without the need for pre-amplification and with an easy readout method, which does not require advanced, specialized laboratory equipment, is highly sought after. Ongoing advances in DNA nanotechnology and related fields have led to the development of molecular sensors for detection and analysis of biological samples at minute concentrations [115–121]. While DNA self-assembly in general and DNA origami, in particular, enables us to build structures with precisely defined geometries and multiple functionalities, e.g. molecular switches, enzymatic cascades or advanced drug delivery vehicles [34–36, 39, 122–127], nanoplasmonic offers control over the optical properties of nanostructures by carefully choosing their geometry and material composition [77, 95, 128–134] . Nanoplasmonic systems have shown the potential to produce strong or amplify weak optical signals [128, 129, 134, 135]. Plasmonic nanoparticles with dimensions significantly smaller than the wavelength of light are able to concentrate incident radiation into highly localized electric fields when excited at their resonant wavelength. The close proximity of neigh-

boring nanoparticles leads to plasmon-plasmon interactions possibly leading to strong electromagnetic fields that are generated in the gaps between the particles [133]. By arranging plasmonic nanoparticles in chiral geometries, e.g. particle helices [136, 137] or twisted stacks of nanorods [98], one can also trigger a plasmonic-chiral response, where the nanostructures absorb light differently depending on the sense of the circular polarization (left- or right-handed) resulting in strong circular dichroism (CD) signals [40, 77, 98, 121, 136, 138–141]. Typically, chiral biological molecules absorb light in the UV region, making the detection of their CD signal challenging. In the case of plasmonic chirality the signals appear in the visible spectrum and can potentially be detected without the need of elaborated equipment owing to the strong absorption properties of the plasmonic particles and the optical rotatory dispersion effect that is linked to the CD signal via the Kramers-Kronig relation and that can be visualized with two linear polarizers. Importantly, DNA structures can be designed to switch their conformation upon recognition of a defined nucleic acid sequence [21, 39, 71, 78, 142, 143], pH [144–149] or light [33, 150–152]. Combining these approaches allows for the construction of molecular machines with switchable optical properties [78, 143, 144, 150], which can thus be used as sensors for the triggering sequence with an optical read-out. Plasmonic switches often employ molecular recognition to trigger a controlled change of distance between plasmonic particles or less-defined aggregation into clusters both resulting in measurable changes of the scattered/absorbed spectra of the particle dimers or particle groups [96, 153–156]. Other plasmonic detection systems rely on a fluorescence-based read-out by exploiting the electrical field of plasmonic particles to enhance fluorescence signals [92, 117]. In this work, we focused on the detection of a specific RNA target with a chiral plasmonic switch. As a first proof-of-principle, we chose a 22 base RNA sequence present in the 5'-end region of a Hepatitis C virus (HCV) genome [157]. As biological samples do not exhibit CD in the visible spectrum, any change in absorption of polarized light occurs due to switched nanosensors enabling both high specificity and sensitivity.

6.2 DESIGN AND MECHANISM

Using the DNA Origami technique, we constructed a 3D gold-DNA-hybrid structure (Figure 1a), consisting of two arms connected by

two single-stranded DNA segments in the center, allowing for flexible turning of the two arms. To each of the two arms, a gold nanorod is attached to generate a plasmonic response. Depending on the reciprocal orientation of the arms, the structure displays left- or right-handed (LHD/RHD) chiral geometry, producing a left- or a right-handed circular dichroism signal [118, 158]. The resonance wavelength of the nanorods determines the spectral position of the CD signal and lies in our experiments at the red end of the visible spectrum and the near-infrared (NIR). The geometry of the structure can be switched from LHD to RHD by the addition of defined nucleic acid sequences and thus presents a perfect platform for the detection of specific DNA or RNA strands by means of CD spectroscopy. The sensing region consisting of two oligonucleotides is located at the end of each arm (Figure 1c). The two strands are complementary and can lock the structure in a right-handed state. Initially, one of the two locking strands is hybridized with a blocking strand, preventing the structure from locking. In the presence of the target sequence, the blocking strand is removed by strand displacement, leading to locking of the structure in a defined handedness (Figure 6.1c). To facilitate the binding of the target sequence, the blocking strand was designed with an unpaired eight bp toehold [21], allowing it to first capture and then fully hybridize with the target RNA sequence via strand migration. As a result, the gold nanorods display a defined chiral orientation leading to a strong CD signal.

6.3 SENSITIVITY MEASUREMENTS

In the absence of any target RNA, we observe a weak peak – dip CD signal at the plasmon resonance wavelength of the nanorods, indicating a slight preference of the unlocked structure for a left-handed state. In order to determine the sensitivity of our nanosensor, we exposed it to target RNA concentrations between 0 and 100 nM. A separate sample was prepared for each RNA concentration and its CD spectrum was recorded (Figure 6.2). Adding the target sequence should lead to a transition from a left to a right-handed signal. Indeed, while target RNA concentrations of 1 pM to 10 pM resulted in decreasing left-handed signals, concentrations of 100 pM or higher clearly induced switching of the structure to the right-handed state accompanied by the evolution of a pronounced dip – peak CD signal. Figure 6.3 shows the difference between the minimum and the

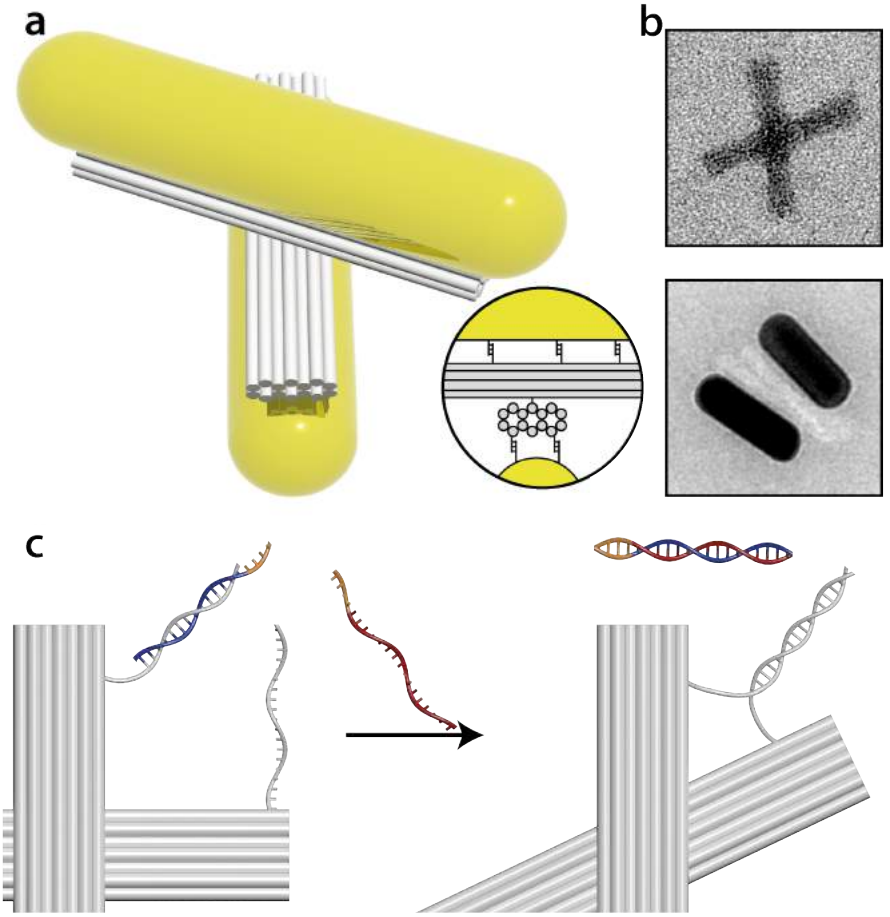

Figure 6.1: a) Schematic representation of the DNA Origami structure. Zoom in indicates the only connecting point of the two DNA origami bundles and the nanorods attachment handles. The gold nanorods are attached to the DNA structure by complementary ssDNA strands reaching out of the structure and hybridizing to the thiolated DNA strand on the nanorod surface. b) TEM images of the structure with and without gold nanorods. Scalebar: 20 nm. c) Recognition mechanism scheme: binding of the two complementary locking strands (grey) is inhibited by a blocking strand (blue). The blocking strand is removed via strand displacement by the target sequence (red). The reaction starts at the 8 bp toehold region (orange). After removing of the blocking strand, the structure locks in a right-handed configuration.

maximum of the CD signal for each trigger concentration. Negative values are used for a right-handed signal and positive values for a left-handed signal. Fitting with a model incorporating the Hill equation revealed dissociation constants kD of 337 pM (red), 478 pM (blue) and 480 pM (yellow) for different batches of the structure. In comparison: Lesnik *et al.* measured a ΔG of 18 kcal/mol for a 21 bp RNA/DNA hybrid duplex [159] which corresponds to a kD of 64 fM. Given that our mechanism involves two steps – first intermolecular

RNA-DNA-binding and then intra-structural DNA-DNA-binding, it was expected to have. Importantly, our detection limit of target RNA below 100 pM is comparable to some of the most sensitive methods such as microcantilever arrays [160]. The specificity of our device was tested by comparing the response to a random RNA sequence, which did not affect the system even at 1 nM (Figure 6.4).

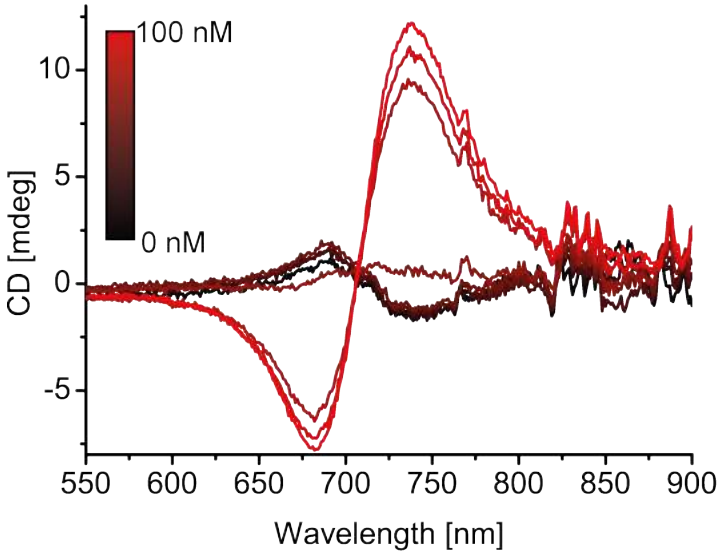

Figure 6.2: CD spectroscopy measurement at concentrations of target RNA from 0 to 100 nM. The concentration of the DNA switch was 10 pM

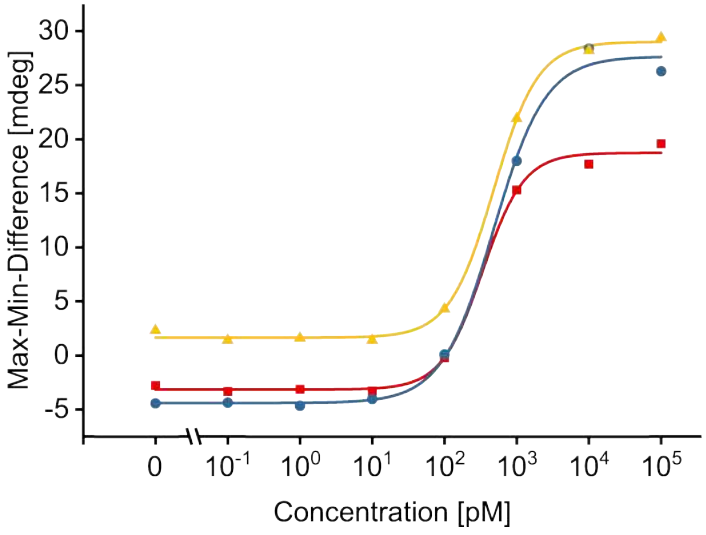

Figure 6.3:) The strength of the CD signal as a function of the target RNA concentration. The data shown was collected from three different batches of nanosensors. Each set was fitted with the Hill equation, which gave a Hill constant of 337 pM (red), 478 pM (blue) and 480 pM (yellow).

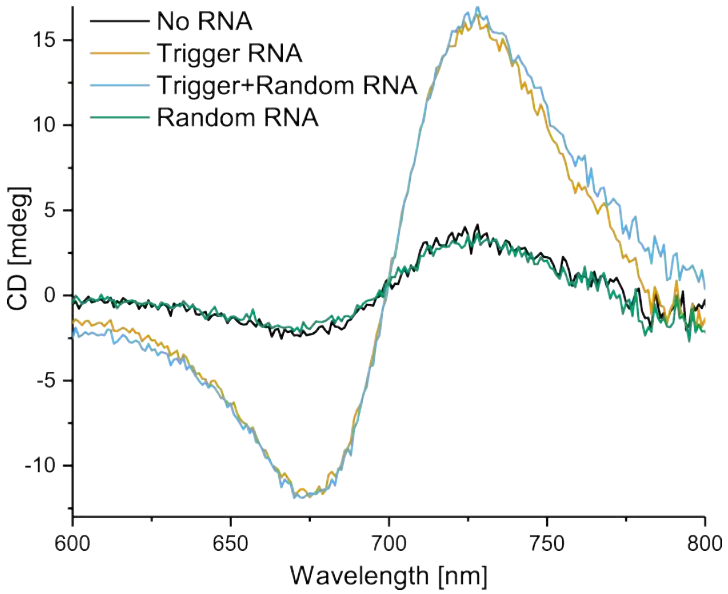

Figure 6.4: CD spectroscopy measurement to show the specificity of the mechanism. 10pM of structures (black) were mixed with the trigger RNA (yellow), a control RNA sequence (green) and both (blue). Only in presence of the correct trigger sequence, the structures switch their conformation.

6.4 DETECTION IN HUMAN SERUM

Having shown the successful detection of low concentrations of target RNA in buffer, we moved on to a more complex and clinically more relevant system. With a distinct signal in the visible spectrum, the nanosensor could potentially be used in a lab-on-a-chip system where blood samples could be tested directly. To investigate if our sensor potentially detects viral RNA directly extracted from blood samples, we performed measurements in human serum. For these experiments, the serum was deactivated by heat treatment and the addition of 0,03 % SDS + 11 mM $MgCl_2$. The origami-gold hybrid structures were then dispersed in the serum in a volume ratio of 1:9 (serum : sensor&buffer). Finally, the target RNA was added to a final concentration of 1 nM. After an incubation time of 30 minutes, CD signals were acquired. The corresponding spectra are shown in Figure 6.5a. In the absence of any target RNA, the CD signal reveals a left-handed geometry (black curve) as was already observed in buffer. This indicates that our nanosensor is stable in blood serum and does not interact with other biomolecules present in the solution. In the presence of the target RNA, the structure switches to the right-handed geometry as indicated by the altered CD signal (red curve), suggesting that

our nanosensor can be successfully applied to detect low amounts of target RNA in human blood serum. Recording CD spectra with only 10 pM of structures in the buffer experiments resulted in signals up to 20 mdeg in min-max-distance. Compared to the serum experiment with 50 times more structures we would expect a much higher signal than the signal shown in Figure 3. We hypothesize that this decrease in signal strength arises from two different factors: ongoing degradation of structures in serum and / or clustering of proteins around the structures. Gel analysis of DNA structures in serum showed that deactivation of the serum and addition of SDS decreased the clustering of the structures. Nevertheless, when investigating the stability of our structures by TEM imaging after exposure to serum, we were able to discern many Au NR pairs, suggesting that structure degradation was limited (Figure 6.5 b).

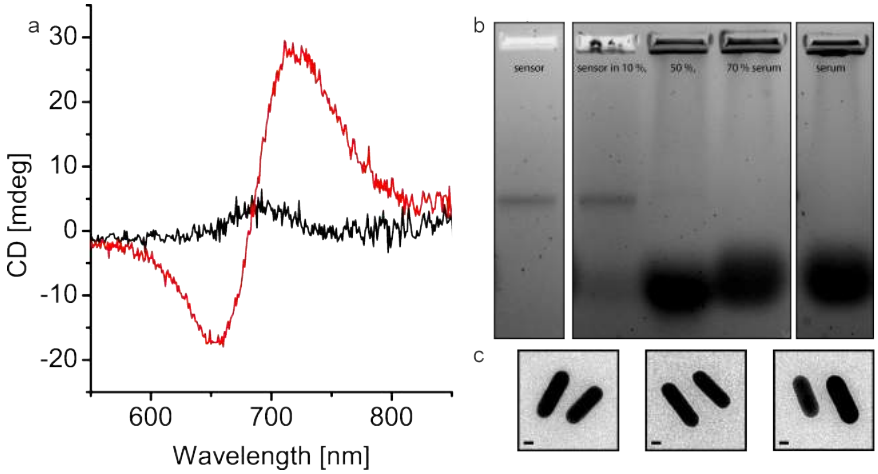

Figure 6.5: a) CD spectroscopy measurements in 10 % human serum of relaxed (black) and switched (red) structures. Switching of the chiral response of the structure was performed at 1 nM of the target RNA. The structure concentration was 500 pM. b) 2% agarose gel with sensor, sensor in 10 %, 50 % and 70 % serum and serum only. c) TEM images of the sensor after incubation in 10 % serum for 3 hours showing pairs of gold nanorods. This indicates the presence of intact sensor structures. Scalebar: 10 nm.

6.5 IMPROVING THE SIGNAL STRENGTH WITH SILVER

It has been shown, that covering gold nanoparticles with silver is a good way to improve CD signal strength [77]. To test this approach we used a commercial silver enhancement kit (NANOPROBES HQ SILVER). The kit is designed to signal from colloidal gold labels in biological samples. Silver salt and a reducing agent are mixed and added

to the sample. The gold nanoparticles function as a seed for the silver growth. The amount of silver grown on the particles is determined by the added amount. To determine the appropriate amount of silver salt for enhancing the gold nanorods in the RNA sensor, different amounts of the solution was added to 48 μl of 1 nM functionalized nanorods in 0,5xTBE+11 mM $MgCl_2$. Figure 6.6 shows pictures of the solution after adding 0.48/1.2/2.4/4.8 μl of enhancement solution and incubating for 1 hour. The solution showed a phase separation with one part changing color from green to slightly blue and an increasing fraction of red coloring with an increasing amount of silver solution. Figure 6.7 shows the absorption spectra of the blue and the red fraction of a sample and Figure 6.8 the respective TEM images. The red portion of the sample consists of almost spherical particles leading to a big blue-shift of the absorption spectrum with strong signal enhancement. The blue fraction shows a small blue-shift and a small signal enhancement with still keeping the rod-characteristics.

To show the effect of the silver enhancement on the signal of the RNA sensor, samples with different amounts of target RNA were measured before and after adding 1 vol% of the silver solution. Figure 6.9 shows the CD signal with 1, 10 and 100 pM of target RNA. After adding the silver solution, the spectra show the expected blue-shift (Figure 6.10). Furthermore, the signal strength doubled for each sample. Achieving higher signals would be essential to construct a real lab-free device, so silver enhancement could be a viable route to achieve this.

6.6 FUNCTIONAL SEQUENCES

All sequences used that differ from the design in [78].

Connecting strands

CTGATAAATTAATGAAAGGCTATCGTAAAACAGGAtt TCA TCC TCA CAC UCCGCCAUGA

GTG TGA GGA TGA TTT AAC CTA GCG AGC GAA CAT GC TT AGGGAACCGAACCACGAAATCCGCGACCTACAACG

Blocking strand

GGA GTG ATT CAT GGC GGA GTG TGA GG

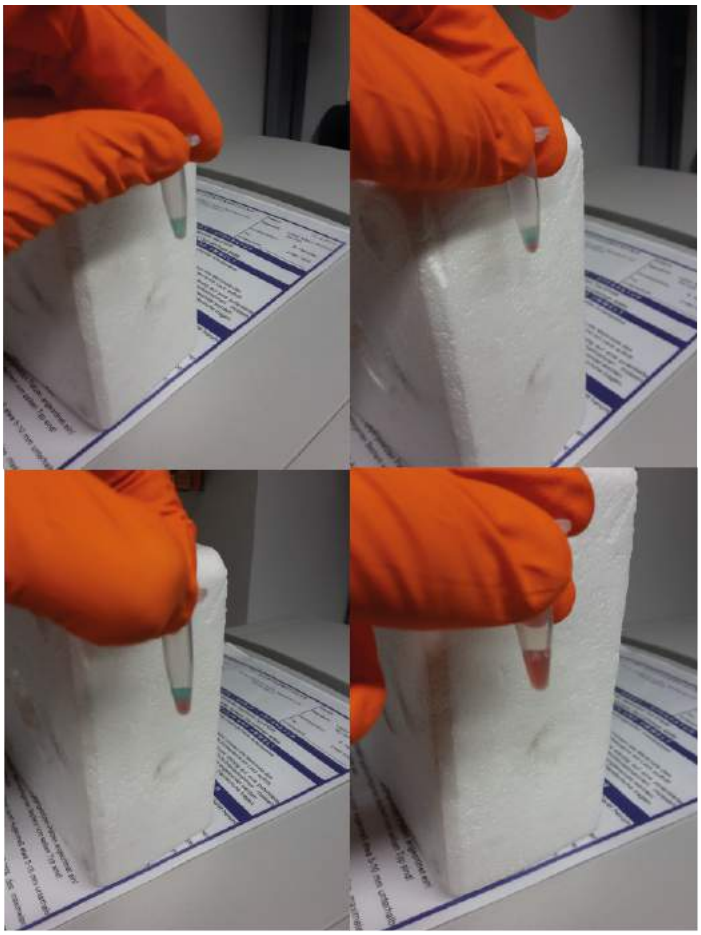

Figure 6.6: Pictures of 1 nM nanorod solution after adding 0,48/1,2/2,4/4,8 μl of enhancement solution and incubating for 1 hour. The solution showed a phase separation with one part changing color from green to slightly blue and an increasing fraction of red coloring with increasing amount of silver solution.

HCV target

ACA CUC CGC CAU GAA UCA CUC C

RNA control sequence

UACAACUAUCUAUCUCCUCUAUCAUA

The HCV sequence was chosen from [157] which reports on the RNA structure of the HCV genome. The chosen sequence is a free (no hairpin) part of the 5'end of the genome displayed in figure 4 in this publication.

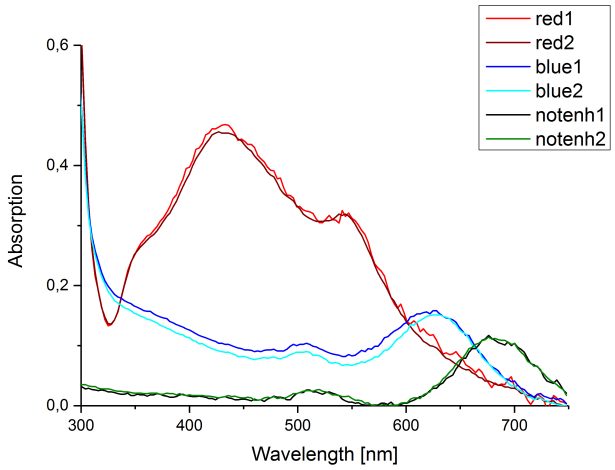

Figure 6.7: Absorption spectra of the blue and the red fraction of a sample. The red portion of the sample consists of almost spherical particles leading to a big blue-shift of the absorption spectrum with strong signal enhancement. The blue fraction shows a small blue-shift and a small signal enhancement

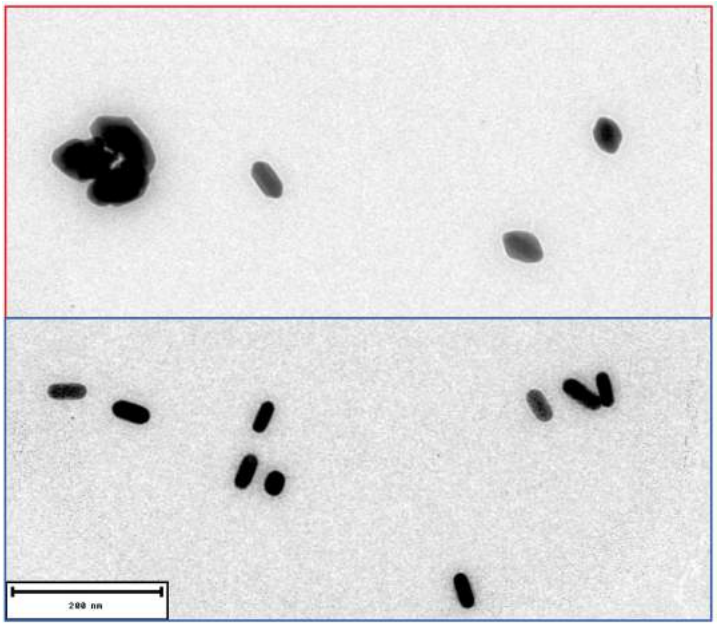

Figure 6.8: TEM images of the blue and the red fraction of a sample. The red fraction shows almost spherical particles while the blue part remains rod shaped

6.7 CONCLUSION

In summary, we showed successful detection of viral RNA at target concentrations below 100 pM in buffer. We furthermore demonstrated that our nanosensors are stable and functional in human serum to detect RNAs with concentrations below 1 nM. The principle could thus

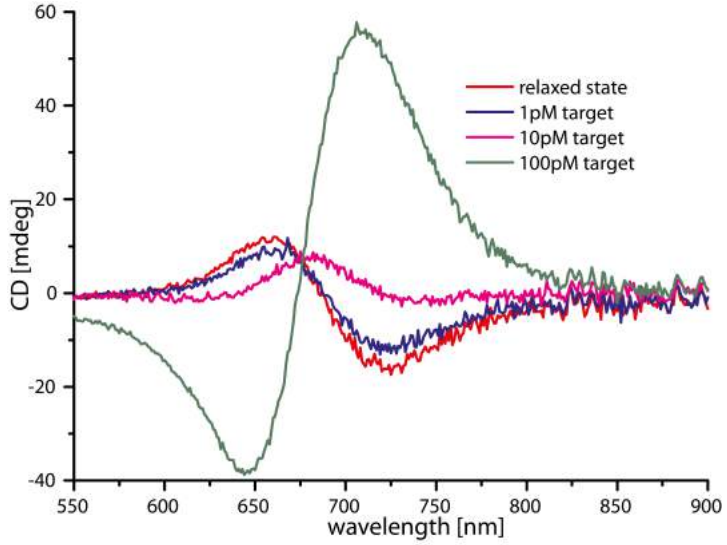

Figure 6.9: CD spectrum of the RNA sensor with different amounts of target RNA before silver enhancement

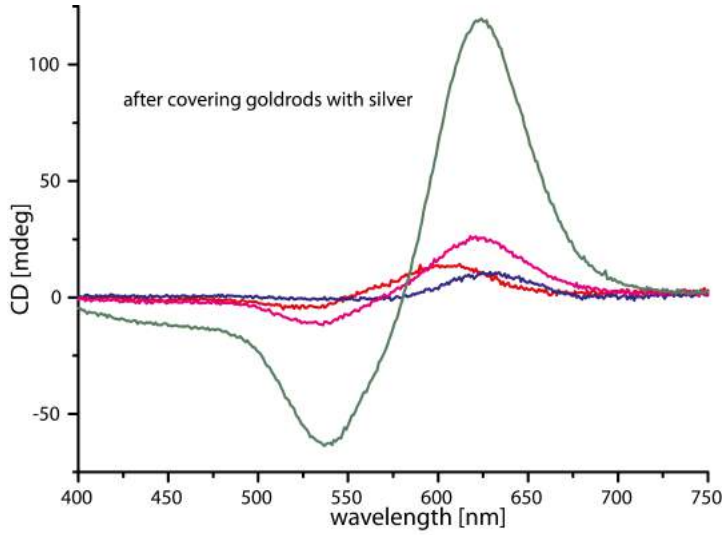

Figure 6.10: CD spectrum of the RNA sensor with different amounts of target RNA after silver enhancement

potentially be applied to selectively detect RNA sequences in clinically relevant environments. Infection levels of HCV can be measured with the "viral load". The viral load is usually described as the number of RNA genomes per ml (often displayed in a logarithmic scale). A typical viral load of an infected individual is 1.000.000-5.000.000 molecules/ml. Concentrations over 2.000.000 molecules/ml are considered high viral load [161]. A concentration of our target RNA of 100 pM corresponds to 60.000.000 molecules/ml, whichis still 10-50 times too high for detection. In order to improve clinical applicability

and to achieve even lower detection limits, plasmonic particles with stronger light-matter interactions, e.g. silver (covered) nanorods have shown to be a good choice. Although the stability of the DNA origami structures is reduced when exposed to human blood serum, protection strategies such as silica or block-copolymer embedding can further aid in achieving the desired stability and thus functionality [62, 162, 163]. All in all, our nanosensors demonstrate a promising route towards the sensitive detection of pathogenic RNA by means of a CD signal readout without the need for extensive sample preparation or target amplification.

6.8 MATERIALS AND METHODS

The DNA origami structures were assembled by mixing a 7560 bp scaffold with a 10-fold excess of synthetic staple oligonucleotides (Appendix) in 1x TE buffer with 14 mM MgCl2 and 500 mM NaCl followed by a thermal annealing process (Appendix).

The Nanorods were produced by a previously reported method [164]. Shortly, CTAB-capped gold seeds were grown in solution containing silver ions, CTAB, and ascorbic acid. The desired size and resonance wavelength was obtained by adding 5-bromosalicylic acid as an aromatic additive.

The nanorods were mixed with thiolated DNA (biomers.net, Germany), SDS and TAE buffer. The NaCl concentration was increased from 0 mM to 600 mM over one hour. After incubation overnight, the nanorods were purified by agarose gel electrophoresis. A detailed description of the protocol can be found in Section 5.2. The purified nanorods were mixed with the assembled structures in 10x excess, incubated overnight and gel purified.

CD measurements were performed with a Chirascan CD spectrometer from Applied Photophysics. Optical pathlength was 3 mm. Each sample was measured twice, averaging the signal at each wavelength over 0.01 s.

7

SWITCHING HELIX CHIRALITY

7.1 INTRODUCTION

Chirality is an essential feature of the 3D world we inhabit. Most of the molecules in living systems are chiral or chirally arranged [84]. Due to a chiral arrangement of electronic dipoles, left- and right-handed light is absorbed differently by these molecules. The spectrum of the difference in absorbance of left- and right-handed light, which is called circular dichroism (CD), has been used to analyze molecules for many years [102]. The CD of these natural molecules usually produces a weak signal in the ultraviolet (UV) region. To achieve CD signals in the visible spectrum, new artifical molecules and nano-assemblies are needed. Recently, assemblies with a strong CD in the visible region have been developed. By using chiral metal nanostructures, CD signals in the visible spectrum could be achieved. These structures do not depend on the chiral arrangement of electron dipoles but exploit the plasmonic interactions of nanosized metal particle dipoles [91, 92, 95, 98]. Because the particles are much smaller than the exciting wavelength, all electrons are excited simultaneously, which creates an enhanced electric field around the particle. The coupling of the fields of two particles creates even higher field enhancement localized between the particles, depending on the distance of the particles [87]. Four or more particles can be arranged chirally to create various plasmonic effects [77, 95]. Plasmonic nanostructures offer a high amount of control over the desired effects by tuning different parameters: e.g. number, size, shape, material, and distance of structures. However, precise control of orientation and position of particles is required for these structures. To address this requirement, two main approaches are used: lithography (top-down) and self-assembly (bottom-up). Regarding the bottom-up approach, DNA was established as a versatile material for nanofabrication [40, 91]. As a well-studied material, DNA offers many advantages for self-assembly. It is programmable, nontoxic, easy to manage and insensitive to contamination.

First chiral assemblies of gold nanoparticles with a CD signal in the visible spectrum were shown in 2009 [165, 166] with a tetrahedron geometry of particles of different sizes. Helical arrangement of gold nanoparticles using DNA Origami has been shown to be an ideal structure for observing plasmonic CD by Kuzyk *et al.* [77]. Consisting of 9 nanoparticles, this nanohelix shows a strong CD signal in the visible region which is consistent with theoretical calculations. DNA Origami was used as a scaffold for the gold nanoparticle helix because of the precise spatial control of particle placement this method offers. In theoretical studies about helically arranged nanoparticles, Fan *et al.* predict a complete inversion of the signals handedness, depending on the number of particles of a 4-pitch-helix [138, 167]. A right-handed helix with N=4 particles will produce a peak-dip signal. Adding the fifth particle would result in a signal change to a dip-peak CD signal even though the particles are still oriented in a right-handed geometry. Figure 7.1 shows the results of calculations of a helix with a 4-particle-pitch. The results of This can be explained by a coupling of the first and the fifth particle along the helical axis (z-direction) and thus changing the interaction chirality. For N=6 the signal shows the same characteristics as N=5, for N=7, the signal switches back to peak- dip. Adding more particles leads to the same signal as N=5 and N=6. The goal of this project was to investigate CD spectrum dependencies on the number of particles in a helix and to show first indications for an interaction of the particles in z-direction. To this end, we measured the CD of a helix with 10 nm particles and a pitch of 6 particles; and a helix with 20 nm particles and a pitch of 4 particles. To eliminate the influence of excitation, sample geometry, and concentration, the chirality often displayed by the chiral anisotropy factor or g-factor: $g = \Delta\epsilon/\epsilon = \Delta A/A$ [168, 169]. Normalizing the CD signal with the absorbance makes it easier to compare samples that differ in structure and concentration.

7.2 9 PARTICLE HELIX

First tests were performed with the helix from [77] with a pitch of 6 particles. According to theoretical predictions, the CD signal of a helix with 6 particles and another with 7 particles should be flipped. To this end, structures with a different number of particles were assembled separately. Each sample contained the same oligos for the core structure, but each with a different set of oligonucleotides for

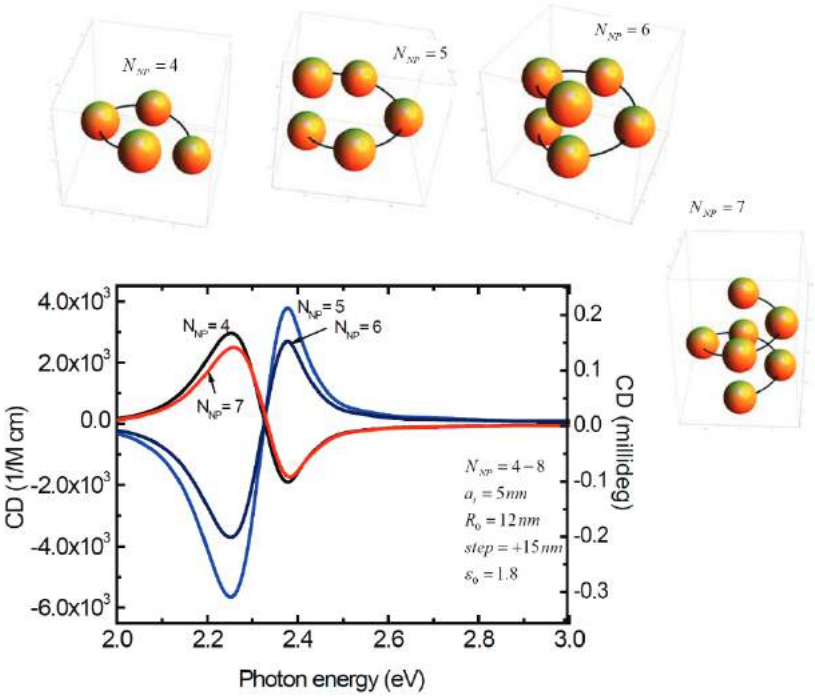

Figure 7.1: Theoretical CD signal for different number of particles on a helix with a 4 particle pitch. Reprinted with permission from [138]. Copyright (2010) American Chemical Society

gold attachment. For each desired particle position, the three handles were added. For the position without particle, oligos without overhang were used. The concentration of each sample was measured by UV-vis spectroscopy and each sample diluted to a concentration of 300 pM. A silver shell was grown on the particles in each sample to enhance their plasmonic properties. The quality of the structures was examined by TEM (Figure 7.2). The recorded CD spectra can be seen in Figure 7.3. The amplitude of the CD signal increased almost linear from sample III to V. From sample V to VI we see a small change. From sample VI to VII the signal decreases by about 40%. Then the spectra were compared by looking at the g-factor of the spectra. To visualize changes in the CD strength, the difference of the minimal and maximal value of the g-factor was calculated. The value of the maxima and minima of the spectrum and their correlated g-factor increase with the number of particles from three to five particles. With the sixth and seventh particle, we see a decrease of the g-factor indicating that more interaction than next neighbor dipole interaction becomes important. This hints to an interaction of the particles in the z-direction of the helix.

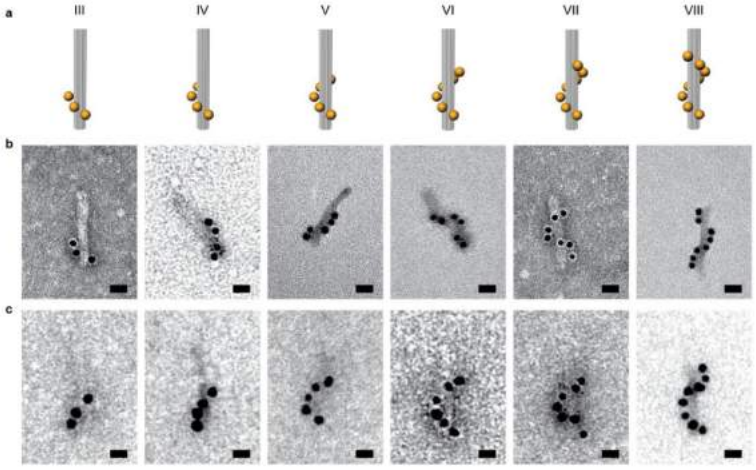

Figure 7.2: Nanohelices with different number of particles. a) Design b) TEM images of assembled structures c) TEM images of assembled structure after silver enhancement. Scalebar is 20 nm.

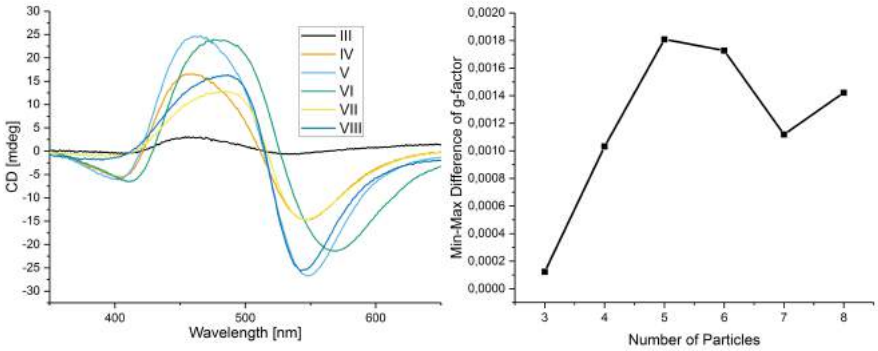

Figure 7.3: Left: CD spectra of samples with different number of particles of the 9 particle helix. Right: Amplitude of the g-factor of each sample

7.3 6 PARTICLE HELIX

To get a stronger interaction of plasmonic dipoles and possibly a stronger flip in the CD after reaching one turn, we designed a new helix of 6 particles of 20 nm with a pitch of 4 particles. Each sample was measured after growing a silver shell on the particles to enhance the plasmonic interaction. Figure 7.4 shows the difference of the minimal and maximal value of the g-factor. The structure shows no CD signal for 1 and 2 particles. However, a small signal can be observed for 3 particles. In theory, 3 particles are not able to form a chiral geometry. In reality, the particles are not entirely homogeneous in size and shape. Additionally, sometimes particle randomly attaches to the DNA structure, then forming a chiral structure. The interesting change happens after adding the 5th particle (starting the second turn). Again, the CD signal shows a significant dip, even stronger than the previously investigated helix with the 6-particle turn. The stronger interaction of the larger particles also leads to a stronger interaction in the z-direction. The predicted flip, however, could not be seen.

All samples were examined with the TEM. For the individual structures, the number of particles was counted. Figure 7.5 show the particle distribution of each sample. Each sample has a peak at the intended number of particles. However, the samples with 5 and 6 binding sites show a very high percentage of large clusters of structures and particles. The distribution of species can be used to explain the missing flip in the CD signal of the samples. Theory predicts helices with N=5 and N=6 to be to be different from all other helices. The dominant species of sample V is the 5-particle helix. Together with the N=6 helix they make up 45% of all structures. Since the CD spectrometer measures an average of all structures in the light path, a weak signal is expected instead of a flipped signal. To explain, why we do not see a flipped signal, further studies have to be made. One reason could be that the interaction in z-direction is significantly weaker or that the large particle clusters are mainly left-handed. The reality is probably a combination of both.

7.4 CONCLUSION

The strength of the CD signal of gold particle helix depends on the number of particles. We could show, that another non-trivial effect

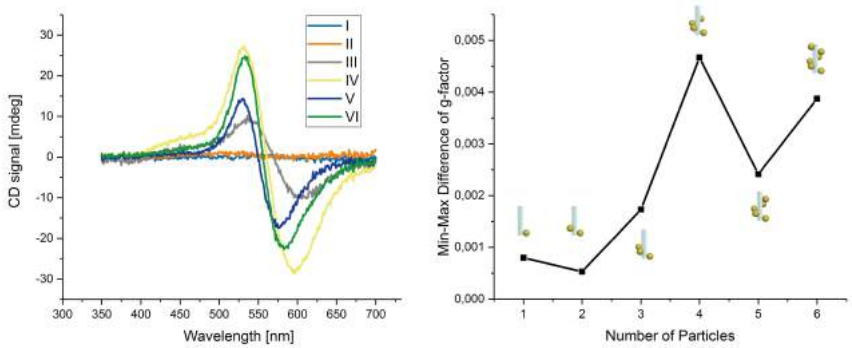

Figure 7.4: Left: CD spectra of samples with different number of particles. Right: Amplitude of the g-factor of each sample

has to be taken into account when dealing with small pitch helices. Chirality is a binary attribute: a molecule can either be chiral or non-chiral. We observe a change in the CD signal and g-factor for a different number of particles, which looks like a "weaker" chirality. With closely located particles, the CD signal becomes significantly weaker when particles additionally interact with each other in the z-direction, in our case when the 7th or 5th particles is added. Theory predicts a complete switch of chirality after one turn. This could not be shown, because the particles not only bind to the designed binding sites, but also bind randomly to each other and the DNA structure. To observe the switching of the CD spectrum, one could either increase the purity of the sample by increasing binding affinity of the particles and sample purity, or increase the interaction strength in z-direction by decreasing the helix pitch. Constructing helices with a very small pitch remains a challenge due to particle repulsion. However, this work indicates that more effects for plasmonic chirality than just next neighbor Coulomb interaction have to be considered.

7.5 MATERIALS AND METHODS

The DNA origami structures were assembled by mixing a 7560 bp scaffold with a 10-fold excess of synthetic staple oligonucleotides (Appendix) in 1x TE buffer with 14 mM MgCl2 followed by a thermal annealing process (Appendix).

The nanoparticles (BBI Solutions) were mixed with thiolated DNA (biomers.net, Germany), SDS and TAE buffer. The NaCl concentration was increased from 0 mM to 600 mM over one hour. After incubation overnight, the nanoparticles were purified by agarose gel electrophoresis. A detailed description of the protocol can be found

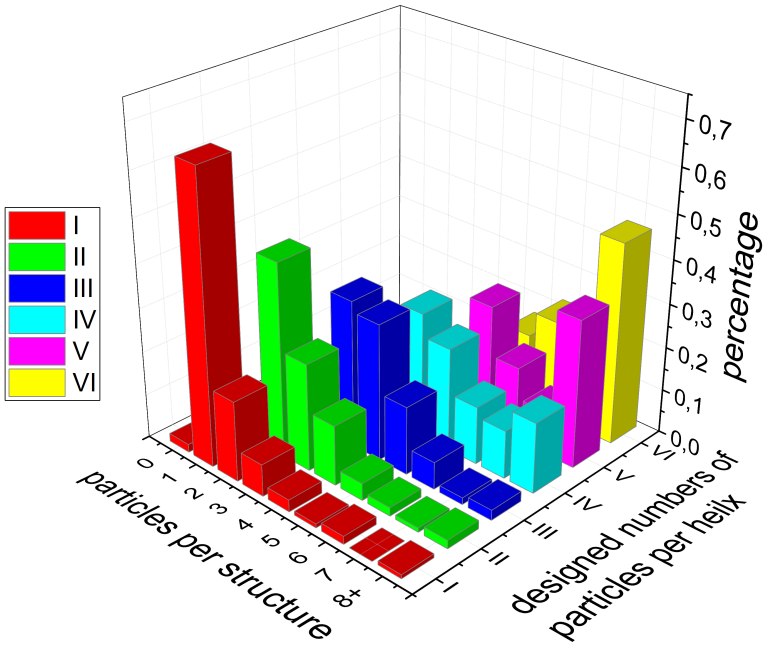

Figure 7.5: Actual number of particles per structure in each measured sample.

in Section 5.2. A silver shell was grown on the nanoparticles using a commercially available kit (Nanoprobes HQ silver) to enhance the CD signal. 3.5 µl of the silver solution was added to each sample and left to incubate without light for 30 minutes. The purified gold particles were mixed with the assembled structures in 5x excess per binding site, incubated overnight and gel purified.

CD measurements were performed with a Chirascan CD spectrometer from Applied Photophysics. Optical pathlength was 3 mm. The signal was averaging at each wavelength over 0.01 s.

8

TOWARDS GOLD NANOPARTICLE ASSEMBLY FOR PRODUCING FANO RESONANCES

8.1 INTRODUCTION

DNA nanotechnology has been used a lot in recent years to try many compositions of nanoparticle systems. Because of the geometrical freedom to arrange nanoparticles in any 3D shape, various shapes have been build and multiple effects have been investigated. One of the many properties of a nanoplasmonic system is heat generation. When exciting nanoparticles, highly localized heat can be generated. There are many current and potential applications for localized heat. In biological systems, heat from excited nanoparticles facilitates cell uptake [170] or can be used to specifically destroy tumor tissue [171, 172]. Other applications are catalysis [173], efficient light to heat conversion [174] and vaporization [175].

With their large absorption cross-section, nanoparticles can produce heat very efficiently. The strength and localization of the heat depend on the morphology of the particle. Heat generation is directly proportional to the square of the electric field in nanoparticles. Thus heat generation can be optimized by tailoring the size, shape, and arrangement of particles [176]. Due to inhomogeneous distribution of the electric field in the particle, heat generation is also inhomogeneous. However, because of the small size of the systems and the fast thermal diffusion, the temperature is uniform over the whole particle even if heat generation is not [177]. To give an example: A 20 nm particle with continuous light excitation at 530 nm with an irradiance of $I = 1mW/\mu m^2$ shows an overall temperature increase of $\approx$5°C. The time to establish a steady-state temperature is in the range of nanoseconds [176].

Arrangements of particles can be designed specifically to maximize the heat generation. Heating effects can be categorized into collective and local heating. Collective effects come from large and dense clusters of particles where the heat flux of individual particles adds up to a high overall temperature [178, 179]. This is useful for heating large areas as it is used in biological tissue. Local heating effects occur in

certain confined volumes in or around plasmonic structures [180]. Interestingly, a dimer with a hot spot is not a good choice for heating. The electric energy gets focused in the dielectric gap reducing the overall temperature increase compared to a single particle [177]. One approach for localized heating is the use of a third particle in the plasmonic hot spot. This was proposed for the first time in [178] in a linear assembly of three particles. A small particle in the center of a pair of large particles leads to a thermal hot spot with the large particles serving as antennas.

8.2 THE FANO EFFECT

To maximize the heat generation, one has to minimize other losses. A general strategy against radiative losses in larger particles is to utilize the Fano effect [80], described by Ugo Fano in 1935 [181]. The first description was about atomic spectra of Helium, where two quantum paths lead to the same final quantum state. Those two paths can interfere with each other leading to a specific asymmetric line shape of the peaks in the spectrum. In nanoplasmonics and metamaterials, there is an analogous phenomenon. Plasmonic nanoparticles have bright and dark modes. While bright modes are highly resonant and can be excited by an incident electric field, dark modes are not very prominent in optical spectra. The total response of a system of metal nanoparticles to excitation is caused by the superposition of fields produced by the individual resonances. The overall response can be very different from the responses of the individual resonances due to interference among those fields. If a broad bright resonance interferes with a narrow dark mode, the resulting spectral shape has the unique peak-dip shape known as Fano resonance.

The lineshape of a normal resonance arises as follows (Figure 8.1): The real component of normal resonance at ω_r is proportional to $\frac{\omega-\omega_r}{(\omega-\omega_r)^2+\gamma^2}$ with γ determining the resonance width. This leads to a dispersive response that changes sign at ω_r [81]. The imaginary part is proportional to $\frac{\gamma}{(\omega-\omega_r)^2+\gamma^2}$, describing an absorptive response with peak at ω_r. The resulting overall response is proportional to the intensity and follows the Lorentzian shape of the imaginary part (Figure 8.1a).

When a broad bright mode with field E_B and a narrow dark mode with the field E_N overlap spectrally, they can interfere, so that the overall intensity is proportional to $|E_B + E_N|^2$. In Figure 8.1 the four

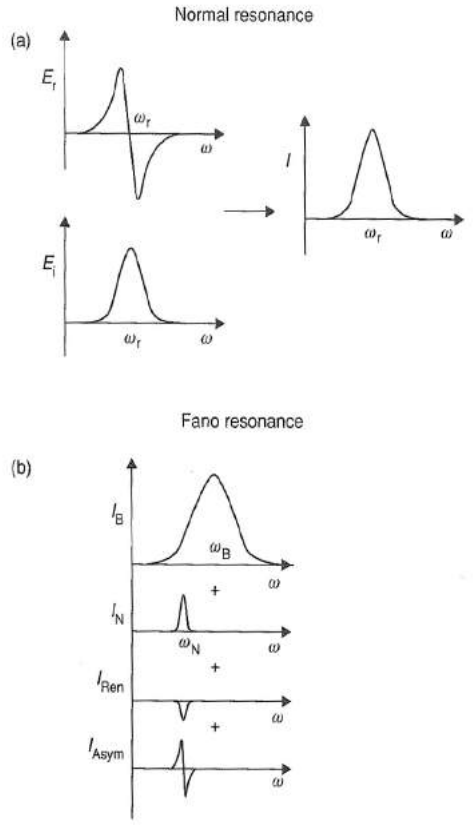

Figure 8.1: a) Real and imaginary components of a field near a resonance frequency and the corresponding response function. b) The four contributions to a Fano resonance. I_B is the resonance from the broad mode. Republished from [81], with permission by John Wiley and Sons

contributing components of the resulting intensity can be seen. I_B is the resonance from the broad mode. I_N is the resonance from the narrow mode. I_{Ren} is the result of interference of the two imaginary components of the resonances. It is a renormalized version of I_N, same lineshape but proportional to E_B. I_{Asym} is the interference of the real components with an asymmetric lineshape following E_N, so that it enhances responses on one side of ω_N and reduces it on the other side. The resulting response at ω_N of $I_N + I_{Ren} + I_{Asym}$ is called the Fano resonance. The overall shape of the Fano resonance depends on the ratio of I_{Ren} and I_{Asym}. When I_{Ren} is larger the Fano resonance has a dispersive shape; when I_{Asym} is larger, it has an asymmetric Lorentzian shape. In real metal nanostructures, however, coupling and interfering happen at the same time so that it is often difficult to clearly separate the effects of interference and hybridization. In single particles, Fano resonances can occur when the particles are big enough to give rise to higher order modes that can interfere.

Considering the fact that Fano resonance also involves destructive interference (Fano dip), the effect can be used to reduce radiative losses of a plasmonic system. At the Fano dip, electric fields in the hotspot are the strongest. Other possible applications for the Fano effect are plasmonic sensing due to stronger hot spots or nanolasers [80].

Artificial nanostructures can be specially designed to enhance Fano resonances [183]. First theoretical predictions of Fano resonances in the optical spectrum with experimental proof were shown in a dolmen-like structure [184] and a non-concentric ring-disk cavity [185]. Fano resonances can also occur in finite clusters of plasmonic particles. One example for such a geometry is a central nanodisc surrounded by a six-disc ring (Figure 8.2) [182, 186]. The spectrum of this structure is dominated by the effects of two of its modes. A bright mode where all disk oscillate in phase (1160 nm) and a dark mode with the inner disk out of phase with the outer disks (1490 nm). Interference between this two modes leads to a Fano resonance. By changing the size and arrangement of the disks, the Fano resonance can be tuned [187].

8.3 THE CONCEPT FOR A SUPERSTRUCTURE

Khorashad *et al.* proposed a superstructure of two large spherical particles with a small nanorod in the hotspot to create Fano resonances and thus increased heating [188]. Simulations showed an even higher heat generation compared to a spherical particle in the hot spot (Figure 8.3). Figure 8.4 illustrates the proposed structure and shows the idea to build the assembly using DNA origami. To create this superstructure using DNA origami and finding a way to measure Fano resonances and heating effects was the goal of this project.

8.4 DIRECT PARTICLE LINKING

To illustrate the strengths of DNA origami for 3D arrangments of nanoparticles, the first try of building the proposed structure will be explained here. It has already been shown, that nanoparticles can be connected into 3D geometries and clusters [95, 103]. Different particles get functionalized with complementary DNA sequences to facilitate their self-assembly in solution. The easiest way to assemble the Fano heater seemed to be this direct linking. To this end, 100 nm par-

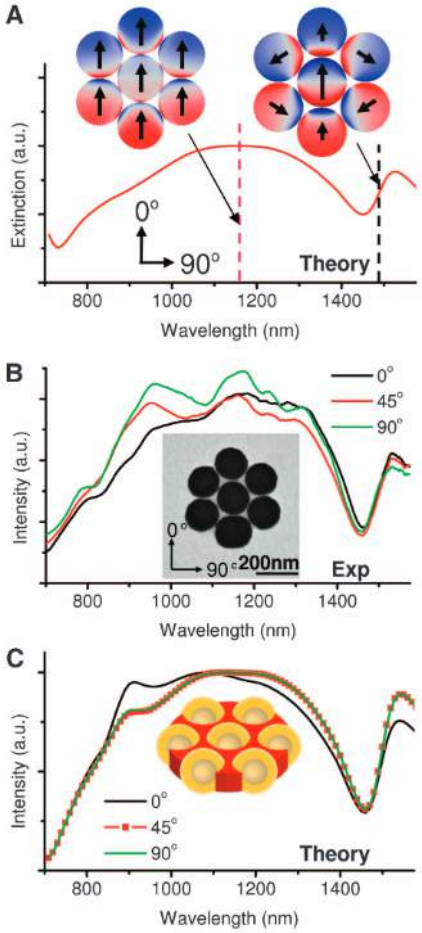

Figure 8.2: Fano-resonant behavior of a plasmonic heptamer. (A) Calculated extinction spectrum and charge density plots for a heptamer excited at normal incidence with a 0° orientation angle. The Fano minimum, characterized by suppression of the bright mode, is at 1450 nm. The charge density plot of the bright mode, whose peak resonance is denoted by the pink dashed line at 1160 nm, shows the charge oscillations on each disk oriented in the same direction, resulting in the constructive interference of their radiated fields. The charge density plot of the heptamer at 1490 nm, denoted by the black dashed line, shows the dark mode at its peak resonance. This mode supports charge oscillations on the nanoshells oriented in different directions, resulting in the destructive interference of their radiated fields. (B) TEM image and spectra of a heptamer at three different incident electric-field orientation angles. (C) Calculated scattering spectra for a heptamer with a geometry matching that in (A), for the three orientation angles in (B). Republished from[182], with permission by AAAS

ticles and small rods with a length of 25-30 nm were covered with thiol-modified complementary sequences. After incubating for one hour, the assemblies were purified with agarose gel electrophoresis. The band with the trimers was cut out and investigated under the

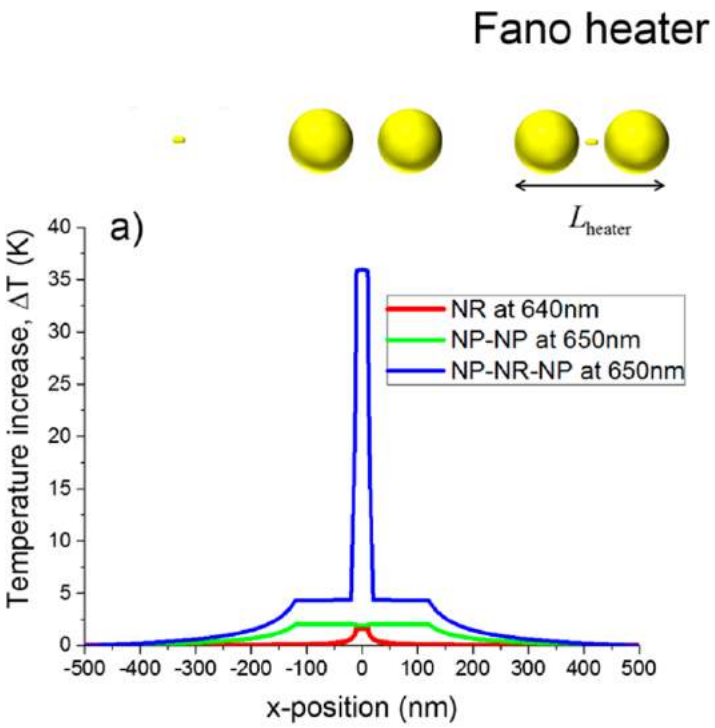

Figure 8.3: Theoretically calculated temperature increase in singe nanorod, particle dimer and trimer structure. The particle dimer with nanorod in the hotspot shows a lage temperature increase because of the Fano resonance. Reprinted with permission from [188]. Copyright (2016) American Chemical Society

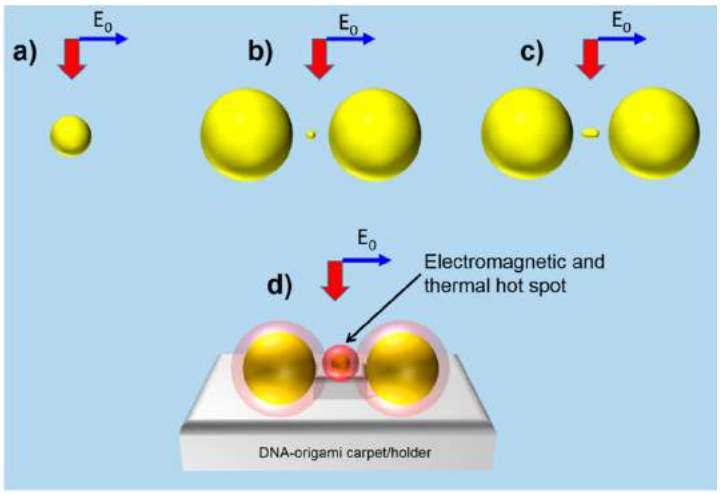

Figure 8.4: Three different heat generating plasmonic structures: A single particle, large particle dimer with a small particle in the hot spot and large particle dimer with nanorod in the hot spot. This project aims to design a structure to fix a nanorod in the hot spot. Reprinted with permission from [188]. Copyright (2016) American Chemical Society

TEM. All the structures show the two big spheres. In some, no rod is

visible, but in most structures, the rod is squeezed between the particles in an upright position or below the particles (Figure 8.5). No linear structure in the desired shape could be found. The result can be intuitively understood when you focus on the fact that the rod is covered completely with DNA. A vertically oriented rod offers more binding strands and thus is favored. A possible solution to this problem would be the regiospecific functionalization presented by Xu *et al.* [189]. With proper tuning of various parameters like oligo, salt and CTAB concentration and the fact that thiolated DNA prefers binding to the [111]-facets at the ends, different sequences can be attached to ends and sides of the nanorods. I tried this method, but after first tests, it was discarded because the nanorods still could connect both ends to both particles, thus not solving the problem.

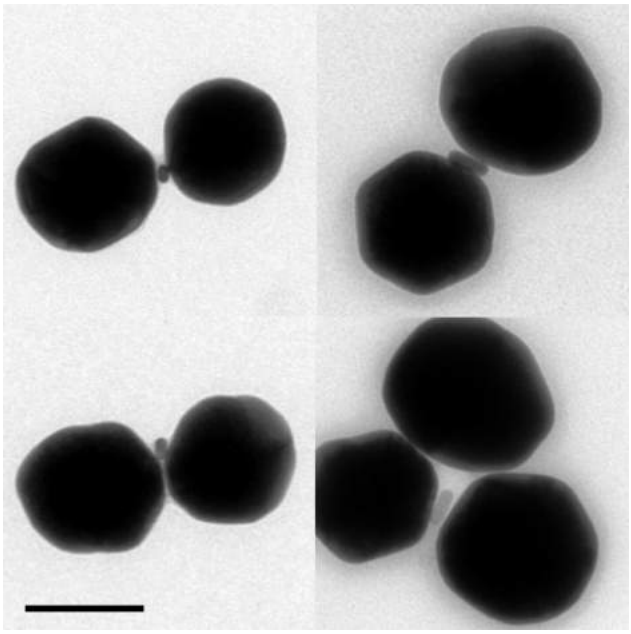

Figure 8.5: TEM images of assembled gold trimers with direct linking of the particles. The nanorod never stayed linear in the hot spot. Scalebar is 100 nm

8.5 FIRST ARRANGEMENT ON A DNA STRUCTURE

To arrange particles at exactly specific relative positions, DNA origami is the perfect tool. First tests for a DNA structure mediated arrangement was done with a 14 helix bundle (14HB), that was already used by Roller *et al.* [190]. Particles and rods were functionalized with different sequences that were complementary to DNA handles on the 14HB. The attachment of particles was done successfully with two

large particles and one rod on each structure and the correct distance between the particles. While the longitudinal orientation of the rods was achieved, the rod was not at all centered between the particles (Figure 8.6). To give a Fano response, the rod needs to be in the center of the hot spot. So we showed, that DNA origami can in principle be used to assemble the trimer, but we needed a more sophisticated structure, taking into account the huge size difference of the particles.

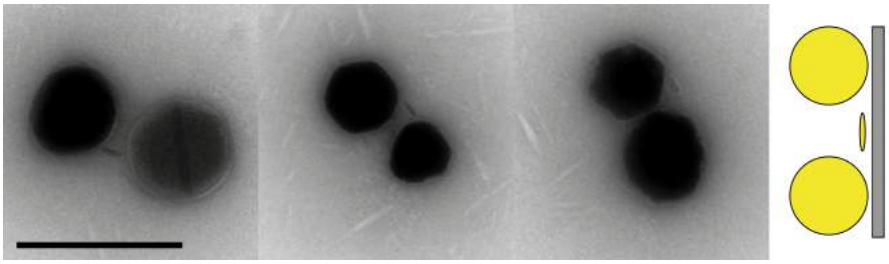

Figure 8.6: TEM images of DNA origami mediated assembly. The particles are attached to a 14 helix bundle. While the longitudinal orientation of the rods was achieved, the rod was not at all centered between the particles. Scalebar is 200 nm

8.6 HALFPIPE STRUCTURE

To center the nanorod exactly in the hot spot of the two large particles, a halfpipe shaped rigid structure was designed (Figure 8.7). It consists of 86 double helices with a length of $\approx$ 25 nm. The inner cavity is designed to fit a 15x25 nm rod that can be attached with complementary handles. The ends of all helices contain poly-A sticky ends for binding the poly-T strands attached to the spherical particles. This structure showed promising results. For the first time, particle trimers with a centered longitudinal arranged nanorod could be found. However, the yield was terrible with $\approx$ 1-2% correct trimers. The procedure to build the structure is as follows:

- First the DNA structures are assembled and gel purified.
- The gold particles were functionalized and gel purified.
- DNA structure and nanorods were mixed in a ratio of 1:5, incubated overnight and gel purified.
- Halfpipe-nanorods were mixed with the spherical particles, incubated overnight and gel purified.

Although the nanorods attach to the DNA structures very reliable, after incubating with the spheres, the rods did not stay in a linear position and some DNA structures seem to have lost the nanorod. Figure 8.8 shows the fully assembled structures with the nanorods in the correct position but in the wrong orientation. Figure 8.9 shows one of the few pictures of desired structures with correct orientation of the nanorod. This shows that in principle it is possible to build this structure. An explanation for the turning and detachment of the nanorods could be the mechanical force of the nanospheres pushing the rods out of the gap when deposited on the TEM grid or even in solution. To reduce pressure from the nanospheres to the nanorods, the next structure was designed to be less rigid and a little bit longer to give more space for the nanorod. Furthermore, to keep the nanorod in place, we wanted to find a way to trap it in the structure completely.

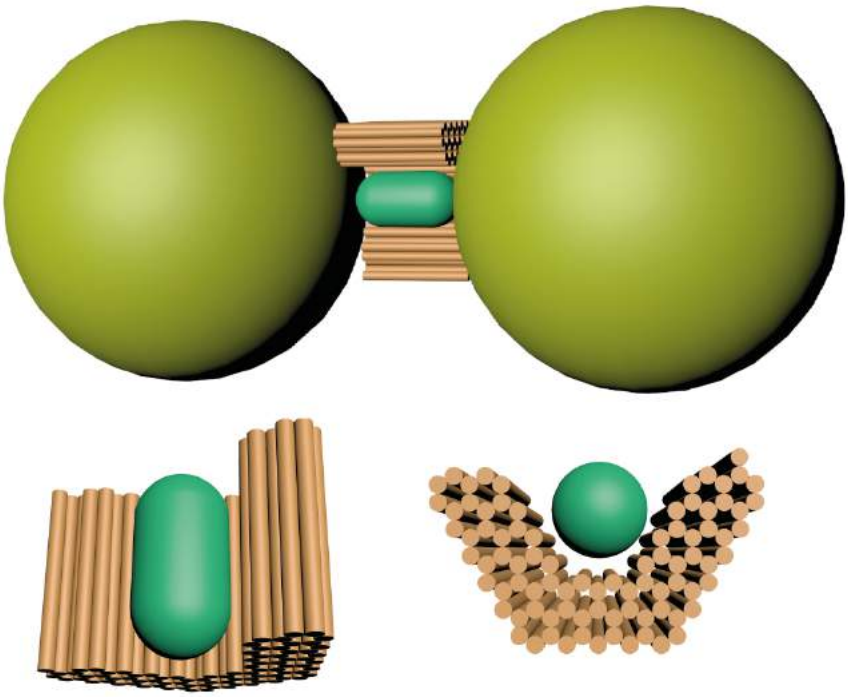

Figure 8.7: First approach for a DNA origami structure to carry the nanorod. It consists of 86 helices of 25 nm length in a halfpipe shape. The rod and the particles are connected to the structure by complementary DNA handles.

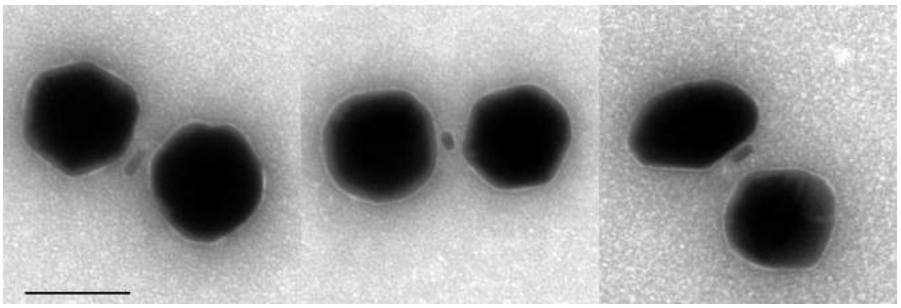

Figure 8.8: Typical TEM images of trimers connected by the halfpipe structure. The nanorods tend to be in the wrong orientation. Scalebar is 100 nm.

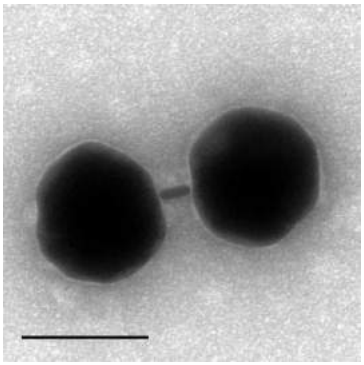

Figure 8.9: One of the few pictures of desired structures with correct orientation of the nanorod. Scalebar is 100 nm.

8.7 BARREL STRUCTURE

To create a loose structure that can trap a nanorod between two particles, I got inspired by the work of Shen *et al.* [191]. My design (Figure 8.10) consists of a 30 nm long tube-clamp of 36 helices with binding sites for the nanorod covering the inside of the tube. The ends of the helices contain sticky ends to connect to the spheres. The procedure to assemble the complete structure remained the same, with a huge emphasis on purification after each step. This led to a yield of $\approx$ 10% correct structures on TEM grids. This seemed enough to continue to find an appropriate method to measure the Fano resonances.

8.8 PROPOSED MEASUREMENT METHOD

To achieve spectroscopy of individual structures, it is crucial to prepare a sample of isolated structures and minimal background. Scattering spectra with almost no background can be achieved by dark-field microscopy. It can be implemented in a way that only scattered light

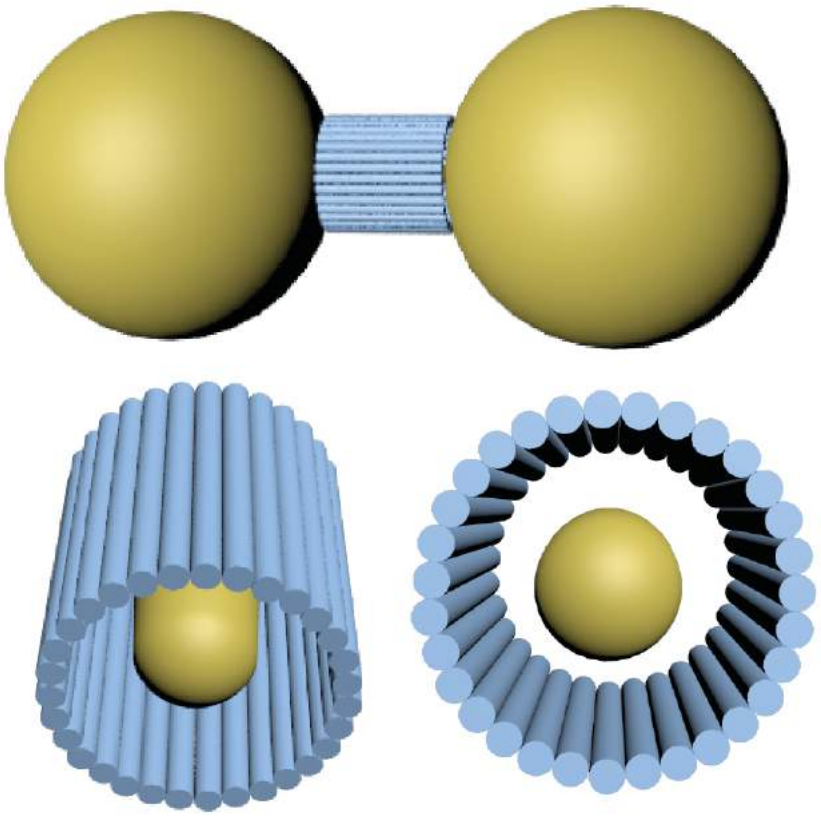

Figure 8.10: 3D image of the second structure to carry the nanorod between the particles. It consists of a barrel of 36 helices of 30 nm length. The barrel is divided into two halves with a hinge like a clamp. Once closed, the nanorod is trapped in the structure.

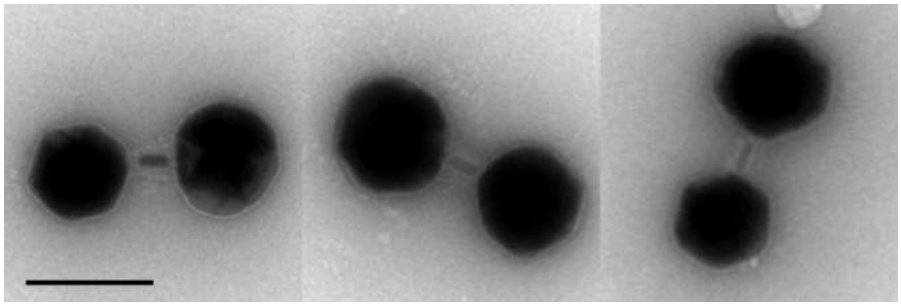

Figure 8.11: TEM images of the fully assembled trimer using the barrel structure. Scalebar is 100 nm.

and no background or absorbed light is recorded. This can be done in transmitted or reflected light geometries. Although dark field microscopy massively reduces the background, the recorded signal still needs to be corrected for weak background and microscope characteristics. This is done with Equation 5.1. Even though the sample on the dark field microscope only shows isolated dots, it is wrong to assume

that each dot consists of a single particle. Small nanoparticle geometries like the ones discussed in this chapter are still smaller than the diffraction limit and show thus also only a dot. Preselecting dots by size and color is still possible, but as plasmonic spectra can be quite complicated, due to plasmonic coupling, the spectrum alone is not sufficient to conclude about the actual geometry. The solution to this problem is the correlation of the recorded spectra with electron microscopy (SEM or TEM). This allows to confirm the particle geometry and match it to the spectrum. To accomplish this correlation, a good choice of substrate and marker are required. We used TEM grids with an asymmetrically marked center so that four distinguishable quadrants could be used to locate particles. The order of experiments is critical here. To avoid damage on the sample by high electron beams, the optical measurements should be done first. Possible damages like structural changes to the nanoparticle due to the high-intensity electron beam, electron-stimulated reactions between the nanoparticles and their substrates, and deposition of contaminants can lead to a resonance shift or a broadened linewidth [192]. To avoid spectral artifacts by a charge mirror image on a conductive surface, we used a TEM grid with a formvar layer without carbon. Figure 8.12 shows an example from the first test of the method. A sample of heater barrels was deposited on a TEM grid and the spectrum of multiple dots was recorded. Afterward, I correlated the measured dots to structures on the TEM. In Figure 8.12 the dot, spectrum (after correction) and TEM image are shown. The spectrum matches the expected spectrum of a nanoparticle dimer. Unfortunately, it turned out that no measured dot contained a correct heater structure. Further investigation seems to confirm that particle dimer with DNA and Rod in the middle collapses on the formvar grid and forms a dimer. Reason for this might be the different charge compared to a carbon layer.

8.9 CONCLUSION

The goal of this project was to build a DNA origami structure fit to arrange three nanoparticles in the proposed geometry. We developed a promising design concept to trap the rod in a barrel like structure between the large particles. To measure Fano resonances in the structures, dark field spectroscopy with TEM correlation seems to be a good approach. However, challenges in sample preparation and deposition have to be overcome to ensure proper placement of the struc-

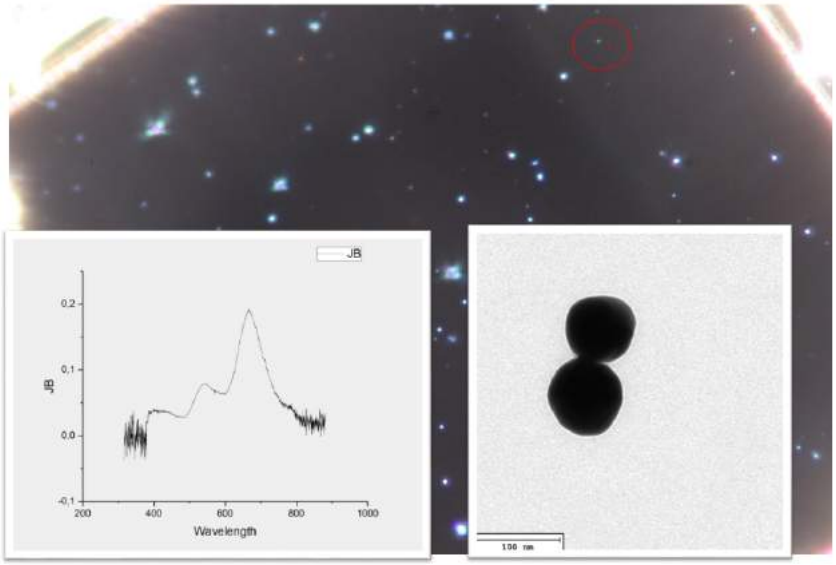

Figure 8.12: The red circle on top marks a dot on the dark filed sample. Spectrum and TEM image of that dot are shown here. The Spectrum has the expected shape of a Nanoparticle dimer spectrum.

tures on the surface. We are confident with some further investigation, this challenge can be solved and finally, Fano resonances and even temperature changes can be measured.

8.10 MATERIALS AND METHODS

The DNA origami structures were assembled by mixing a 7249 bp (barrel and halfpipe) scaffold with a 10-fold excess of synthetic staple oligonucleotides (Appendix) in 1x TE buffer with 16 (halfpipe) or 20 (barrel) mM MgCl2 followed by a thermal annealing process (Appendix).

The nanoparticles (BBI Solutions) were mixed with thiolated DNA (biomers.net, Germany), SDS and TAE buffer. The NaCl concentration was increased from 0 mM to 600 mM over one hour. After incubation overnight, the nanoparticles were purified by agarose gel electrophoresis. A detailed description of the protocol can be found in Section 5.2. The purified nanorods were mixed with the assembled structures in 5x excess, incubated overnight and gel purified. Then the structures+rods were mixed with the large nanoparticles, incubated overnight and gel purified. All sample containing the large particles were kept in a rotator to avoid sedimentation.

9

CONCLUSION AND OUTLOOK

The research field of DNA nanotechnology is a broad and diverse field with endless possibilities. Even only looking at the plasmonic applications of DNA origami offers various exciting questions and problems to be solved. The combination of DNA as a flexible and multifunctional material and gold nanoparticles with their tunable optical properties has shown to be a promising platform to investigate nano-optical effects and construct switchable optical structures. Optical switches can be used as detectors if the structure is designed to switch with a specific input trigger molecule. In this thesis, I could show that a chiral plasmonic switch can be used as an RNA detector. A specific RNA sequence from the HCV genome could be detected at concentrations of 100 pM. To prove the potential use as a virus detector, I investigated the sensing in human serum. The stability and ability to sense a specific sequence in serum could be shown. Next step is to test which concentrations are needed to actually make the changes in CD visible to the naked eye and what optical setup suits that purpose best. To finally obtain a functioning lab-free diagnostic tool is still a lot has to be done. To study chirality of plasmonic geometries further, I looked at helical arrangements of gold nanoparticles and the influence of different numbers of particles on the CD signal. With an increasing number of particles, the strength of the CD signal increases. Additionally, theory predicts a flip in the CD with the particles forming more than one turn. This could not be shown, but a significant weakening of the signal when helix had one more particle than was needed for one turn. Further studies to find a structure that actually shows a flip in the CD signal are planned. A helix with a bigger radius and a smaller pitch is a promising candidate to give rise to strong interactions in the z-direction and thus a potential CD flip. By absorbing light arrangement of nanoparticles can generate heat in a nanoscale space. To increase the efficiency and confinement, the Fano effect can be utilized. In a structure of two big nanospheres and a nanorod in the middle, the broad plasmonic mode of the spheres and the narrow mode of the nanorod can exhibit destructive interference, reducing the scattering losses. The needed sizes of the spheres of 100 nm turned out to be a significant struc-

tural challenge with DNA origami structures usually being much smaller. I could develop a functioning origami design to place and orient the nanorod in the correct position. The next step is to verify the occurrence of the Fano effect with single molecule dark field microscopy. The spectrum should show a characteristic dip at the wavelength of the Fano resonance. Further studies about the actual heat generation by embedding the structure in heat activated polymers are also planned.

Part III

Appendix

A

APPENDIX

A.1 DARK FIELD DATA ANALYSIS WITH ORIGIN (LABTALK)

When working with SpekWin data recorded on the full CCD:

- Import all spectra in a single workbook (File>Import>Multiple ASCII – select desired files – click Add/OK).
- Check box "Transpose Data" and select "Import Mode -> Start New Sheets"; choose correct comma option
- Once imported, open command window (Window>Command Window, or Alt+3) to perform column operation on All open sheets

Eliminate All third and first columns (delete col(1) command did not work for me)

```
doc -e LW {range rr = 3;delete rr;range tt=1; delete tt}
```

Add additional columns at the end (called I to V now)

```
doc -e LW { wks.ncols=wks.ncols+5};
```

Copy Row 1 to "Comments" row

```
doc -e LW // Loop all worksheets in active workbook
{
        worksheet -s 0 1 0 1;  // Select first row
        wks.SetAsLabel(L,-1,0,0); // Set as Long Name and
        // remove first row after
}
```

[Set first column as X. Not needed if you use plotxy]

```
doc -e LW {wks.col1.type=4} // Use wks.colN.type=4, where N is
    the column number. Use type 1 for "Y", and 4 for "X"
```

Find relevant columns with signal from the particle. sum them up in column I (I_S in Equation 5.1). Example:

```
doc -e LW {csetvalue formula:="WCol(151)+ WCol(152)+ WCol(153)+
    WCol(154)+ WCol(155)+ WCol(156)+ WCol(157)+ WCol(158)+ WCol
    (159)+ WCol(160)+ WCol(161)+ WCol(162)+WCol(163)" col:=258};
```

Take the same number of columns left and right of signal as background to column II (I_{BG} in Equation 5.1). Example:

```
doc -e LW {csetvalue formula:="WCol(150)+ WCol(149)+ WCol(148)+
    WCol(147)+ WCol(146)+ WCol(145)+ WCol(144)+ WCol(164)+ WCol
    (165)+ WCol(166)+ WCol(167)+ WCol(168)+WCol(169)" col:=259};
```

column III = column I - column II

```
doc -e LW {csetvalue formula:="WCol(258)-WCol(259)" col:=260};
```

Copy I of noise(black) to II of white to get IIIbw ($I_{DC} - I_{STD}$ in Equation 5.1). Copy IIIbw to IV of all other columns. Example to sheets 1-20:

```
loop (num, 1, 20) {colcopy irng:=22!col(260) orng:=$(num)!col
    (261) data:=1
        format:=1 lname:=1 units:=1 comments:=1;}
```

Finally compute V=III/IV. The result is the real spectrum of the particle by using Equation 5.1

```
doc -e LW {csetvalue formula:="WCol(260)/WCol(261)" col:=262};
```

Create graphs:

```
doc -e LW {plotxy iy:=(1,262) plot:=200;}
```

A.2 FOLDING PROGRAM

- 65 °C for 15 min
- 64°C - 60 °C for 5 min each
- 59°C - 40 °C for 1 hour each
- 39°C - 37 °C for 30 min each
- 36°C - 6 °C for 5 min each
- 4°C

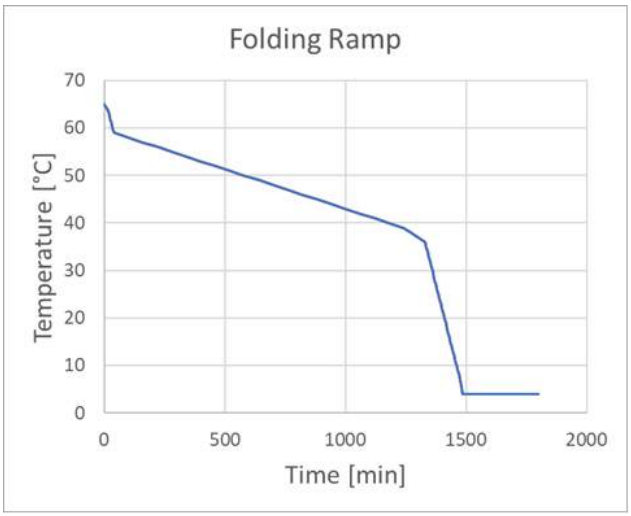

Figure A.1: Temperature ramp for folding the DNA structures

DESIGN HEATER HALFPIPE

HANDLES FOR LARGE PARTICLES

AAAAAAACAGACAATATTTTTGCGTAAGAATACGTGGCAAAAAA

AAAAAATAAAGCATCCCAACATGTAATAAAAAA

AAAAAAGTATTAACACCGCCTGAGAGGTGAGGCGGTCAAAAAAA

AAAAAACTGAATATAATGTTTGCTC

GCAGACCCAAAAGAACTGGCATGATTAAGAAAAAAAAAA

AAAAAATAGAAGGCTTATTTACCAACGCTAAAAAAA

AAAAAAAGACTGGATATCAAAAATAATAAAAAA

AAAAAAGTTTGGAACAAGAGTCCACTATTAAA

AAAAAACGAGCACGTATAACGTGCTTTCC

AAAAAACAGTAAGCGTCATACATGGCTTTTGA

AAAAAACCGTTGTAGCAATACTCCATCACGCAAATTAAAAAAAA

AAAAAACATCAATATGATATTCAACTTGCATCAAAAAAAAAAA

AAAAAAAGGAAACGCAATCGTAACAAAGCTTCTTTCCAAAAAAAAAA

AAAAAAAGGTGAATTTCTCGCATAACCGATAAAAAAAAAA

AAAAAACATTCAGGCTGCGCAACTGTTGG

CCGAGATAGGGTTGAGTGTTGTTCCAAAAAAA

AAAAAAGTGTAGATGGGCGCATCGTAAACCAGGCAAAGCGCCATTCGCAAAAAA

AAAAAAATACCTACATTTTGACAAAAACGCTCATGGAAAAAAAA

AAAAAAGCTGTCTTTCCTAAGGTAAATAAAAAA

AAAAAATTTAGACAGGAACGGTGGCCGATTAAAGGGATAAAAAAAAAA

AAAAAAAGCGACAGAATCAAGTCAGCACC

AAAAAACTGAGTTTCGTCACAGACAGCCCTAAAAAA

AAGCGCAGTCTCTGAATTTACCGTTCAAAAAA

AAAAAATAAAACACTCATCTTTGACGAATAGCGAACGTGGACTCCA

AAAAAAGAATTGAGGAAGGTTAAATCAACAGTTGAAAGAAAAAA

AAAAAAAAAATTTTTAGAACCCTCATACCTTTAATTGAAAAAAAAAA

ATAAATATTCAGAATTTACCCTGACTATTATAGAAAAAA

AAAAAATCAATAACCTACTAATAGTAGAAAAAA

AAAAAAATAAGTGCCGTCGTGTATCACCGTAAAAAAAAAA

CACTGCCCGTATGGTTGCTTTGAAAAAAAAAAA

CATTCCTCAACATACTGCGGATGGCTTAGAGCTTAATTGAAAAAAAAAA

CGGTGTACAGACCAGGCGCAAAAAAAAAA

AAAAAAGATTAAGAGGAAGAACCCATGTACCGTAACAAAAAAAAAAA

AAAAAACGCAAAGACACCAACGAACTAACGTCAGATAAAAAAA

AAAAAATAGCATTAACATCCAATAAAGTTGATTCCCAAAAAAA

AGAAACCAATCAATAATCGAAAAAA

GTAGCTATTTTTGAGAGATCTACAAAAAAAAA

AAAAAAATTCTGCGAACGGTAACAGTGCCCGTATAAAAAAAAA

AAAAAAGGTCAATCATAAGGGAGGAACGAGGCGCAGACAAAAAA

TTTGGCTCATTGTTATCAGCTTGCTTTCGAAAAAA

AAAAAACAAACAAATAAATCCTTTGGCCTTGATATTCAAAAAAA

AAAAAAGAAGAAAGCGAAAGGATGGCGAGAAAGGAAGGAAAAAA

AAAAAATGCGATTTTAAGAACTTGTGTGAATTACCTTAAAAAAA

AAAAAAGCTTGCATGCCTGCAGCGACGGCCAGTGCCAAAAAAAA

AAAAAACGCCAGCTGGCGAAAGGGCCTCTTCGCTATTAAAAAAA

AAAAAAATCGGGAGAAACAATATAACAGTACCTTTTACAAAAAAAAAA

AAAAAATTATTCATTTCAATTAATCGCGCAGAGGCGAAAAAAAA

AAAAAATTGCCCGAACGTTATTACTCGTATTAAATCCTAAAAAA

AAAAAAAAAGGAGCCTTTCTCGTTTACAAAAAA

AAAAAAGAACCAGAGACCCTCAGAAAAAAAAAAA

AAAAAACGCCAAAAGGAATTACTAATGCAGATACATAAAAAAAA

AAAAAATTCTGACCTAAACATATGCGTTATAAAAAA

AGTTTTAGTTAATTTCATCAAAAAAAAAA

AAAAAAATAGGCTGGCTGACCTTCATCAAGGAACGAGGGTAGCAACGGAAAAAAAAAA

AAAAAAGTCTGAGAGACTAAGAACGCGAGAAAAAAAAAAA

AAAAAAACATTATGACCCAACGCAAGGATAAAAAAAAAAA

AAAAAATACAGGGCGCGTACCTGCGCTTAATGCGCCGCAAAAAA

AAAAAACATAGTTAGCGTAATCCCCCTAAAAAA

AAAAAACAAATGCTTAAAAACAGGAAGAAAAAA

AAAAAAAGTTTTTTGGGGTCGAGGTGCCGTAACCATCACCCAAATCAAAAAAA

ATTTCATTTGAATTACCTTAAAAAA

AAAAAAGGCTATCAGGTCATTGCGATAATACA

AAAAAAGAAAGGAACAACAAAATGTTTAAAAAA

AAAAAACAGTTAATGCCCAGTACCAGGCGGAAAAAA

AAAAAACAGACGACGATTAAATGTGAGAAAAAA

AAAAAATTGCCCCAGCAGGCGAAGCGGTCCACGCTGGTAAAAAA

AAAAAAGAGCCGGAAGCATAAAATTCCACACAACATACAAAAAAAAAA

AAAAAAAGAGCCTAATTTATGAAAATAGCAAAAAAA

AAAAACAGGGAAGCGCATTAAAAAA

GAAACAATGAAATAGCAATAAAAAA

ATTTTCGTGTTCAGCTAATGCAGAACAAAAAA

AAAAAACATTGGCAGGCGCCCAATAGCAAAAAA

AAAAAACTACAGAGGCTTGTAATGCCACTAAAAAAA

AAAAAATTTTAATGGAAACAGTACATGAAAACATAGCAAAAAA

AAAAAACGAGTAACAACCCGTCGGAAATGGGATAGGTCACGTTGAAAAAA

CORE STRUCTURE

TCGTTAGAATCACAAATTGCGCCTGTCGCGCGTAAGCTGGCAGACGGGG

ACGGAGAAACCCTAAAGGGAG

TGAGTAGTCCAGAAGTTGAGAAAGCCGTAGTACCGGCTATCCCATCCTA

TAAAACTAGCATGTCAATCAACTAACAA

AAAATACTGATAGCGGCTTTTCACTCATCGGAGCAACACTAT

ATTTTTATATGTAACACCACC

ACTAAGTCAATAGTGAATTTATCAAA

AGCTTTCAGGGGACAGGGACATTCTGACGGCGGAT

GTGATGAATCACAGCTGATTGCGTCACGCTGTGCCAGC

TTCTGTAATTAGAGCAAGAAAAATAAAAAAGAAGT

AAATAGACGTTCTAGCTGATAAATTATT

TACCGAAGCCCAGTTACCAGAAGG

TGCATTAAGCTAACTTTATCCAGAACCGGATATTCATTACCC

TCAATTCTGTTTAGCTATATTTTCATTT

ACGCATATTATCACATTTGGTCATAGCTGTTAGCTCGAAAACACCCTAT

ATAAATAAAATATCGCGTTTTAATTCGAGCTTCAAGCGAGCC

CAAAATAAACAGCATTTTTTAAATTGT

TTCAGTGAACAGGAACGCCAG

TACCAAGCTGAGAATCCCTTAGGAGTGTACTGGTAAAAGTAT

CTTTGATCCAAATAAAAAGTT

AGGAGCATCAATATCTGGTCACAAATAT

CTTGATAATTCATATATACCAATACCACCCTTGCTGCTTCTG

CCTAACCCACAAGAATTGAGTAATATCA

GAAGGGGATTCAACGAGGCATAGTAAAG

AGGTTTAGTACCGCCACCCATAGCCCAGAGGTC

AACCTACTACTTCTTCAGATGGGAATTA

GACTGCTCACAGTGTAAAGCCTGGGTGAA

CAAACTCGAGTAATGTATCCTGATTGTT

TTGATATGCGGGGTCTGTAGCATATAACATCATACGGTGGCA

CTTTTGCGGTTGCGTAGATTTTTATATAGTTTTAAAAGGATTTATTCTG

TGGATTACATATCAAAATTATAGATGAATAACCTC

TTGCTATTAACGTCTTGCACGTAAAACAGAAATAA

CAGTTTGCGGCACCGGTAATAAAGAACTCAAACTA

ATCTACGACGCGAGGCTACAACTTGCCCTGACGAGATTCGTA

CCAATAGGCCCGAATAGAGAGTATATTTGAAGCCTTTATTTCTGTAATA

GTGCCGGAACCGTGCATCTGC

TTTGCGGAACGTAGGCACCCAGCGTTTTAGCGAACCTCCCGA

CGGGAAGATCGCACACCGCCATAACATCCCACCGAAGAAGTG

TATCACCGGGCGACTAAACCATTTTATTTAATAAAGACGACA

CTGAGGCTTGCAGGGAGTTAAACGAAAGATTTTTCA

AAAGCCGAAATCGGTTTGTATGAACAAAGTCAGAGGGTAATTAAGTACA

TCCATTAAACGGGTTGACCAA

TTTTTAACCAATAGAAATTGTATCAGAAGTAATCG

TTAGTAAGCCATTGCAACAGGGCTCAAT

AATTATTGGGAGGGTATCATTCATTACCATTCACCTGAAATG

GATTATACATGTTAACGGGCAGGCCAACGCGCGGGGAGAGGCGGTTTGC

CCACCACCAAGACAACCTTTTTATACAGACGGATTCGCCTGA

TTCACGTTGAAAATATTGCGATCAA

AGAGAGAATTCACCCGCCTTCCAGTCGGGAAATTGCGCT

AATTAACTGAACACCCTCAAACAT

GGAGAGGTTTGAGGATTAGAGCCGTCAATACTGAGA

CAAACTACATTTCGGTCATAGCCCCCTTTCATTTT

GTATCGGCCTCATCAGTCACACTGAAAGAATGGCTATAAAACCAACAGT

ATCATAAGCCTTAAATCAAGATTAGTTGAGAACGACTTGACACAAAAGA

AGAGAGTCAGTGAGCTTAGCCACCGAACAAAATACTGAGGAC

TTAGTAAATCGTCGCTATTAAATAACCTAAGAAAA

GGGGCTCTGCTTCTGTTTGACCATTAGATACATTT

AGAGCGTTCAGAACAGCAAGC

CGCGAACCGAACGATTAAATCTGTTAAAATTCGCATTGCTGA

TGAGTGATTAATTTGAAGTACGGTGTCTGGAAGTTT

GGACAGAGTGCCTATGAAATTGTTATCCCTAGAGG

AAACATGATAAGTTTTAACGGGGTCAGTGCCTTGAAGTAGAT

GGAATCATTTCATCGGCATACTTGTCGTGGTCGTC

CCAGCATTGACAGGAGGTTGAGCCGCCACCGCCAC

TTTTTATAACGCCAGGGTTTTGGTACCGTCCTGTGATGA

TGAGGTTGGGTCAGGTTTAAGCAA

AACAAGCTTTAGGAGTCAGGACGTTGGGAAGAAAA

AGTAGCACAACAATAGATAAGAACAACAAGCCAGT

ACATTATTACAGGTAGAAAGATTCATCACAATATTTCCAGCC

CCTGCCTATTTCGGAACCTATAGGATTAAACGCCG

CATAACCAATTGTATCGGTGTTTACCAG

TCAGGATAGACTTCAGGCGTT

CTAATAGATTTAGATCAAAAA

CGGCTTATGCAAATCCGGAAG

GAGCCAGTGAACCTGTTGGCATCTAAAATATCTTT

ACGTCAACTTATAAGGTGGTTCCGAAATCGGATTT

CCTCACTCCCTCAGAGCCGCCCCACCACATAATCA

CCCCCGCCGAAACAGAGCGCTTAAGCCCAATAATAGAAAAGTAGAA

CTAGGGCCCACCACGCCTGATGTTTAACGTCAAAAGCCAGTTA

GCGGAACAGGTAAAGATTCAAAATGCCTCAACAGG

CAGGGATCGCCACCCTCAGAACCAGAACATGC

AATCCTGGTAAAAGTCTAAGATTAATAAACGGAATAAGTTTATTTTGTC

TTTGATAGGAATAGGAGAGGG

GACTTTACAAACAAAAGCCAAAGCCTGT

ACCACCCATTAGCGAGACTGTAGCGCGTTAATTACCCGTGTG

ATACCGATAGAAAACGCTCAACAGTAAAAGTATTA

AGAGCTTAGTGTAGCGCCTTCACCGCCTGGCCCTG

TAAGACAGAATGGATGATACAGAATCCTTAAATCATTTAACA

TTCTGACCGACCAGTTCATCGTAGGAATCCAAGAAAGCATGT

CAGACGACATTAAAGCGGCTGAGACTCCTCAAGAGATATGCA

TCAGGTCAACGAGAGTTGATAAAACGTTAATATTTAGCTCAT

TTTGCCAAGCGAGACCTAAAATGGGAACAAGCCAACAGAGATAGAACCC

ATATAGTAAAGAAAGAGTAACATTATCATTATGCC

CTGAAAAAGGCAAGTCAGAGCATAAAGCTAAATCGGTT

TGACCGTTTCTCCGCAGCTTTCATCAACATAAAAA

TTTTCACTGCAGCAAAATCCTGTTTGATATCAAAACCCCAGC

CGCCAAAATAGAAACCGATAGTTGCGAATACATACATAAAGGGTTA

GCAGAAGATTAGTCTTTAATG

GTCGAAATCCGCGACCTGCTCCCAAGCGAAAATCCAGGGCGA

TAGATTAAGACGTTACAAACCTGAGCAAAAGAAAATTACAATATATG

CAGTAAAGTTGCCTGTACGAGAATAAACACC

AGAAAGATAAATGCAAGGGTGAGAAAGG

ATCCCCGCCCAGTCACGACGTTGCTGCAGAGG

ATATACGAACCAGACCAATCGCCTCAGAGGCAGGT

TCTGTCCAAGTACCTAGGGCTTAATTGAGAATCGCCATATTT

AACAACGACCTTGCCAGCAAA

TCGCGATCGGTGCGGGGGATGTGTAAAAGTC

TAAAGACCAGCATCGAGTAATGTAGTAAATTGGGC

AAAACCGTCTATCAGGGCGAT

ACAACTTATAATAATTAGCCA

CAAAATTGATGATGAAACAAACAGCGAG

TAAAGCCGCAAAGAATTAGCAAATTGAA

AAATCAAAATAACGGAATATCGTCACCCTCAGCAGGGCCGCT

ATTTACGCGGGTATATTCAACCGATTGACATTAAAAATCACC

GAGAGATAAAACGAAAGAGGCAAAAGA

TTATTACCTGAATCCCGGTATAGTCTGTTCTTTGA

AATAAGAGAATATAAGACGACATTTTTGACCACCA

CCAAAATGAGGGGGAATACTGCGGAATAAAGTAAT

TGAGGGCAGATAGCCGAACAATTTTTAAAGAGCAA

TTCCTGTAGCCATCGCCATTA

TTTGGGATGGGATTGACGTTAGTAAATGAAAACCA

GGCCCACTACGTGAAAGCACTGCGAACGGCGGGCG

TTAGTATTTTAATGAAGGAGCATGGCAATTCATCA

CAGTATATTCGACAAATTTTAAAAGTTTCCACCAGGTTTGAA

CTTGCGGAGGCGATTAAGTTGGGTAATCAGTGAGGACTTGCC

HANDLES FOR NANOROD

TTTAACCGACAATGACAACAACCATCGCCCATAAACAG ATG TAG GTG GTA GAG

CCGGAAACGTCACCAATGATT ATG TAG GTG GTA GAG

TCGATAGTTGCCTTTAGCGTCTTTGCCA ATG TAG GTG GTA GAG

ATGAACGAAGCCCCTAAACAGTTCATTGAACGATCTTTCAGC ATG TAG GTG GTA GAG

ACAATCAGACAAAAGTCACCGACTTGTT ATG TAG GTG GTA GAG

CAAACCCTCATATGTACCCCGATGACCAGACAAAACTTTCCATTGCTAA ATG TAG GTG GTA GAG

GCGCCTGTTTATCCATTACTGACGGA ATG TAG GTG GTA GAG

TTAGGCAGAGGCGTAATCAAGCAAGG ATG TAG GTG GTA GAG

AATATTTGAACGCCAGCGTCCTAATAGTTAAAGGACTCCAAA ATG TAG GTG GTA GAG

GCCACAAGACAATATCCTGAACCAGCAAGGTGAAT ATG TAG GTG GTA GAG

ATGAGCGGGAGCTAAATAAGGTTTTATCGCAGTATTGGCAAC ATG TAG GTG GTA GAG

AGCAAAGGCATTCCACCAGTA ATG TAG GTG GTA GAG

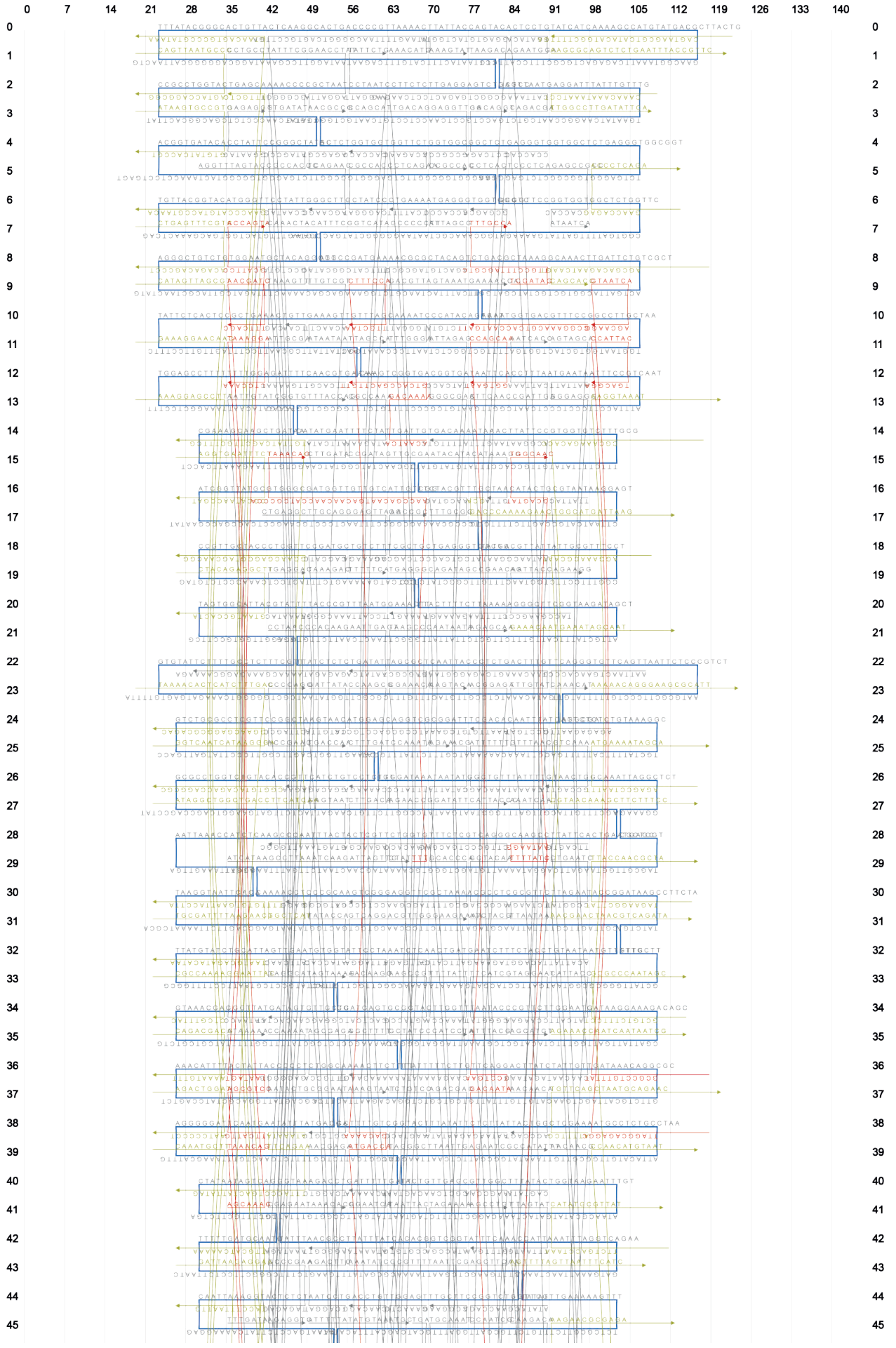
0 7 14 21 28 35 42 49 56 63 70 77 84 91 98 105 112 119 126 133 140
0 1 2 3 4 5 6 7 8 9 10 11 12 13 14 15 16 17 18 19 20 21 22 23 24 25 26 27 28 29 30 31 32 33 34 35 36 37 38 39 40 41 42 43 44 45

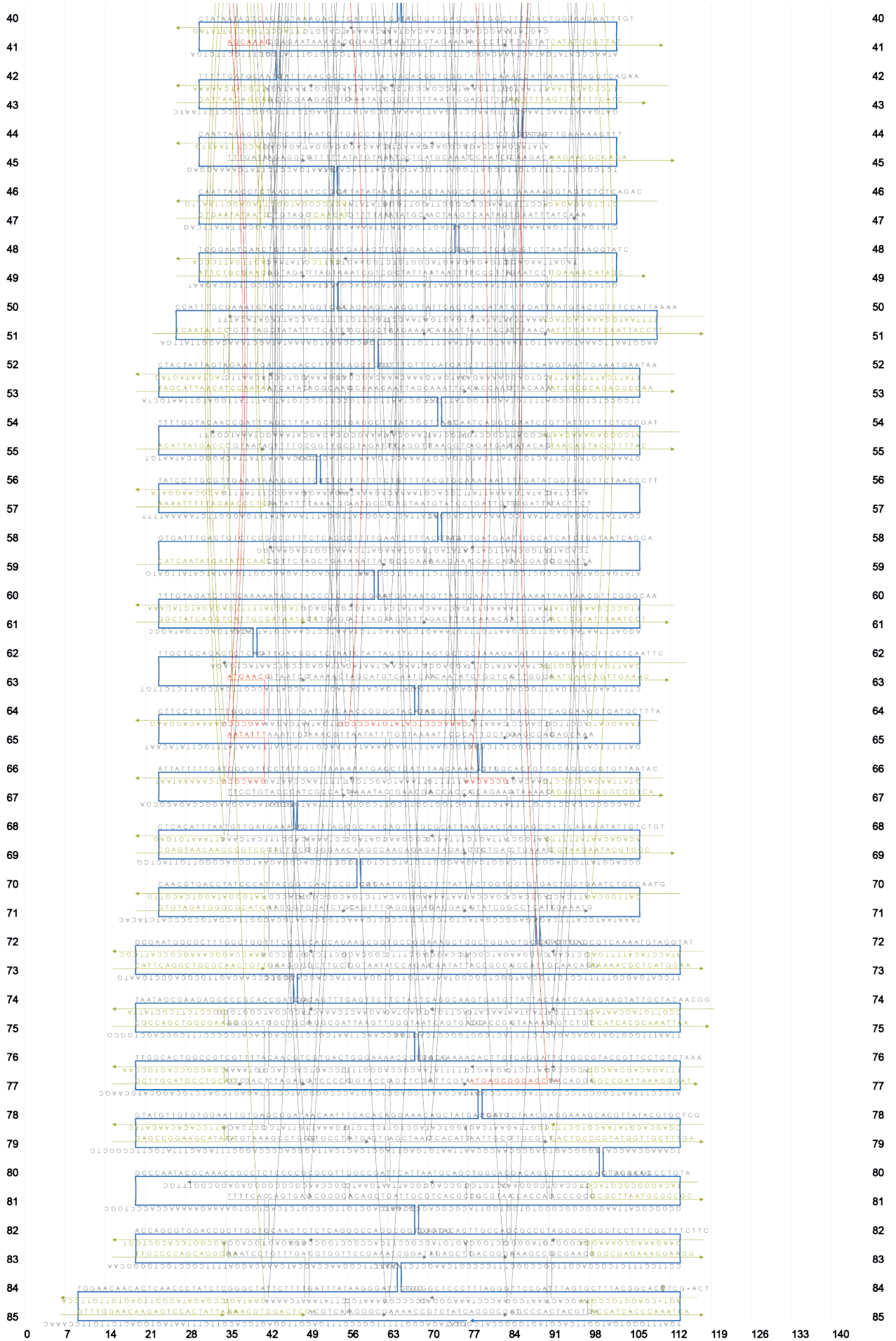
40
41
42
43
44
45
46
47
48
49
50
51
52
53
54
55
56
57
58
59
60
61
62
63
64
65
66
67
68
69
70
71
72
73
74
75
76
77
78
79
80
81
82
83
84
85
0
7
14
21
28
35
42
49
56
63
70
77
84
91
98
105
112
119
126
133
140

DESIGN HEATER 1 LAYER BARREL

HANDLES FOR LARGE PARTICLES

AAAAAATTATTAATTTTACATCAATATAATAAAAAA

AAAAAAGTAAAAGAGTCTGTCCTCAGTGA

AAAAAAGAAACACCAGAACCAGCCAGCTTTAAAAAA

AAAAAAAGTAATAAGAGAATAGATAAGTCCAAAAAA

AAAAAATCAAATATATTTTAGTTAAGAAAAAGCCTGTTTAGTATAAAAAA

AAAAAATGAACAAGAAAACGCACTCATCGAAAAAAA

AAAAAAGCAAAAGAAGATGTGAGTGAATAACCTTGCTAAAAAA

AAAAAAATCCGCGACCTGCTCCATGGAACGGTGTACAGACCAGGAAAAAA

AAAAAACATATGCGTTATCATTTTCGAGCCAAAAAA

AAAAAAATCGCCATTAAAAATACTGATAGCCCTAAAACAAAAAA

AAAAAACCAAAAAAAAGGCTCCAAAGCGCCGACAATGACAACAAAAAAAA

AAAAAAAAAGAGGCAAAAGAATACACCTGATAAATTGTGTCGAAAAAAAA

AAAAAAAGCACTAACAACTAATAGATAAATCCTTTGCCCGAACGAAAAAA

AAAAAAGAATTTTCTGTATGGGATT

AAAAAACGCATAGGCTGGCTGACCTATAAGGCTTGCCCTGACGAAAAAAA

AAAAAATGATTGCCCTTCACCGTGAGACGGGCAACAGCAAAAAA

AAAAAAGGGTTGAGTGTTGTTCAGAATAGCCCGAGATAAAAAAA

AAAAAACCAGCTGCATTAATGACGGGAAAGCCTGGGACGAGCC

AAAAAAACACTGAGTTTCGTCACCATTTCCAGACGTTAGTAAATAAAAAA

AGAACGCGAGAAAACTTTTAAAAAA

AAAAAACCGGCACCGCTTGCTGGCGAAAGGAAAAAA

AAAAAACCTGATTGTTTGTTTAACGTCAGAAAAAAA

AAAAAATGAATATACAGTTCAATTACCTGAAAAAAA

AATCAAACAGTTTGTAGGAACCCATGTACCGTAAAAAAA

AAAAAACTAAAGCATCACCTTGCTGTATCTAAAATATCTTTAGGAAAAAA

AAAAAAGAACAAGCAAGCACCATCACCAAAAAA

AAAAAACGAACGTGGTACTATGGTAAAAAA

AAAAAACAAATCAAGGAAAGCCGGAAAAAA

AAAAAAGCAACAGGAAAAACGCATTACCGCCAGCCATTAAAAAA

CTTTAATGCGCGAACCGAACGCCAGCAGCAAATGAAAAATAAAAAA

GATATATGATAGTTAGGAGCCTAATAATTTTTTCACGTTGAAAATCTAAAAAA

CORE STRUCTURE

GCAAATCCAATCGCTTCTGAC

CAACGCCGCCAACGCTCAACAAGAATAATAATGGTTGCTGAT

GTTATCCTCACATTAAAAAGG

TTACTTAATCATCGCTAAAACCACTACGAGAGGCTTTGAGGAGTGAATT

ATAAATCTTTCCCTTAGAATC

CTACCTTCGTCACCCTCAGCACATAACC

GCGCCAGGCAAGCGAAATCGGTATTAAATTTCAGGGATAGCACTACAAC

AATCAATACCGCCTCAGAGGTGAGGCGGCAGACAA

GGCAATTAAAGTTTGAGTAACCTCGTATTTAGAGCGGAAGGT

TCCATTAATTATACCAGCTTT

TTTCAGGGATTATACTTCTGAAGATGAT

CCAGATACCCAAATACCGTGC

GAATTGACGTCAATAGATAATAAACAAT

CGTGGCATCGTAAAACGACGG

AGCCAGTTTGAGGGTTCAGGC

AACCTCACTGAGAGAACCACCAGCAGAATATTAGT

TAAAGCATCTATCAAATCATTACCGCGCCTTATCA

CGCTGGCGCCCCAGCAGGCAA

AGTTGCAGGTGGTTTTTCTTTAACGCGC

CTGGTTTAAGTGTAGCATTGGTGCGTGG

CGCTATTAATTAATAATATATGATGAAACAAACATGCGAATT

ACAGTATGATGGTTTAATTTACAACGTAAGAACCGAACTGAC

TACGCCACTGGTGCCGGAAACAGGAAGA

CAAACTGTTGGGAAAGTCACG

AGTCCACCAAAATCCCTTATACTGAGAG

GACTCCATGATGGTGGTTCCGGTCCACG

GGAACCGGATATTCATAGGAG

AAACTATCTTCTTTGATTAGTGACAGGA

AGAAAGGGCTTGCTTTTGAGA

GCCACCAACAGACAGCCGGCTGTCTTTCCCAATAGAGGGCGA

TAGAGCTGGAAGGGAAGAAAGAATGCGC

TAATGCATAAAGTAATTCTGTTATTTAA

CTTGAAAAATGGAAACAAAATTAATTACAAGTTAC

ATGTAAATTGAAATACCGACC

TTTCAGCTAGCGTAGCATTCCCCCTCATGAACGTG

ATGAGTGGCCCGCTTTCCAGTATCGGCCTCACCAGCCTGGCC

CGCTTTTCTGAGGCTTGCAGGTTTCTTATTTATCAAACAACT

AAGGCGATTAAGTTTCGCTAT

CGGAATTACCATATCAAAAAG

GAATACCATTTAACAATTTTT

TCAACAGAAAGGAATTGCGAATTTAATT

TATTCCTTTTTGCGGAACAAAACTTTACACATTTGTCAACAG

GGGGAGAGCTCACTAGCTAACGCTCACA

ATGAGGAAGACGCTGAGAAGA

CGCTACATATAACGTTTATAAATCACGC

AAAACCGCTAAATCGGGAAAATCCTGTTACGTCAACATCAGA

TATTTTTGAATGGCGATAAAAGCAACAG

GTGTGGTGGTTATATAACTAT

GATTTTAAATAACATCACTTT

GCAGAGGACAAATTCTTACCAATTACTATTTCATCAAGACAA

TAGATTAAGCATTTGAATTAC

GGCCCACGGGTCGAGGTGCCGCCCGATT

ATCGCCACCAGACGACGACAT

ACCACCACACCCGCGAATCAGGCCAGAAAGCAATA

ACGGTACAGCGGGAGCTAAACGCGCGTA

GAAATAAACAACATCCAATCA

TTTTTTGTACGTGACGTTTTTATTTTCAATTAAAC

GAACGCGTAATTTAAACGGGTTCGTAGGGGGCGAT

ATATCCAAAATTAACCGTTGTTCCTGAG

GTATCGGAACAGCTTGATACCTCGGTCGGCGGGATTTTAACC

GGCCTCTGGGTAACGCATGCC

AATGCCTGAGTAGAGATTATT

AAGTGTTTGCTTTCCTCGTTACGCGCTTCGAAAGGGGGAGCC

TTGCTAATGTCGTCGTACAAAAGCCCAAGAACAAG

TCGCACTCGAGTAGTAAATTGTCAGTGATCATCAAGACAGAT

GTCAATACTAAAGAAAAATACGTAATGCACTCATC

AAATAAAAAGGGTTAGAACCTATCATCA

CCCTAAAAGCGGGCGCTAGGG

TGCAGGTAGATAGAACCCTTC

CTTTTTTACATAGCGATAGCT

CCAGTGCAAAGCGTAAGAATA

TATTATTTGCACGTATTCGCC

CTAAATTACACCGGAATCATAGTATAAAAACATGTCAAAAGG

TCACGCTAGGAGGCCGATTTTGCGTTGCGGCGGTT

GAAATTGCATCGGGCGCAGAGCAAGAAAACAGTAC

TGACCTGCAAGCTTGCCAGGGTTTTCCCGGGCGAT

CGGTGCGAGCGCCATTCGCCAGACGACG

CAGACGGCAAAGTACCCAGCGAACGGGTCTTTTTC

ATCTGAAGTATTAGGAAACCA

TCCGGCTTAGGTTGTAAAGGC

AGGTGAAGAATAAATAAGGCG

CTTGACAACAAAGCTGCTCATGGCTTGACGGCCTCCAGGCAA

TGCGCGTTGGCAAAAGGATTT

TCGACAAATTATCAGATTATCATAATGG

ATCAACAATATAAAGTACCGAAATTTAG

CGAGGCGCAACTTTGAAAGAGGAGTAAT

TCATAGCATTCCACACAACATGTGCCTA

TGCCACGAATATCAAACCCTCTTGAAAG

GGCCACCCTTTGACGAGCACGGGGCGCGCGAGAAATGACGGG

TTAAATAGTAGGGCTTAATCG

ACGTTAGTATTAACATCTGGT

HANDLES FOR NANOROD

TGTTTCCCACCAGTCACACGACCAGTAAATCATGG ATG TAG GT

TGATTAGCGCGAAATCAATCA ATG TAG GT

TTCCAAGCGAGCATGTAGAAAGTTCAGC ATG TAG GT

GCCTGTAACGATCTAAAGTTTACAACTT ATG TAG GT

AAAATCGAGAAACAATAACGGAAAACAG ATG TAG GT

GAACAATTCATGGAAATACCTACATTTTGCTGGTA ATG TAG GT

CGGCCTTGACGCTCAATCGTCTGAAATGAGAACTC ATG TAG GT

ATTCATTAACAGTACCTTTTACGTAGAT ATG TAG GT

TACATTGGCAGATTTGTGTGA ATG TAG GT

ATAATCCTCATAGTGGAGTGA ATG TAG GT

CAAGTACATAATATCCCATCCCCTGTTT ATG TAG GT

TTTGACCCAACGGAGATTTGTGCCGGAA ATG TAG GT

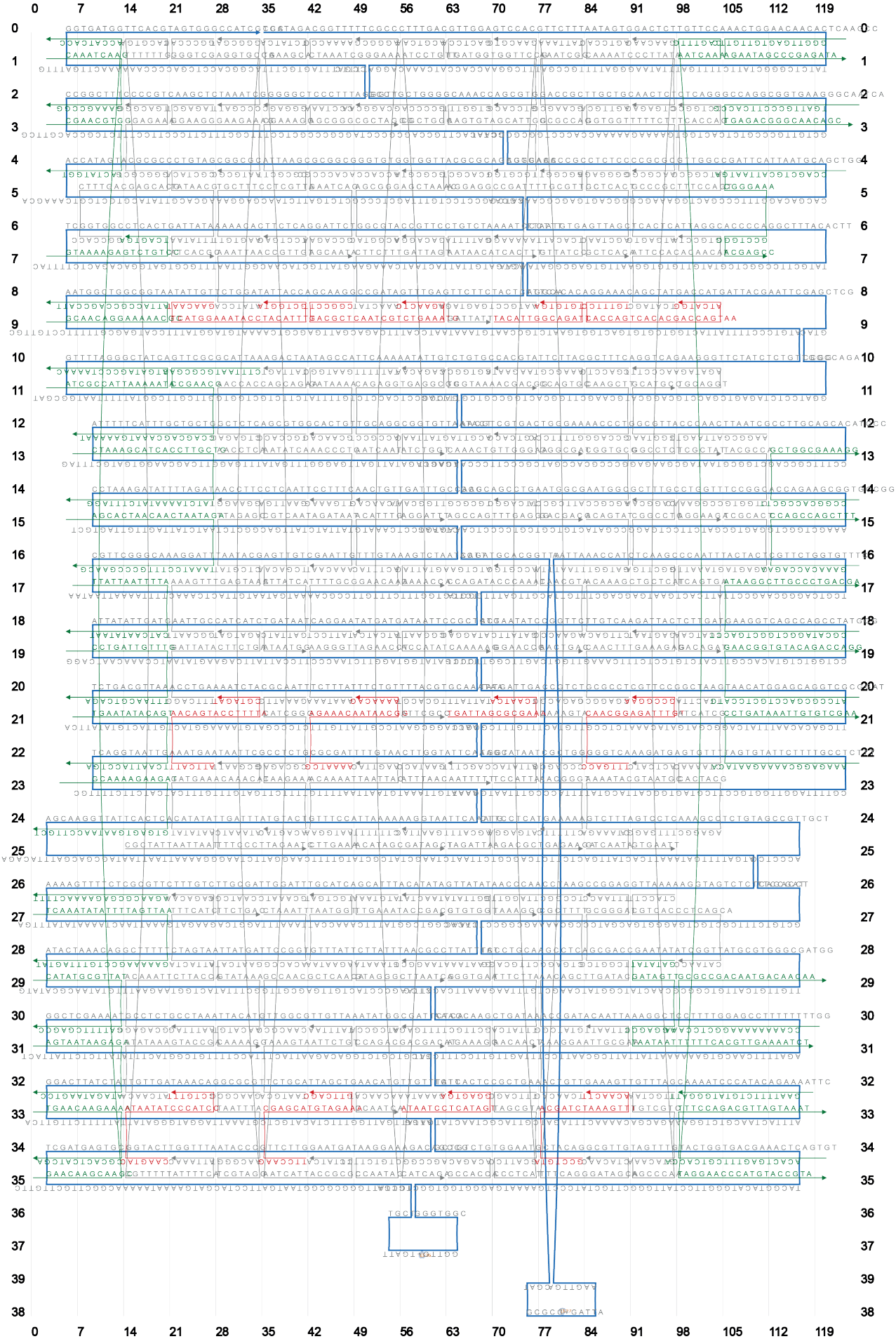
0 7 14 21 28 35 42 49 56 63 70 77 84 91 98 105 112 119
0 1 2 3 4 5 6 7 8 9 10 11 12 13 14 15 16 17 18 19 20 21 22 23 24 25 26 27 28 29 30 31 32 33 34 35 36 37 39 38

DESIGN RNA SENSOR

CORE STRUCTURE

AACGAGCGTCTTTCGCCATATTTGTTTAGAAGCGCATTAGAC

AGGTTTAACGTCGACACCGCCTGGAAGGGTTAGAAGATTTTC

TACTTTTTCTAATCTATTTACAGAAAGGTGCCTGAAACAGTGAGGCCAC

AAGAAGTCCAAAATTAGAGAGCTTAATT

TTTGAGATGTTTTTATAATCGCATTCGC

AATTTTAATTTTCAGCAAGGCAAAGAAT

TCGACAAATTATCAGTCAATATAGGTCTGAGAGACGTGAATTACGAATA

ACTCGTCAATCGGAGAGTAACCTCGTATGAGCACTGGAAGGTAACCTCA

CTCATAATGTTTAGACACCCCCAGCGATAAGAGGA

CATAACCTTATTACCCCTCAGAACCGCCCCAGGTCATTTTTG

CCGGCTTAGACGCTCGGCTGACGCATTTCCCAAATGAGCGGATGGAGGA

TGTCCATCACGCAAATTAACTTTTAGACAATAGGAACCCGTCGGCAAAT

AATTAATTTTCCCTCTCCTGGTTGGTGTGTGGACT

AGGGAGCGCCATCTAAAGCCTCAGAGCA

GTCAATACTAACTTTTTCAAATTAACACGCAAATGAAAAATC

TATTCTGAAATAAAGGTGGAATAAATTGAGGTTAAAGGTAGCAAG

TATACTTAGATACATTTCATCACAGAGGTCACCTTGCAGACA

GGCAATTTTCTGAATAATGGCAGTTACAAAAATTAATTACAT

GAGATTTACCTAAAACGAAAGGCCACTAAATCATTTTGGGAAGAATTCC

CCAAAGAAGAAAATACAAACAACTGGTAATAAGTTCAGTGCCTCAAGAG

GTGGTTGTGGGAAGGGAAACCAGGCAAA

CATACAGTTTGGGGAGTATCATAATGGTGAACCACTGAATGG

AACCGCCGAGGCAGGTCAGACGATTGACCACGCCACCCTCAG

GTTTGATGGTGGTTCCGTAGCCCGTGTTATCCTGTAAATCTCCCCGGGT

AACGGCTAGGGATAAAACTACAACGCCT

GGAGGTTACCCTCAACCACCGTAGCGCGTTTTCATATCGATAAGCACCA

CGAGTAAGTAATAAAGGGTGATATTTTAAATGCAA

AGAATCCAAATCAGTTGTAAACGTTAATCCCCAAAAACTAGCATGTCAA

ACCATCACACATAAGATAGCTTAGATTAAGGTTGG

GAGGTTTTTTTAGCGCGGGGTTTTGCTCAGAACTG

AATATCAAACCCTCTTGAAAGGAATTGAAACAACTTAGTTAATTTCGCA

GAAACACCAGAACGAGTAGTAGTGAGAA

AGCTAAACAGGAGGAATTCGCATTAAAT

AATTGCTGACGACGATAAAAATTTGCCAAGCGTCCACAGTTC

CTTGATATTCAACCTGAGAGTCTGGACCAAGGGATTTGACGA

AAAGAAATTACATCGGGAGACGCTGAGACATAAAACAGAAAT

AAGATTAGTATTCTGGCGGATAAGTGCCACTAATAACGGAAT

TTTGCCCGAACGCCCTGAAATGGATTTACTAAATTTATGCGT

AAGGATTCCTTATTGTCAGATAGCCGAACTGAATCCTTGCGG

CCTCATTTTGTCACAGAAAATACATACACATGAAAAACAGTT

GCATAGTATCAGTTTCAGGAGGTTTAGTCTTAGAGTACCTTT

ATTTAAACTCATTTTTTAACCAGGAACGCATTGCCGTTCTAG

CGTAATCAGTAGCGAGAGCCAGCAAAATTTGAGCCATTTGGGACCAGCG

ATTAACGAGGCGCAAACGGTGATCAAGA

GAGGCTGCAAACGTAATCAATCAAAAGGCACCGACCACCAGTGCAGCAC

AAACAGGACGTCAAAAATGAATTACAAATAGCCATATTTAACCGGAGCG

AATACGTGGCACTGTATCTAAAAATTTACATTGGCGCGTAAG

TTAACGATTGCCTTGATATTCTCATATGACGCAGT

TTCGAGGAATTGTAAGGAATTGCGAATAACAGTTTACCATCGGCTTGCA

AAGACGGAGGAGTAAACAGGGCTTAAGCTA

GAGGAAACGCAAGGTAATTGAGAATCGCTATCTTAGGAAACC

ACAGACATTAATTTCAACTTTCGAAGGCCTTTGAG

ATGTTAGAGACTCCTTGAGTAACAGTGCGGAGTGTAATAAAT

CAATATCCTATGGTGTGTAGCGGTCACGGTGCTGACCTCTAA

AATAAATTCGAGCTCAGGTCAGGACGAGTAGATTTAGCCAGT

CGGAGACTACTTCTCGGGCGCTAGGGCGGACAATGACGCAAGATGTG

TATTACCGCCTTGCTGAAAAGAACATCC

TTTGGGGCTTGAATGAGAAGAGTCAATATACCTTTTTAACCT

CATTTATATTATTTGCACGGTTGGCAAA

ACTAATCGGTTTATTGACCAACTTTGAACCGGATAAGGAACA

TGATTGCAGTAACAGTACCTTTTGCGTACCTACCA

GCACGTAGCGCGTATGGTGCCGGCGATCGGTGCGGGCCTCTATCACCAT

ACCAGAACCGAAGCCAATGAAATAACCCACCCTGAACAAAGT

GGGAACAAGTAACAACGCCATCAAAAATCCGATTAAGTTTGAGGCACCG

ACCCAAAAGTACCAAAGAACGCGAGGCGTGAAGCCGCTACAA

TTATCAATCCCATCCTCATTGAATCCCCAGGTCTTTACCTGT

AGTAATAAAAGGGACTCATGGGCGTTAAATAAGTT

TTAACCTGCCTAATGAGTGCACCTGAGACAAAATCCCATGAT

CTATTAGCCTGAAAAGATTCACCAGTCATGACGCTACCGACCGAAAAAG

AGAGCCAAATCTACGTTAATACAGGACGGTGAATTCTGACGA

GGGAGTTAAAGGCAGTATCATCGCCTCACAGCGGAAATTGGGCTCTGTA

GTTATTACATAAATACATAGCATCATTTCTCCGAAGGCCCACCCTGATT

CTTAAGTGTCCTTACTGCGCGCTACAGGTAACGTG

TTTGCGGAGATGGTGCCCTCATAGTTAGCCAGTACGCAAGCCCAATAGG

GTGTGATTCGCCATTGCGCGAACTGATAACAGAGATAGAACC

AATGCCCTACATGGGAATGGAGAGCCGC

AGCACTAGGTGGGCTATCAAAATAAATTAAGCAATGTAAGCA

CAGAGGGTAATTACAATAAACTGTACAGAGAGAATAACATAA

CATTTGAATAAATCCCAACGTGGGCGATCTCTGACTAGAATC

AATAATACAATAGATAAGTCCAACATGTTTCTGTC

GCTGAATACCGTACGAGATTTAGGAATAAAAGGAAGGGCACT

TATCAAATGTTTGGCGAATTATTCATTTCCAAACAATAACGG

GGGAGAGTAAGAAACGATTTTTATTTATCAAGAAACCTTTTT

ATTAAATTTTTGTTTGAGAAGGATCTACCCGGAGAGGGTAGCATTCAAA

GTAGCAACCACCCTCATTTTCACAGAGGACCCGCT

TGAAACCCGGCATTCCGGAACCAGAGCCGAGCCACTCACCGTGCGACAT

AACGCCACCACATTGGAATAGGTGTATC

TAGAGCCTCAACAGAATCAATATCTGGTGCCAGCACGCCTGC

AGAAAAGGCTGGCTGACCTTCTACAGACCAGGCGCCAAAAAG

ATCATTCTTTTATTAAGTTTCATTCCATCCAACGCTCAACAG

GCTTGCCACCTTATGTAAAATTCATGAG

TAATAGTTTTACCACCTTTTGATAAGATCACTCATCTTTGCGGAAGCAA

CAGACGAAACGCCAATCAATAATCGGAGAATAGCAGCCTTAACAAGAAA

ATCAGTTATTACCTTGTGAGTGAATAACCTTGCTTCGAATTT

TAGAATTCATTACCCAAATCATGACAAGAAAGAGG

CAGATATGGGTTGATATAAGTTTTTAAATATGCAA

ACTCACAACGCGCGGGAGATGAATATACTTTGAATACAGCTA

CAAAAGGAGCCTTTTGAATTTCAATGACAAGATAAATTGTGTGCTTGCT

TCAACCGGTTTATTAAAGCCACTTTTGATGATACACCGTATAGTATTAA

CATCGAGTTGATTCTGTAGCTCAACATGATAGCCCCAACTAATGCAAAT

TTTTATCCAAAGTTGCATGATTAAGACTAGGATTAGAACCTCCCGGGGT

AGAAAAGATTTTGTTAAAATTCTGGCCAGCCGGTTGATAATC

AAAGTAATCAGCTAATGCAGAACGCGCCTACCGACAAAAGGT

AAAAGAAAAATCGGGAGTTGCTGCCCTTGAGGCGGTTTGCGTTCGGC

AGCTGATAGCAAGCCTGGGGTCACAATTCCACACAACAT

ACTCCAATCAAAGCCAAATATAAAGCGGATTGCATATACGAGAATGACC

ATAAATCCAGAAGCCGCGTTTTAGAGAATATAAAGCTGACTA

GCTTTCCGGGGACGCGTAACCGATTGACCGTAATG

ACAGATGGACGGTCTGTTACTTAGCCGGTATACCAAAAGCTG

AAGAAAAGTAAGTTAACAATAATAAGAGCCCAATCCAACGCT

CAGACTGGAACCGCCTCCCTCAGAGCAATTTGCCTTTAGCGT

AGAGCCGAAAATCATTCGGTCATAGCCC

TTACCATTGAATTACACCCTCCGCCAGCATTGACA

AAACCAAGTACCCTGTCATAAATATTAA

ATAATCCATTATCAAGATAACTATATGTAAGATGA

GCTGCATTAATGAAATTGGGCGGGCAAC

TCGGAACGAACCCTCACGCTGAGCCCACGCATA

TACCAGTAAACGAAGAACCGCCACCCTC

TAAAGCATGAGGCGGTCAGTATATATTTAATAGAT

GTGAAATAGATAGGCACTATTAAAGAACAATGAGTCGCTATT

ATTGTCACCAGGGTTTTCCCATGTAAAACCAGG

GTGAGCGAACGGCGGTGCATCTGGCAAACAAGAGATCTCCGT

GTAATCTACGTAACAGCGCGAAGAATACACTAAAATAAACGG

CTTGAAACAATATATTTTTAAAGAAAACAAATCGC

CCCAATAGCAAGCAAAGCCGTCAAGAACGCATGTAGAAACCAACATGTA

CATTAATTGCGTTGCGGTAAAGCGGTCCACGCTGGTT

AATAAATTAAAGCTGACAGTGCGGCCCTCCCCGATATTTATT

AGATTGTATAAGATATCGATGAACGGTAATCAGGTGTACGCC

CGTGGCGGCTCGCCTTATGACCCTGTAATGCCTGA

CAGGAAAGTAGAAGACGTGTAGGTAAAGTAAATAA

GTAGCAAAGTCAAAAAAATTTTTAGAACCCTCATAGAAAGGC

GACTCTAGGAAAGCACTATCGGCCAGCCTACATTTCACGACC

TTGACGGTGATACCAAATCGGTTGTACCTAGCATTGTGGCATATTACTA

TCTAGCTGGCGAGGAGAAGCGACGGC

TAAATGAATTTTTGGATCGTCGGGTAGC

GTAATTAATAGTAGAAAAACACTGGAGT

CGAGCTTTCTCAAAGGGGGGATTCGCTATTACG

CAGTGCCGGTAACGACCTTATCTGGCAATGCCGTT

HANDLES FOR NANORODS

CGGATGGACCGCCAAGGTAGAAAGATTCAAGAGCAACACTATAAAAAAAAA

AACAGTGCAATTACGATAATATTTAGAAAAAAAAAA

CTAATATCAGAGAGATAGCAAATAAACACAGAGCCAAAAAAAAA

AAGACAAAGAACGCGAGAAGAGCAAAAGAAATGCTCCAGAAGCAAGTTTAAAAAAAAA

TAGGGCTTGTCTGGTTCATCGTAGGATGCCCTGTCTTTCCTTAAAAAAAAA

GTATTAGGAAACCAGATGCAAATCCAATCGCAATGTTTTGCGGCCGTAAAAAAAAAA

GAAGTTTACCCTCACTAACGGAACAACACTACTGGCTCATTAAAAAAAAA

CTAAAGTGTCGAGAAGAAGGCTTATCCGGTATCATTACCGCGAAAAAAAA

TGAAACAAACATCATGGAAACTCATATTTACGTGAAAAAAAAA

AGCCCGAAAGACTTGAACCAGACTGGATGAGGGGGAAAAAAAAA

CCTGTTTCGCGAGCTGGTAATTTAGAGCAAAAAAAA

TTATAGTAAAAATCCTCAAATGCTTTAAAATACTGCGGAATCTTTGCAAAAAAAAAAA

ATTCGCCGCAGAGGATTATACCATCAATAAAAAAAA

GCGATTTTAAGACGAATCAGTGAATAAGAAAAAAAA

TCATATGTACCCCCTAAAACAAAATAAGAAATACCATTGCAAAAAAAAAAA

TAATTTGCTATTTTGCACCCATTAAATCAAAAAAAA

TAGCACAACCTGTTTAGCTATAAAGTTTACCCTAAAAAAAAAA

CTTCTGATCTTTAATAAAAATACCGAACTTGAAATCAATCGTAGAACAAAAAAAAAA

ACACCGGAATCATACAATTCTAACTCAACGGCGAAAAAAAAAA

ATTTTCGAGACCAGTATAAAGATAACAGAACAAGCGATACATAAAAAAAA

ATTTAGGCAGAGGCTTTACGAGGGTATTAAAAAAAA

TAGGGGCTCGAGGTGAACAAAACTTTACAAACAATAAAAAAAA

ATAATGCCCAATTCTGCGAATAGCGAGATTACGAGAAAAAAAA

ATATTTTCAGCAGAAGATAAATTCTGACTCTTTAGTAAATCCAAAAAAAA

RECOGNITION HANDLES

CTGATAAATTAATGAAAGGCTATCGTAAAACAGGAttTCATCCTCACACUCCGCCAUGA

GTGTGAGGATGAtttAACCTAGCGAGCGAACATGC ttAGGGAACCGAACCACGAAATCCGCGACCTACAACG

GACTAAAGACTTTTACGTAATAGGCAAAAACAAAGTGCTCCAAATCATAttGCATGTTCGCTCGCTAGGTT

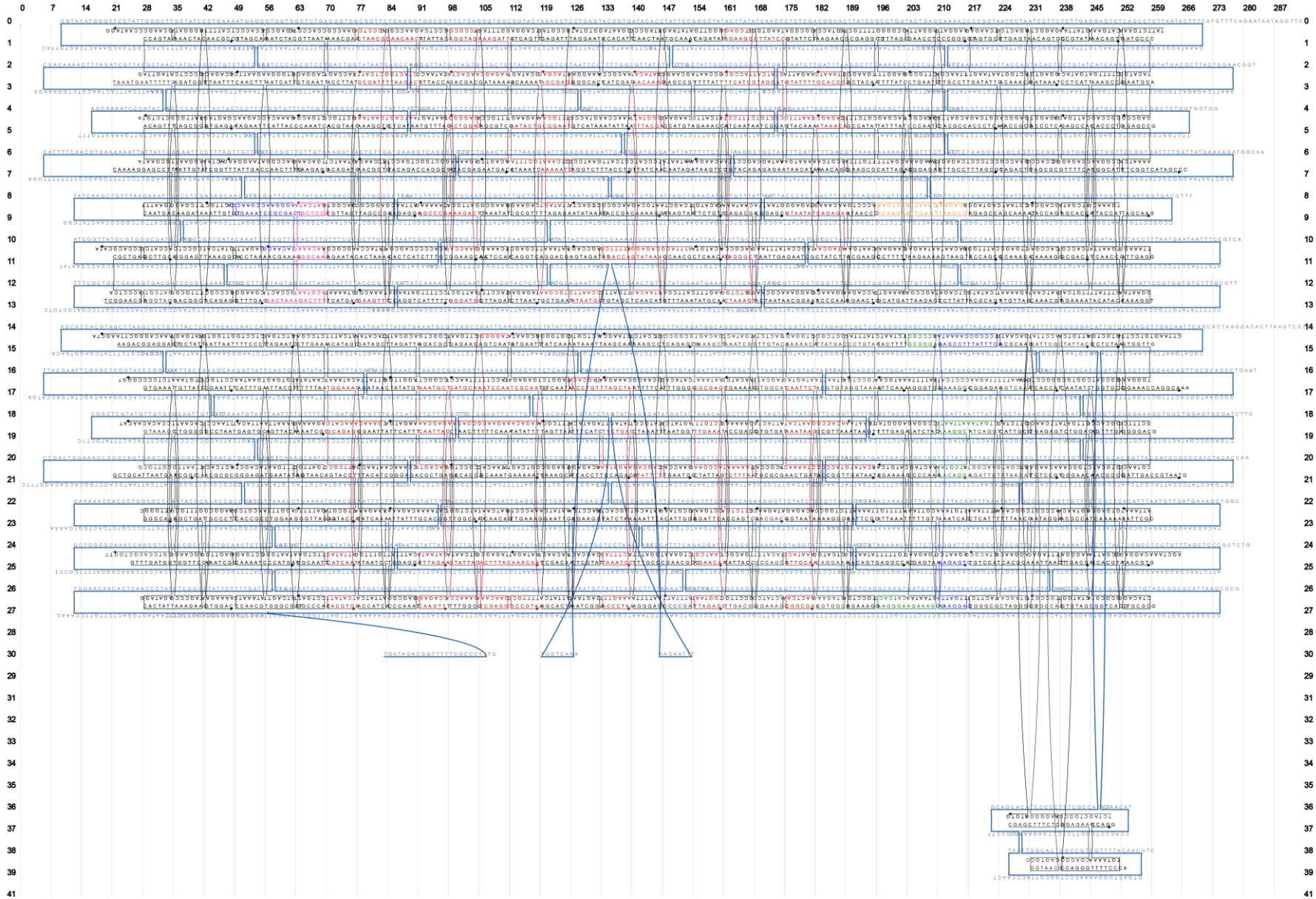

DESIGN 9 PARTICLE HELIX

CORE STRUCTURE

TAACCCCTCCTTAGCGTAATGGTAACAACCCGTCGGATTCTCCGTGGGC

GCGAACCAGAGAGTATCCAATATTAAGCAATTTAATCATTGTGGGAAGA

GTATCGTCACACTGGCTCATTATAACAACATTATTAGCTTT

GGGATAGTTTGCTAAACAACT

CCCTCAGAGCCACTGAGACTTGCTCAGACCATTAACCATCG

AAGATTACGCCTGTTTATCGCGTAGATTCGTATTAAACAATT

ACAATGATTGTTCATATTCCT

GAATTCTAAGTCAGGAGGGTTGTAGAAGAGTGA

CCTTACCAGGAACAAACGGCGGTGCATCTGCCAAATTC

CAGAAACGAGCGTCAACAGCCATATTATAGATAAT

AACCTCCCCCAGCTATGTTCAAAATAATATAATTGAGCGCTAGAAACAA

GCCCGAACGTGACAACTTTCAGGTCAGAAAT

GCACTAAATTAGACTATTTTTTAAAAATACTTGCA

ATATTGAGTTACACTCAAATATCGCCAATACTCAGAAA

AGGAGGCATTCCACTTTTGCGACCGATA

AGGTGAGGGTTCAGACTGACAGAAT

ATATTTCCAGAATCTTAAGAGCAAATATCAG

CAGGGATTTTTGCGGATGGCTTAGACATGTTTTAAATTTGAGAGG

TCAAAAAGCAAAGCCCTGACGGAGATGG

CGATCTAGGAAGTTTCCATGCTTATCGGA

TTCCAGAGGACTAATACGAAGGCTAATCAGTAGCGTAGCGCG

TCACGACTTGGGTAATTACGCGGCGATCGGTGCGGGGGGTGCCGGAAAC

ACGAGAATGACCATAGACTGG

CCCTCAACAATACACTAAAACCGCGAAA

CGGATTTAGTAAATTTTGACCCAACCTA

AGCCTAGGGGGAGGGAAGGTAAATATTGAAAA

GATTGAAGGAGAAAGTTTCAATTTCAGATGAT

GATTAAGGTTGTAAACGGTAACGGT

AACTAAAAGTTGATTCCCACTAAAACCGAAGGCTA

ATAGCGTCGTTTTAGAAGCCCGGACGTTGAATTAC

TGCGGAAAGAGGGGATAAAAACCAAAATAGC

GGATCAAGCCCACGCCTGTTGATACGCCCACG

TTCAAGCCACCCTCCACCCTCGGCCTTGCCGCCAC

GAGAGAAAGAATTAACTGATTGGAAAGCCGTCACC

ATATATCCTGAGCCTAAGAAAAGTAAGCATGA

CCAAGTATTTTGCACGACTTGATTTAGGTAGGGCT

GAGTTTCCTTAGAAACCAATCAATAATAGAA

CATCAATTAATGGAAGGGTTCCTGGCAATAGGTCT

GGGATTAGGCTGCGCAACTGTAGCGCCACCAGCCAGTATCGGGGCGCAT

TCAGCGGAACAGTTAATGCCCCCTGCCTATTT

TATTAAGCCCCGATGGGAATTAGAGCCA

TTCTGAAATAATCCACAATTCTATTAATACAAAATTGAG

TTAGTTATCATTCCGGCCCACTCGAAATCCGAGAGA

TTTACCAAAGAGCAAACTAATGTTGAGAAACGAAC

AGGGTCCGCGCATTAGAAAGGTCATTAA

ATTTACGACAAGAAGCTAATGACGACGAAAGAGAA

CCTACCATATCAAAATTATCGATTATAC

CAGGCAATGGGAAGCAGCTGGGACTCCAGAGAGTC

CGCAAATGCATTCTGCGAACGAGTAGAT

CATTGACCATTAGACTATATTTTCATACCTTCAAA

CACGTTGAAAGGAACCAAAAATTCAGGTAGAAAGA

ACAGTGCCCGTATTGCGAA

AGAGATATAACACCCTGAACAAAGTCAG

GTCCTGAAGCATGTATCATTCAAAGGAGTTAACCTCCGGCTT

AAAGAAATTAACAATAGATAA

CGTAAAATTAACGTTACAGTAGGATTCG

CTTCTTCAATAACCAAGCAAAGGTATGC

TAAGTTTTAACGGGGTCTGAGTTAA

TGAAAACACAATTTAAAACAGAACGTCAACGGAAAAAAAGGG

GGTGGCATCGTTTGAGGGGACGACGACAGCTTTCCGCCAAAA

ATTTGGGGCGCGAGGTAGCATTACTACGTTAATAATTTAGGA

TTCATCAGCAGATACATAACGTTACGAGG

TATCAGCTCTCCAAACCCATGAAATATTCATTGGTATG

TAATTGTTCTTAAACAAAATAAATCCTCCAGGAGTGTGCCTT

ATAATTAAAGCCAGAATGACGATTAGAACCGAAT

CCAGAATAATACCAACGCTTTTACA

TGTCCAGCAGAACGGTTGCTACCGCACTTCGTAGGTATATGTGAAC

CTTTTACATGTAAAGTAATTC

CGTAACCGATTGACTGCT

TACTACAGGCAAACAGGTTGATAAGAGGTCTGGCGTTGT

TAACGGACCAGTCAGAAAGACGTCAGAATCAGGTCGGC

CGAGTGCGCCGCAGTACACCTCATAGTTAGACGAGCAGG

AATCAATAAACATAGCAATAGCTATCTTACCGTT

TATAAAGACATGTACGGGAGGCGGTATTGCAAATCATTTTCA

GAAAAGGCGAATTTTAACAACGCCATACCGACAAAAGCGGGA

CCTGATTGCTTTACGGCACAGACGAATACAGATAATTT

TCACGGCCCACGACTTAAGTGGCTTCTATCGC

AAAATACACAAAGATTAAGAGATTCGAGCACATTCACACTAT

CTTATGCTGGGCTTAGAAACAAACGTAAGAACCGG

CAACTCGCTGAGGCTTGTAGTAAATGATTTTAAGAACAATGA

CACCACCCTCAGAGATATTCACAAACGCTAGTTTAGTACCGCATTTTCA

CAGAACCCCTCAGAGAACCGCGCCATCTGGTCAT

CAACAGCAGAGGCATTTTAATTTAGCG

TAATTGAATACAAAAAGCCTGAAGGCGTTCTGACCTAAATTTAAT

TTTCACATCAAGAAAAATATGCGTTGAATCGCCATATATTCA

CAAAATCAATCGTCTGAGGGAATACCAAGTTTTTAGGA

GTAGCCAGCTTTCATCAACATTTTGGTTTAAC

AGAGCATTAGCAAAAAATCATAATAGTACTGAAAA

TTTAATTTCAACTATAAATAA

TATTCGGAACCATCCGATAGTGTGAATTATCGGTT

CCCTCAGAGCCATAGGGGAACCAGAGCCCGTACTC

AAACGCAAGCCGCCACACCACCAGAGCCGC

AGTATAAAGCCGTTACCAGAAGGAAACCGAGG

GAAACAAAATTACCCGCGCAGCAATAACACAGTAC

CAATAGGAATTCATGCGCATGCATTTCCTGATTGGCCC

CATCAAAAATAATTCGATGTTCTTGTCAA

GGCTTGCGGATTGCATCAACTTTGCTGATTAAATGTGAT

GAGTTAAGCGAAAGACAGCACCCAAATCCCAGAACTATT

AACGGAATATTACGCAGTATTAGCGTTTCTCCCTCAGCCCGGCCACCCT

AATTACGCGAGGCGTTTTGATTTTTTAACATATAAAATTC

CATTTAAGAGTAACATTATCACAAAGAAACCACCAATCAGA

TTTTTGTTAAATCAGCTCATTTGGACGGGCAACTAAATTGTAAAC

CGGGAGAACATTATCTCCTTTCAGGATTAGACCGGTGTTTAGTACATTT

CTCAGCAAGGCCGCAGACAGCAACTACAAATAGGAAAAAAAGATTTTTT

ATCAAAATCACCATAGAGGCTTTATCGGCATTTTCTTTCATA

AATAAACACCGCATGATTAAGACTCCTTACCCAACAAA

GATAAATTTTAGTAGCTTATCTTTTGAAGCCTTTCCTTT

GTTAATATTTTGTTTTCAAAAAAGC

ACAACAAAGCTGCTCATTCAGTGATACTTTTG

ATATTCAATAGGCTTTTACCCAAACAGT

ACGAGGGTAGCAATTCATGAAAGTTTTCTAATCC

AGCCCCCTTTAGCGTGATATAAGGGGTTTCCTCAAGATGAAAG

TTTTCGACGAAGTGCCGTCGAGTATCACACCACCGACCGCCA

CGGAACTTATGTTAGCAAACGTAGAAAAACGCAAACCAAATAAAATAGC

AATATATTTTAGGCGTGCC

CCTTACATAAGAATTACCTTTTTTAATACCGACCGTGT

CAGCACCCCAAAAACAGTAAGCAA

GAAAGGCCGGAGACAGTCA

ATTCAGGACAGATGAACCTTCATCAAGAGTTATATAAA

ATACGTAAGAGGCAAAAGAATCATAAGGGCTAAACGGGTAAA

CAAGTTTCAATGAACCATTAGGCCATTTTTAGAGC

GTCACAACAACCGATTGAGAAACGTCACGCTAAGTTTATTTT

ATATGGTTTACCAAAACTTTTTCC

CTTAAGACAAAAAATGCTTACCTTTCGGGCGC

TGATAATCAGAAAAGGGAAGAGAATC

ACCCTCGTAAAATTGCCTACGTCAA

ACTTTGAAAGAACCGTTCTAGCTGATAATCAATACAATGCCT

AAACGAAATGCCACAGACTTTCGGCTACCGTCACC

ATAGCAGCACCGACCCATCACCAGTAGCTACCAGG

CGACATTTCAATAGAAAAGAATACAT

GCGAGAGCGCCAAAGACTTGGGTTA

AAGTGTTTTTATTAGATTAAGACGCTGAGCCAATCGCAGAA

GATGAAACGACGGCCAGATCTGTGCTGCAAGGC

GTAGCTATTTTTGCTAGCTCAAGCTTAATTAATTGGACCCTGAAGCCTC

CTTAGCCGGAACGAGGCGCGATTTGTCAAGTTTTTTGGGGTCG

TATAACAATCATTACCGCTTGGTTAAA

AATCAGAGCGGGAGCAACCCTCAATCACATTTGAGA

TGGAGCAAACAAAATATTAAAGAACGTGCGAAAGG

TCAGGTCACTAGCATTCCCAG

TCTACATCTATCAGGGCGATATATAACGTACGGT

CTGATAAATTGTGTACGTGAACCATCATAAAATGTTTAGTTACCCTCG

CAAAGTACAACGGAAGACGGTATGCTTTTGCGTAA

GCAAACAACCCTAAAGGGAGCAGCAGTT

GACTTGACAAGGCCGATTAGCGTATTTATCCCAATGACACCA

AGGTGAATTATCACCGGCGAA

AGGTTATAAGGGAAGAAAGCGCAAGAACGGGTAAACATCCTA

GAGAGACGATGCAACGTTTTTGACGGAATTTTGAGTCCAAAATTAATTA

TAACGTGCTTTCTTATCAAAATCAGTGTAGCGGTCACGCTGCGCG

AGGGCGACTTCGCTACGCCAGCTTGACAATGTCCCGGCACCG

CGGAGCGATTATACCAAGACTCATCGAATTTTGTCGTCT

TTGACGGCTGAAACAGAAGGATACCGCCA

CGTGGCGAGACGGGTAAC

TAGGGCGGGCTGTCAACAAGCAAAAATC

HANDLES FOR NANOPARTICLES

CAATAGCAACTAAGAACTAGAAATTCTTACCAAAAAAAAAAAAAAA

AATTTGAGTGATCAGTGAGGCCACCTGAGAAAAAAAAAAAAAAA

TGAAGAAACGCCAGTTAAAGAACTGGGAATCATAAAAAAAAAAAAAAA

TGATGGGCATAAGAGTCAATAGTGAATCTCGTTAGAAAAAAAAAAAAAAA

GTCTGGAAATGCTGGACCTGCTCCATGTTAAAAAAAAAAAAAAAA

CGGAACCTATACCCACAAGAATAGTGCCTTGAGTAAAAAAAAAAAAAAAA

CATAGTGACGACGGTAATAGCCCAAATATCATCGCAAAAAAAAAAAAAAA

TAATAGCTCCAAAAGGAACTGGTAAAAAAAAAAAAAAAA

AAAGAATAAAGCTAAATCGGTCTGGCCTTCCTAAAAAAAAAAAAAAA

ACCAAAAAGCCTTTATTTCAATTCGCATTAAAAAAAAAAAAAAAAA

GCCCTAAGCGTCATACATGGCTTTTGATGAAAAAAAAAAAAAAA

ACATAAAGGTGTTAATTTCATCTTAAATAAGAAAAAAAAAAAAAAA

ATATTAGACTGCCAAGCTTTCTGGTTGTGAACGCAAAAAAAAAAAAAAA

TGACGGTGTACAGACCAGGAACCGAACTGACCAAAAAAAAAAAAAAAA

TGGTTGCTTTGACGAGCACGTAAAAAAAAAAAAAAAA

AATAATAATAATAATCAAAAGAAGTTTTGCCTCGTCATTACC

AATAATAATAATAATGAGAGGCTTAACAACTAAAGGAATAAGTGAGAAAT

AATAATAATAATAATCTGAATTTACCGAAGCCCTTTTTCGAGCCAGT

AATAATAATAATAATCAGGAGGTTGAGGCAGGTCAGGAAAGCGCAGTCT

AATAATAATAATAATCGCCAGCATGATAGCCGAACAAAAACGCT

AATAATAATAATAATAAAATTTTTAGAACCCTCATATATAATCTTG

AATAATAATAATAATGGTTTGAAATGGAAACAGTGCTTCTGTAAA

AATAATAATAATAATGAGTAATGTGTAGGTAAAGAAAAACGCAAGGATA

AATAATAATAATAATTCGTCGCTATTAATTAAGATATAATTTTCACATC

AATAATAATAATAATAATCACCAATTAATGCCGGTCAATCATATGT

AATAATAATAATAATTCCTTGAAAACATAGCGATAGCTAAATAA

AATAATAATAATAATAGGTGCCGTAAAGCACTAATAGAAAGGTTG

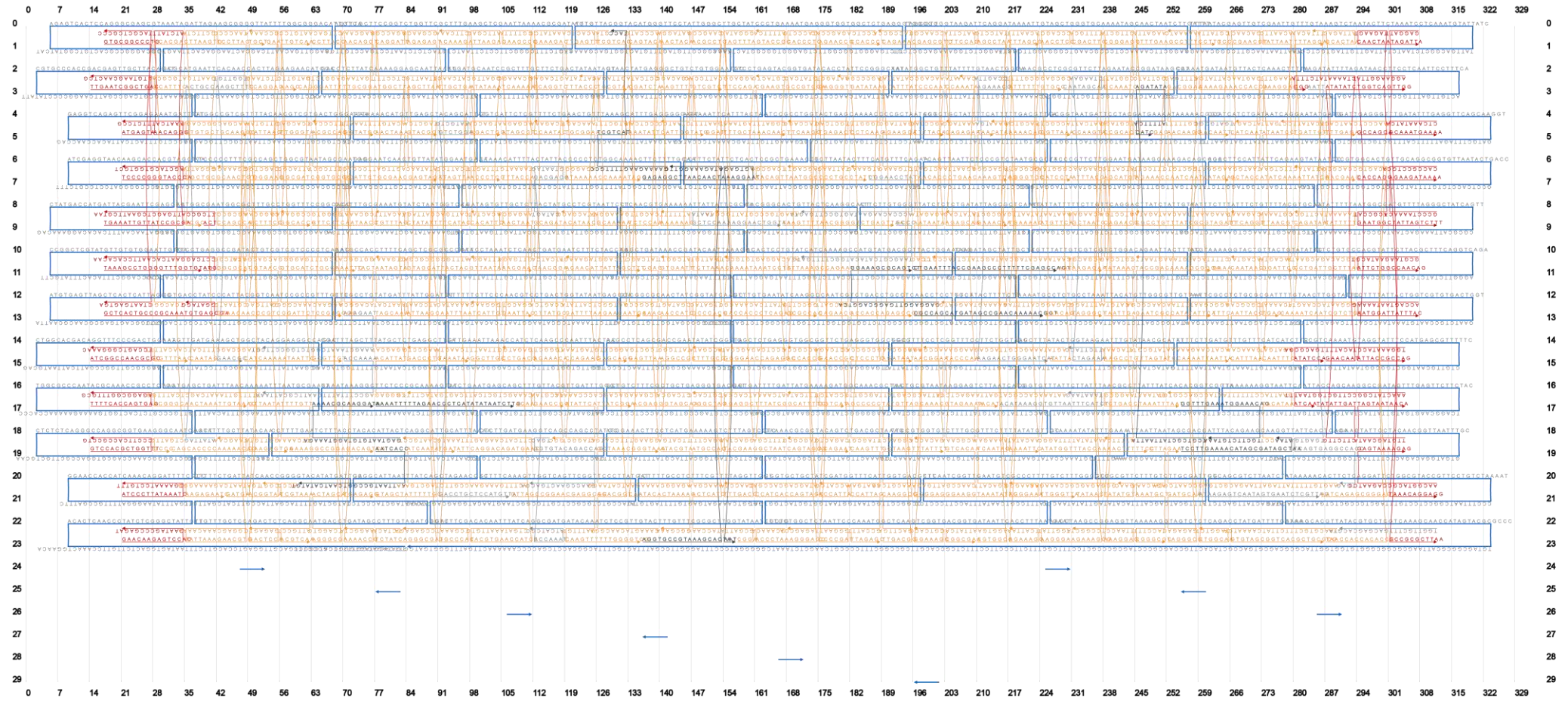

DESIGN 6 PARTICLE HELIX

CORE STRUCTURE

TTTACCGCGAAACAACATGTT

GGCACCGAAGATCGAGGCAAATAACATCTTAGCTACAAATATAGCATGT

TCCGGAATCATTTTTAGTTAATATGCGAATCGCAGAG

GGCCAATGACAACAACCGAATTTCCCACCCTTAGCCCGCCACAGA

GGCTTGCTTCAAAGCGAACTTTCACCAGAAGTACAGGCGCAG

CCAATACTGAGAGGCTATATAATTTGTACCTTTAATTCATAACG

GCCGAACCCTTTTTAGAATTGGCTAATAAACAGGGAAGCGCACAGA

CAACAGTCAAGCTTTCTCACGCCATTAAATTAACA

TACGCTCGATGGTGGTTCCATACATTATGTGCGGGTCCCAGT

CAGCGATTTTGTATAACACTGTAGCATTGAATAGGACAACTAAAAATCT

TAACTGAAAATGAAAAAGCCTGAAATACTCTTCTGATTTTCACATCGAG

AGAACCCAACGCTAAAACGATTTTTTGTAGTAAATGATTTTA

AATCATAAGAAAACAAAATTAATGATGATTCCATAAGACAAATGGG

AATGCTGAAGATTGTTTGGATACGTAAAACAGATT

TAACTGACTATTCAGAAAAAGAACTGGCATGATCATAAAGGCGCA

TAGGGTTATGGTCATAGCTTCACTGCTTGTTACCT

AGGCTTCTGGTCAGGCTGCGCAACGCTATTACGGTTGTCGGG

CGGAAGCGAGGTCACACATTCACACTATCACTCCA

TCCAGAATCGGCCAACGCG

TAAAATAGTCAGTTCTTGCTTTTTTAATTTAACAA

TTTTAACGAGTAACGCATCAAAAGTGAATTTATCAAGGTTTG

GCACCAGAAGGAAACCGCAATAGCATAAGAGAAAGTCAGGAGAAT

CCTTATGACAATGTCTATGATCAGCAGGAAAAGAA

CGTAACCTTCTCCGTGTGAGCCAATAGGTTGTTAA

CAAGCCAAGAAAACGTCTGGATCAACAGATAAGAGGCAGATA

TCCGGAATTATCATCATATTCAATAAAGTT

GATAAATTAATGTGGTGTAGG

AGTTTAGAATGAATAACGGCAAATCAACAGTTGAAAAAAAATATA

ATGTTGTAACGAAAATGAAAACAGTTTCAGCGG

ACAATGAATCGTCAATGACCA

TCAGAGCCAGGTCAGACGATTGCTAAACTGCGAATATAAGTACAGAACC

ATCCTCCCGTCGGAGTGCATCTGCCAAAACCACCACAATATA

GGGAATAGTACATTAAATGGGAACAAACGGCGTAGATGCCTC

TCAGGTTTGTCACCATCAATATGATATTATCTACATTAGTTTATTT

CGTCATATCTCTGACATAAA

TCCACCCATGGAGAAGCCAGGTAGTGCTGAATTATACGTGGCCTAAAAC

TTTCATTCAATTACCAATTCTGGTGATGCAAATCCCCTTTTA

CACGACGAAATGAATAAGAGGCGGTTTGTGATTGC

CCCGCTTCTAATCAAAGGGCGATATTCATGCGCACAAATAAC

GGTTAATAATCCGGCTTAGGTGAACGCGGATGAATTTGCTTT

GGGTGGTTTTTCCGCCGCCTG

TAGAAGATGTCCATGGGTCGAAGGGCGAAGTTTTCACCAGTGCAAGCGG

ATCAAAAATATGCAGAAAGTAATTCTGTCCATTTAGGCCATATTTTATG

CGATAAAAACCAAAATAAAGG

TCATTGTGGGAAGAAAAATGTCACAGAC

GCACACTCCATAGGTCACGTTGGTGGATTGACCAGCTTTAAT

AACCTGTCAATAAACCTGTAGCCGTAATGGCGGTG

ATTAGTTGCGCCGATTGCAGGGACTACGTTAATAATTTAGGA

GTTTTCACCCAGGTGATAACATA

GCTCATTCAGTGGAAGCGCGAAATGGCTGACCTTCCAAAGCT

TGACGCATGGAAATTCACCAGTCACACGACAGTGCAATCGGC

TAGGCCATAGCAAAGCGGATTTTCGAGCCCTGACGGAGATGG

CGGCAAATTTGGAAACCGAGCTCACAATTCAATCG

TTGCCAGAAGTATTAGACTAGATTAGACGCTGATTTTCCCTGAT

GGCACGACTCTGACCTCCTTTTCGAAAT

AACCGACCCTGAACCAAGAAAAGTATCAAACAACGCTCAACAATCCTAA

CCAAAGCTTCAGGTAGAAAGATTCATCAGCAGATAGCTCCTTAGCT

CGTACTAGAAAATAGCACCAATCCAAATAAGACGA

TAAGAACGCGAGGCGTCGTTTTTACCTAAAGCTG

GTAAATCAGATATATAAATCAAGGAACCTACCATAGTTTAAC

GGTAACGCCACCTTGCATTTTAATCAAAAGTCTAGCT

TCCCTGAGCAGAGGCGAATTATTCGAGGAGA

CAGCAGCTTGTAAAAAGTGGTTGTGACGGAACCGC

GAGGTTTCCACCCTTAAAGGCGTAGCAACGTTTAA

AACCAGGGACGACAAAGCAATTTCTACTGCGCGAGAAAACAGCCGGTTG

AACAAGCAGGAGCATGTAGAA

CAATAAGTGCTAACAACTAATTTACAAA

AGCCCTTCAGAGGACAGATGATGACAAG

AAGATTCTTATAATTGAAACTAAAGAACAAGGGCTGTCTTTCCTT

CACTAAAACACTTGTGTCTGCCTTGCAGTAAGGGTTGATAACACCC

TAAGCATCAAACAGACCGGGAACC

AAAGGAGGCTTGATACCGAACTTCTCAG

CTCAGGTAGTAACCGATATATTCGGTCGGCGGGATCACCCTCGCCCAAT

AGAGATATATGGCTCATTATAACAACAT

TACTTAGCCGGAACGAACGGAGATATACCAAGGCACC

GGCGTTAATATTTTCGTCTGGCCGGTTGGTGTAATGATCCCC

CACATTATTAAAGTTCCAGATCCCTTCTCCGAAATATAGG

AGAAGATACAGCTATTTAAGAGAATCGATGA

TACAAAACGCCTGAATACAGTTTTTCAGTCAAAAT

GCCACCTCATGCTTTCGAGGTATCGCCC

TTTAACGCCATCAAAAATCATCAAGTAG

TTTGCCCACCGACCAGTAATAGAGTCAA

ATCATATATTAGATAAGTCCTGTACGGTTTTTTCAGTTAAATTAG

TATTATAGCGAACCTGAATCTATGGTTTGTGAAAGACTTCAAGAGTTTA

TACGAGCTATCCGCTCGAATTGACGGAGGAGTAAA

GCTCCAGTATATAAACAAATAACATAAACAG

CAATCATAGCAAACTTGAGAGCAACCGTGGTGAGA

GAGCCGGAATATAAGGCAATATATACCGCGCTATTAAACCAAGTAAATA

AACAACATAAAGTACCGACAAGCCAGTATAGG

GATTATGGCGAATCGCCATTGCCGGA

CAGCTAAATATCCCTGTTTTAAATTTCACGACCGTCTACAATTCTTTCC

TAGCCCAAAAATCAGGTAAGAGGA

AATGTTGAGAAACGAACTAACGGACCAGTCAAACAGGTGTTT

ATAATCAATTCATTGCCTGAGAGTCTGGATGTACCGAAGATTTAAA

CTGGCCCCCTGTTTGCCCTGGCCATCTGTAAGCAACTCGTGAGCCTATT

AATGGAGCTGTAATGCCTGAGAAATCTA

GGGTGCCACTTACAGAGGCTTTGAAACGAGGCGCTTTTCTGA

GGCCTTGGGCCCTGAGTGACTCCCGCCAGACTTAA

ACGGTCAATTAAGAGTTGCTTTAAACAGTTATAGT

GCATAAAGTGTAAAGCAGGTT

AACAATAACGGATTTCGCGCAAAAGAAGATTACATGGAAACAGTACATA

AAGGCCGTAGAACCATTTCAAGCATAAACAAAATTGTATCGGGGCGCAT

CAGAACATGCGGATGAGGGGGACCCTCGTTTACCAAAGAGCAAACT

AAACTATAAAAACGCCGTAAAAGGCTGG

CGTTGAATTACCTTATGCTGGGC

AACCTAATACGTAAATAGCAAAGAGCCAAGTACCGTTAAACACCTTTAA

CTCAAATATCAAACCCAAATTTTGAGACAGTCAAAAA

AAAAGAAGTACTGGATTCATTGA

TAAATAAGCAATAATAACGGACCAACTT

TCGGTTAAAATTCGCATGTATAAGTATT

CAGGGCTATCATTTATAAATCCGAAAATTGAGAGATTCTTCTACGACGG

TGTTTAGTTTGCCAGGCTTAGTTGATAAAAACTCCGGA

ACGCACGCGTTTTCTCAAAATCCTCAAG

TAGCCTGCTCATTTCACATAATAAGCTACGTGGTC

ATCAGCTAGCCCCACTGAAAAGCGAACGATGCTATTAATTAAGAAGAGT

TGAGTAAACCTTTTTAACCGAAAAGCCAACCCACAAAGAAAA

TAAAGATATGCAATACTTTTGACCAAAAACAG

TTATTTTCGAAAGGTAACGCGCCTGTTTATC

CCAAAAAAAAGGTATAGAATAGAAAGGATGTATCA

TGTGAGTCCTTGAAAACATGCAGTTTCAAACAAACACCAAGT

AGACTGTCACCAATAGGCTGACCGTATAGGGTCAGGATC

TTGTATCCACGTTGAAGGAATAACTTTCTTTTCTG

ATTTATACAACCCAATATATCTTACCGAAGCAAAG

ACCTGTCGGTGCCTACGTCAAGGCGAGA

ACGTCAAACGATATTCATTACCCAAATCCCAGAACATATCGCCAGGATT

GTGGAATTGAGGAAAATAGAT

ATCCCCCTCAAACTAGTAAAA

AAAGACAGCATCGGGGACTAAGGTAAAAAACGAAATGACCCC

CCTTCCCAGTCCACTAATTGCCACAACA

TATTTGCTATACTTTATAACTAGGTCTGGATTAAGAGCCGTCGGTTATC

TTACCTTCTGTAAATCGTCAATCAATCA

ACGGTCAGTCCGGAGAGGGTATTTCGCA

AGATTTTGCGGAACAAAAATCATATATGTA

CATCGAACAAATAAAGAAATTGCGTAGAAACAGTAAATCGCATAAC

TGAATCCGCGAATACATAATTTACCTTTTGGCCTTGATATTCACAA

TAAAACTTTAAATTGTAAAGTCATCAAT

CAATTAAGCGCCATAGGGGGACCTCAGACGCAAGGAGTAGATAAGGCTA

CCAGTGCGCCACGCGGCGCCAATTAATGTCGGGAA

AAGCATCAGGGTTTCCTCTTCTGTTGGGGCTTTCC

GATCCAAGAACGGGCCAATAG

TTGCCAGTTACAACTGATTATCAGAATGGAAG

GTGTCCTGTGGATGGTTGCAGAGAC

AGGAATATTAAACGAGACTTTTTCATGAACCAGCG

TATTAATTTTAAAATCAGAGAGAATTTGAGGATTTCGAACGT

AGAGCCTATTTATCGCCTTTATTAGACGGAGGGTAATTGAGCAGTT

TTTAATTTCAACGCACAATAA

TGAAAATGAAATAGAGGAAACCATGTAAGACGACG

TTAGAAACAAACGTAAATCAAGAGTAATCTACG

ATTTTTTGGTTTATCAGCTCCGGAACCACCTCAGAGCCACTA

AAGAATAGTTTCCAACAGTGCGACCTCAGAACCGCCGTCACC

ACGTAGAAACCTGCTCTGATAAATCATCTTGAGGCAA

AGTGAATTTCCAGACGTTAGTTCTAAAGACGCCTGAGTTTCGTTCA

CGATAAACGTAATCGAGTGTTGAACGTGCAACAGCCGTATTGTGAGAGC

HANDLES FOR NANOPARTICLES

CGGGGATCGCTCACTGCCCGCTTAAAAAAAAAA

GGGGACTCCAAATGAGTGAGCTAACTAAAAAAAAAA

TCCTGTGTGAAATTGTCGGAAAAAAAAAAAA

ATATCTGTCTTTAGGAGCATGCTGCAAGGCAAAAAAAAAA

CATGAATTAGGCTAAATCGCCAGCAGTTGAAAAAAAAAA

TTCGACCATTAGCCTTTCTCATATTGAACAAAAAAAAAA

TTACTGAATATGATGGCAATTCATGAAGGAAAAAAAAAA

AATACTAACAGCGATAGCTTAAGAGACTCATTAAAAAAAAAAA

AGGGGACCACGACAACTCGTATTAAATCCTAAAAAAAAAA

CCATATTAATTTGCTATTTTGGAAGCCTGAAGGCTTAAAAAAAAAAA

GCGTTTATCCTCCCGACTTGCGGGAGAAAAAAAAAA

ACCAATCCCGCACTTCGTAGGTATTCAAAAAAAAAA

GAACTGAATACCCAAACGAGATAAATATAGCGTAAAAAAAAAA

GTGTAAAGATTCTTTACCTTGCTGATTTGCAAAAAAAAAA

AATTACGAGGCATAGTGACGAAAAAAAAAAA

CAGCCTCAGCCCATGTACCGTCATCGCCCATGTAAAAAAAAAA

CCGTATTAACTACATTTTGTCCTCCTTATTACGCAGTAAAAAAAAAA

TATGGGAGTCTCATAGTTAGCAGCAAAAAAAAAAAA

ENDCAPS

CCCCGAAAGGAGCGGGCGCTAGGAACCACCACACCCGCCGCGCCCC

GTCACGCTGCGCGTGCGCTGG

CACGCAACCACCGAGTAAAAGCTGATTTTAGACAG

CCCCAGCGACAGAATCAAGTCAGCACCGTAATCAGTCCCC

CCCCTTTGATTAGTAATAACATCACTTGCCTGAG

CCCCGATAAAACAGAGGTGAGGCGGTCAGTAAATACCGATA

CCCCATATTACCGCCACCCTAAAGGGAGCCCC

CCCCAAGTGTTTTTATAATCACGCCAGAATCCTGAGCCCC

AGAAGGATTAGGATCCATCTT

GCCACAGACAACCTGAAAGCGTAAAAAGGGA

GGTGGCAACATATAAAATGGAAACAAATAAATCCTCATCCCC

AGCGCAGCATGGCTTTTGATGATACAGGAGCCCC

ACAATCAATAGAAAATTAATAAGTTTTAACG

CCCCTACCAGCGCCAAAGACAAAAGGGCCGATTGAGGGAGGAGGTGAA

CCCCTAAAGCCAGAAGAAACGCCCCC

CCCCGCTCAGTACCAGGCGGATAAGAACCACTCAGAA

CCCCTATTAGCGTTTGTAGCGGGGTTTTCCCC

CCCCAGAACCCTTCTGATATTTTTGAATGGCTATTCCCC

CCGCCACGAGCCACCACCGGAACCGCCTCCCTCCCCC

CCCCGGAAATTATTCATTAAGAAGGTAAATATTGACCCCC

CCCCTCAGAGCGGGAGCTAAGCTTTCCTCGTTAGAACCCC

GAACGGTAGTGAGGATTAACCGTTGTAGCAATACTTCCCCC

GTTGACGTGCTTGCCAGCTGC

CCCCGCCAGCATTGACAGGAGGTTGAGGCGCCACCAGTGCCGTCGAGAG

CCCCAGTCTTTAATGCGCGAACTGAACGAACCACCAGCAGAACCCC

CCCCCCCCCGATTTAGGAAAGGAAGGGAAGAAAGCCCCC

CCCCCTTAATGCGCCGCTACAGGGCGCGTA

CCCCGAAATGGATTATGCCAACAGAGATCCCC

GGCGAACGTGGCGAAGCTTGACGGGGAAGCACTAA

CCCCATCACCAGTAGCACCAAATTAGAGCCAGCAAACCCC

TTATCACCGTCAAACATTCAACGA

ATCGGAAGCCATTGTTTTGACGCTCAATCGTCTCCCC

CATTCTGTTACATTGGCAGATACCTACACAA

CCCCAAAGACACCACGGAATAAGTTTATTT

CCCCTGTACTGGTCATATGGTTCCCC

GGCCGACTTGAGCCATTTGGGTTACCATTAGCAAGGCCGGAA

CTATGGTAGCACGTATAACGTACAGGAGGCCGATTAAAGGGG

CCCCAGAGCCGCCACCCCACCAGAGCCGCCCC

TTCATAAATCGGCATTTTCGGTCATAGCCCCCTCCCC

CAGGCGGCCTTGCTGGTAATATCCAGAACACCCC

CCCCCGTGAACCATCACCCAGGGCGATGGCCCACTACCCC

GAAACCATCGATAGTTGCCTTTAGCGTC

CAAGTGTAAAACCGTCTATCAAATCAAGTTTTTTG

AACAGTTAATGCCCATGAAAGTATTAAG

CCCCCCTATTATTCTGAAACCCTGCCTATTTCGGAACCCC

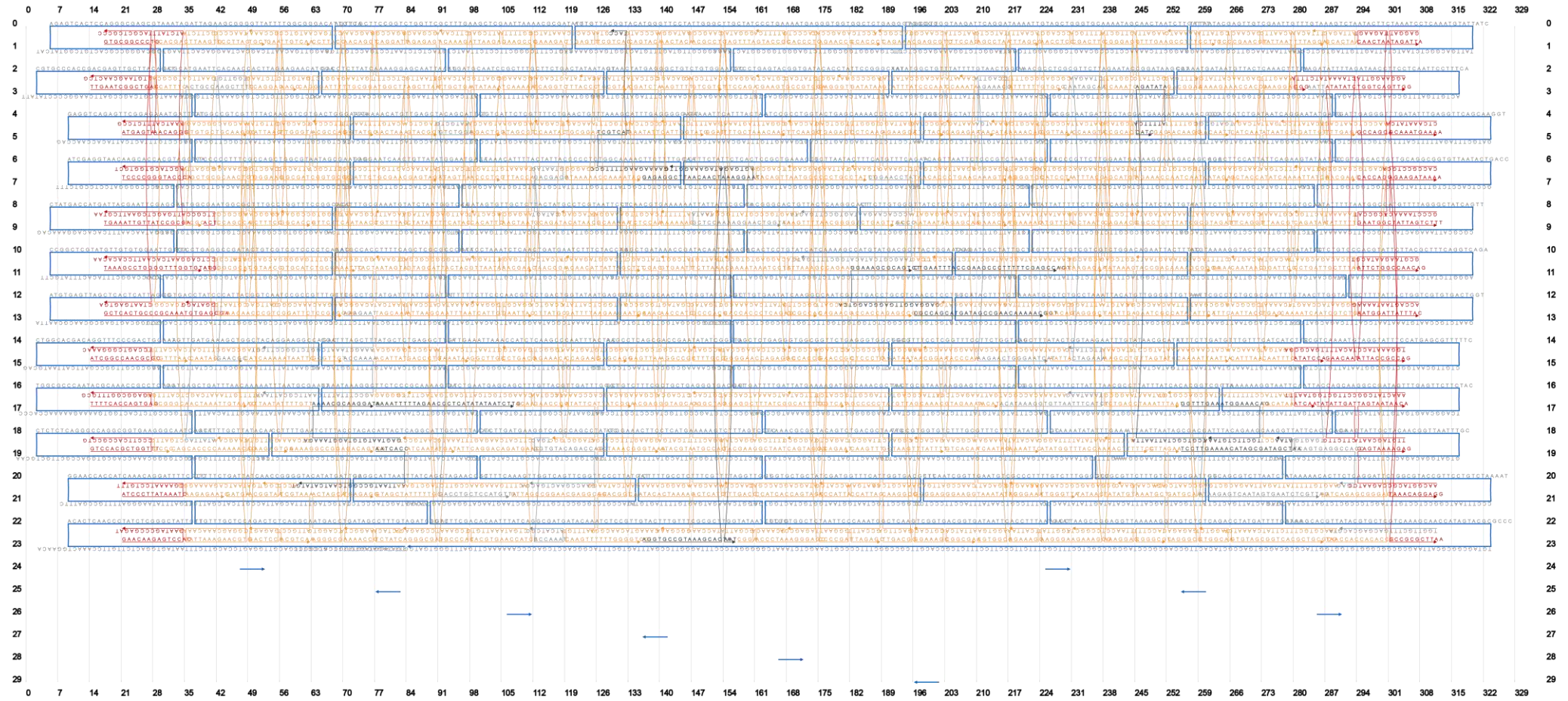

BIBLIOGRAPHY

[1] Michael Faraday. "X. The Bakerian Lecture. —Experimental relations of gold (and other metals) to light." In: *Philosophical Transactions of the Royal Society of London* 147 (1857), pp. 145–181. DOI: 10.1098/rstl.1857.0011. URL: http://rstl.royalsocietypublishing.org/content/147/145.short.

[2] Martin A. Schwartz. "The importance of stupidity in scientific research." In: *Journal of Cell Science* 121.11 (2008), pp. 1771–1771. DOI: 10.1242/jcs.033340. URL: http://jcs.biologists.org/content/joces/121/11/1771.full.pdf.

[3] K. Sanderson. "Bioengineering: What to make with DNA origami." In: *Nature* 464.7286 (2010), pp. 158–159. ISSN: 0028-0836. DOI: 10.1038/464158a. URL: <GotoISI>://WOS:000275366100013.

[4] Thomas Schlichthaerle, Maximilian T. Strauss, Florian Schueder, Johannes B. Woehrstein, and Ralf Jungmann. "DNA nanotechnology and fluorescence applications." In: *Current Opinion in Biotechnology* 39 (2016), pp. 41–47. ISSN: 0958-1669. DOI: https://doi.org/10.1016/j.copbio.2015.12.014. URL: http://www.sciencedirect.com/science/article/pii/S0958166915001779.

[5] Friedrich Miescher. "Ueber die chemische Zusammensetzung der Eiterzellen." In: *Medizinisch-chemische Untersuchungen* 4 (1871), pp. 441–460.

[6] Albrecht Kossel. "Ueber Nuclein der Hefe." In: *Zeitschrift für physiologische Chemie* 3 (1879), pp. 284–291.

[7] Oswald T. Avery, Colin M. MacLeod, and Maclyn McCarty. "Studies on the Chemical Nature of the Substance Inducing Transformation of Pneumococcal Types : Induction of Transformation by a Desoxyribonucleic Acid Fraction Isolated From Pneumococcus Type III." In: *The Journal of Experimental Medicine* 79.2 (1944), pp. 137–158. ISSN: 0022-1007 1540-9538. URL: http://www.ncbi.nlm.nih.gov/pmc/articles/PMC2135445/.

[8] A. D. Hershey and Martha Chase. "Independent Functions of Viral Protein and Nucleic Acid in Growth of Bacteriophage." In: *The Journal of General Physiology* 36.1 (1952), pp. 39–56. ISSN: 0022-1295 1540-7748. URL: http://www.ncbi.nlm.nih.gov/pmc/articles/PMC2147348/.

[9] Linus Pauling and Robert B. Corey. "A Proposed Structure For The Nucleic Acids." In: *Proceedings of the National Academy of Sciences of the United States of America* 39.2 (1953), pp. 84–97. ISSN: 0027-8424 1091-6490. URL: http://www.ncbi.nlm.nih.gov/pmc/articles/PMC1063734/.

[10] J. D. Watson and F. H. C. Crick. "Molecular Structure of Nucleic Acids: A Structure for Deoxyribose Nucleic Acid." In: *Nature* 171 (1953), p. 737. DOI: 10.1038/171737a0. URL: http://dx.doi.org/10.1038/171737a0.

[11] Web Page. URL: http://www.exploratorium.edu/origins/coldspring/ideas/printit.html.

[12] Rosalind E. Franklin and R. G. Gosling. "Molecular Configuration in Sodium Thymonucleate." In: *Nature* 171 (1953), p. 740. DOI: 10.1038/171740a0. URL: http://dx.doi.org/10.1038/171740a0.

[13] M. H. F. Wilkins, A. R. Stokes, and H. R. Wilson. "Molecular Structure of Nucleic Acids: Molecular Structure of Deoxypentose Nucleic Acids." In: *Nature* 171 (1953), p. 738. DOI: 10.1038/171738a0. URL: http://dx.doi.org/10.1038/171738a0.

[14] Marshal Mandelkern, John G. Elias, Don Eden, and Donald M. Crothers. "The dimensions of DNA in solution." In: *Journal of Molecular Biology* 152.1 (1981), pp. 153–161. ISSN: 0022-2836. DOI: https://doi.org/10.1016/0022-2836(81)90099-1. URL: http://www.sciencedirect.com/science/article/pii/0022283681900991.

[15] Web Page. URL: www.wikipedia.com.

[16] Robin Holliday. "The Induction of Mitotic Recombination by Mitomycin C in Ustilago and Saccharomyces." In: *Genetics* 50.3 (1964), p. 323. URL: http://www.genetics.org/content/50/3/323.abstract.

[17] Nadrian C. Seeman. "Nucleic acid junctions and lattices." In: *Journal of Theoretical Biology* 99.2 (1982), pp. 237–247. ISSN: 0022-5193. DOI: https://doi.org/10.1016/0022-5193(82)90002-9. URL: http://www.sciencedirect.com/science/article/pii/0022519382900029.

[18] Neville R. Kallenbach, Rong-Ine Ma, and Nadrian C. Seeman. "An immobile nucleic acid junction constructed from oligonucleotides." In: *Nature* 305 (1983), p. 829. DOI: 10.1038/305829a0. URL: http://dx.doi.org/10.1038/305829a0.

[19] Chengde Mao, Weiqiong Sun, Zhiyong Shen, and Nadrian C. Seeman. "A nanomechanical device based on the B–Z transition of DNA." In: *Nature* 397 (1999), p. 144. DOI: 10.1038/16437. URL: http://dx.doi.org/10.1038/16437.

[20] Nadrian C. Seeman. "DNA in a material world." In: *Nature* 421 (2003), p. 427. DOI: 10.1038/nature01406. URL: http://dx.doi.org/10.1038/nature01406.

[21] Bernard Yurke, Andrew J. Turberfield, Allen P. Mills, Friedrich C. Simmel, and Jennifer L. Neumann. "A DNA-fuelled molecular machine made of DNA." In: *Nature* 406.6796 (2000), pp. 605–608. ISSN: 0028-0836. DOI: http://www.nature.com/nature/journal/v406/n6796/suppinfo/406605a0_S1.html. URL: http://dx.doi.org/10.1038/35020524.

[22] Nadrian C. Seeman and Hanadi F. Sleiman. "DNA nanotechnology." In: *Nature Reviews Materials* 3 (2017), p. 17068. DOI: 10.1038/natrevmats.2017.68. URL: http://dx.doi.org/10.1038/natrevmats.2017.68.

[23] Kalle Gehring, Jean-Louis Leroy, and Maurice Gueron. "A tetrameric DNA structure with protonated cytosine-cytosine base pairs." In: *Nature* 363 (1993), p. 561. DOI: 10.1038/363561a0. URL: http://dx.doi.org/10.1038/363561a0.

[24] Ghodke Harshad B., Krishnan Ramya, Vignesh Kasinath, Kumar G. V. Pavan, Narayana Chandrabhas, and Krishnan Yamuna. "The I-Tetraplex Building Block: Rational Design and Controlled Fabrication of Robust 1D DNA Scaffolds through Non-Watson-Crick Interactions." In: *Angewandte Chemie International Edition* 46.15 (2007), pp. 2646–2649. DOI: doi:10.1002/anie.200604461. URL: https://onlinelibrary.wiley.com/doi/abs/10.1002/anie.200604461.

[25] Yang Yang, Zhou Chao, Zhang Tao, Cheng Enjun, Yang Zhongqiang, and Liu Dongsheng. "DNA Pillars Constructed from an i-Motif Stem and Duplex Branches." In: *Small* 8.4 (2012), pp. 552–556. DOI: doi:10.1002/smll.201102061. URL: https://onlinelibrary.wiley.com/doi/abs/10.1002/smll.201102061.

[26] Liu Dongsheng and Balasubramanian Shankar. "A Proton-Fuelled DNA Nanomachine." In: *Angewandte Chemie International Edition* 42.46 (2003), pp. 5734–5736. DOI: doi:10.1002/anie.200352402. URL: https://onlinelibrary.wiley.com/doi/abs/10.1002/anie.200352402.

[27] Tao Li and Michael Famulok. "I-Motif-Programmed Functionalization of DNA Nanocircles." In: *Journal of the American Chemical Society* 135.4 (2013), pp. 1593–1599. ISSN: 0002-7863. DOI: 10.1021/ja3118224. URL: https://doi.org/10.1021/ja3118224.

[28] Wenmiao Shu, Dongsheng Liu, Moyu Watari, Christian K. Riener, Torsten Strunz, Mark E. Welland, Shankar Balasubramanian, and Rachel A. McKendry. "DNA Molecular Motor Driven Micromechanical Cantilever Arrays." In: *Journal of the American Chemical Society* 127.48 (2005), pp. 17054–17060. ISSN: 0002-7863. DOI: 10.1021/ja0554514. URL: https://doi.org/10.1021/ja0554514.

[29] Youdong Mao, Dongsheng Liu, Shutao Wang, Songnian Luo, Wenxing Wang, Yanlian Yang, Qi Ouyang, and Lei Jiang. "Alternating-electric-field-enhanced reversible switching of DNA nanocontainers

with pH." In: *Nucleic Acids Research* 35.5 (2007), e33–e33. ISSN: 0305-1048 1362-4962. DOI: 10.1093/nar/gkl1161. URL: http://www.ncbi.nlm.nih.gov/pmc/articles/PMC1865044/.

[30] Yukiko Kamiya and Hiroyuki Asanuma. "Light-Driven DNA Nanomachine with a Photoresponsive Molecular Engine." In: *Accounts of Chemical Research* 47.6 (2014), pp. 1663–1672. ISSN: 0001-4842. DOI: 10.1021/ar400308f. URL: https://doi.org/10.1021/ar400308f.

[31] Daniel Hoersch, Soung-Hun Roh, Wah Chiu, and Tanja Kortemme. "Reprogramming an ATP-driven protein machine into a light-gated nanocage." In: *Nature nanotechnology* 8.12 (2013), pp. 928–932. ISSN: 1748-3387 1748-3395. DOI: 10.1038/nnano.2013.242. URL: http://www.ncbi.nlm.nih.gov/pmc/articles/PMC3859876/.

[32] Takahiro Muraoka, Kazushi Kinbara, and Takuzo Aida. "Mechanical twisting of a guest by a photoresponsive host." In: *Nature* 440 (2006), p. 512. DOI: 10.1038/nature04635https://www.nature.com/articles/nature04635#supplementary-information. URL: http://dx.doi.org/10.1038/nature04635.

[33] Hiroyuki Asanuma, Xingguo Liang, Hidenori Nishioka, Daijiro Matsunaga, Mingzhe Liu, and Makoto Komiyama. "Synthesis of azobenzene-tethered DNA for reversible photo-regulation of DNA functions: hybridization and transcription." In: *Nature Protocols* 2 (2007), p. 203. DOI: 10.1038/nprot.2006.465. URL: http://dx.doi.org/10.1038/nprot.2006.465.

[34] Paul W. K. Rothemund. "Folding DNA to create nanoscale shapes and patterns." In: *Nature* 440.7082 (2006), pp. 297–302. ISSN: 0028-0836. DOI: http://www.nature.com/nature/journal/v440/n7082/suppinfo/nature04586_S1.html. URL: http://dx.doi.org/10.1038/nature04586.

[35] Shawn M. Douglas, Hendrik Dietz, Tim Liedl, Bjorn Hogberg, Franziska Graf, and William M. Shih. "Self-assembly of DNA into nanoscale three-dimensional shapes." In: *Nature* 459.7245 (2009), pp. 414–418. ISSN: 0028-0836. DOI: http://www.nature.com/nature/journal/v459/n7245/suppinfo/nature08016_S1.html. URL: http://dx.doi.org/10.1038/nature08016.

[36] Shawn M. Douglas, Adam H. Marblestone, Surat Teerapittayanon, Alejandro Vazquez, George M. Church, and William M. Shih. "Rapid prototyping of 3D DNA-origami shapes with caDNAno." In: *Nucleic Acids Research* 37.15 (2009), pp. 5001–5006. ISSN: 0305-1048. DOI: 10.1093/nar/gkp436. URL: http://dx.doi.org/10.1093/nar/gkp436.

[37] Carlos Ernesto Castro, Fabian Kilchherr, Do-Nyun Kim, Enrique Lin Shiao, Tobias Wauer, Philipp Wortmann, Mark Bathe, and Hendrik Dietz. "A primer to scaffolded DNA origami." In: *Nature Methods* 8 (2011), p. 221. DOI: 10.1038/nmeth.1570https://www.nature.

com/articles/nmeth.1570#supplementary-information. URL: http://dx.doi.org/10.1038/nmeth.1570.

[38] Do-Nyun Kim, Fabian Kilchherr, Hendrik Dietz, and Mark Bathe. "Quantitative prediction of 3D solution shape and flexibility of nucleic acid nanostructures." In: *Nucleic Acids Research* 40.7 (2012), pp. 2862–2868. ISSN: 0305-1048 1362-4962. DOI: 10.1093/nar/gkr1173. URL: http://www.ncbi.nlm.nih.gov/pmc/articles/PMC3326316/.

[39] Ebbe S. Andersen et al. "Self-assembly of a nanoscale DNA box with a controllable lid." In: *Nature* 459 (2009), p. 73. DOI: 10.1038/nature07971https://www.nature.com/articles/nature07971#supplementary-information. URL: http://dx.doi.org/10.1038/nature07971.

[40] Anton Kuzyk, Ralf Jungmann, Guillermo P. Acuna, and Na Liu. "DNA Origami Route for Nanophotonics." In: *ACS Photonics* 5.4 (2018), pp. 1151–1163. DOI: 10.1021/acsphotonics.7b01580. URL: https://doi.org/10.1021/acsphotonics.7b01580.

[41] Bryan Wei, Mingjie Dai, and Peng Yin. "Complex shapes self-assembled from single-stranded DNA tiles." In: *Nature* 485 (2012), p. 623. DOI: 10.1038/nature11075https://www.nature.com/articles/nature11075#supplementary-information. URL: http://dx.doi.org/10.1038/nature11075.

[42] Yonggang Ke, Luvena L. Ong, William M. Shih, and Peng Yin. "Three-Dimensional Structures Self-Assembled from DNA Bricks." In: *Science* 338.6111 (2012), p. 1177. URL: http://science.sciencemag.org/content/338/6111/1177.abstract.

[43] Hendrik Dietz, Shawn M. Douglas, and William M. Shih. "Folding DNA into Twisted and Curved Nanoscale Shapes." In: *Science (New York, N.Y.)* 325.5941 (2009), pp. 725–730. ISSN: 0036-8075 1095-9203. DOI: 10.1126/science.1174251. URL: http://www.ncbi.nlm.nih.gov/pmc/articles/PMC2737683/.

[44] Dage Liu, Mingsheng Wang, Zhaoxiang Deng, Richard Walulu, and Chengde Mao. "Tensegrity: Construction of Rigid DNA Triangles with Flexible Four-Arm DNA Junctions." In: *Journal of the American Chemical Society* 126.8 (2004), pp. 2324–2325. ISSN: 0002-7863. DOI: 10.1021/ja031754r. URL: https://doi.org/10.1021/ja031754r.

[45] Tim Liedl, Björn Högberg, Jessica Tytell, Donald E. Ingber, and William M. Shih. "Self-assembly of three-dimensional prestressed tensegrity structures from DNA." In: *Nature Nanotechnology* 5 (2010), p. 520. DOI: 10.1038/nnano.2010.107https://www.nature.com/articles/nnano.2010.107#supplementary-information. URL: http://dx.doi.org/10.1038/nnano.2010.107.

[46] Walther Andreas, Loescher Sebastian, and Groeer Saskia. "3D DNA Origami Nanoparticles: From Basic Design Principles to Emerging Applications in Soft Matter and (Bio-)Nanosciences." In: *Angewandte Chemie International Edition* 0.ja (). DOI: doi:10.1002/anie.201801700. URL: https://onlinelibrary.wiley.com/doi/abs/10.1002/anie.201801700.

[47] Erik Benson, Abdulmelik Mohammed, Johan Gardell, Sergej Masich, Eugen Czeizler, Pekka Orponen, and Björn Högberg. "DNA rendering of polyhedral meshes at the nanoscale." In: *Nature* 523 (2015), p. 441. DOI: 10.1038/nature14586https://www.nature.com/articles/nature14586#supplementary-information. URL: http://dx.doi.org/10.1038/nature14586.

[48] Florian Praetorius, Benjamin Kick, Karl L. Behler, Maximilian N. Honemann, Dirk Weuster-Botz, and Hendrik Dietz. "Biotechnological mass production of DNA origami." In: *Nature* 552 (2017), p. 84. DOI: 10.1038/nature24650https://www.nature.com/articles/nature24650#supplementary-information. URL: http://dx.doi.org/10.1038/nature24650.

[49] Thomas Gerling, Klaus F. Wagenbauer, Andrea M. Neuner, and Hendrik Dietz. "Dynamic DNA devices and assemblies formed by shape-complementary, non–base pairing 3D components." In: *Science* 347.6229 (2015), p. 1446. URL: http://science.sciencemag.org/content/347/6229/1446.abstract.

[50] Linda K. Bruetzel, Philipp U. Walker, Thomas Gerling, Hendrik Dietz, and Jan Lipfert. "Time-Resolved Small-Angle X-ray Scattering Reveals Millisecond Transitions of a DNA Origami Switch." In: *Nano Letters* 18.4 (2018), pp. 2672–2676. ISSN: 1530-6984. DOI: 10.1021/acs.nanolett.8b00592. URL: https://doi.org/10.1021/acs.nanolett.8b00592.

[51] Klaus F. Wagenbauer, Christian Sigl, and Hendrik Dietz. "Gigadalton-scale shape-programmable DNA assemblies." In: *Nature* 552 (2017), p. 78. DOI: 10.1038/nature24651https://www.nature.com/articles/nature24651#supplementary-information. URL: http://dx.doi.org/10.1038/nature24651.

[52] Mahsa Siavashpouri, Christian H. Wachauf, Mark J. Zakhary, Florian Praetorius, Hendrik Dietz, and Zvonimir Dogic. "Molecular engineering of chiral colloidal liquid crystals using DNA origami." In: *Nature Materials* 16 (2017), p. 849. DOI: 10.1038/nmat4909https://www.nature.com/articles/nmat4909#supplementary-information. URL: http://dx.doi.org/10.1038/nmat4909.

[53] Kevin Martens, Timon Funck, Susanne Kempter, Eva-Maria Roller, Tim Liedl, M. Blaschke Benno, Peter Knecht, Antonio Garrido José, Bingru Zhang, and Heinz Kitzerow. "Alignment and Graphene-Assisted Decoration of Lyotropic Chromonic Liquid Crystals Containing DNA

Origami Nanostructures." In: *Small* 12.12 (2016), pp. 1658–1666. ISSN: 1613-6810. DOI: 10.1002/smll.201503382. URL: https://doi.org/10.1002/smll.201503382.

[54] Florian Praetorius and Hendrik Dietz. "Self-assembly of genetically encoded DNA-protein hybrid nanoscale shapes." In: *Science* 355.6331 (2017). URL: http://science.sciencemag.org/content/355/6331/eaam5488.abstract.

[55] Jean-Philippe J. Sobczak, Thomas G. Martin, Thomas Gerling, and Hendrik Dietz. "Rapid Folding of DNA into Nanoscale Shapes at Constant Temperature." In: *Science* 338.6113 (2012), p. 1458. URL: http://science.sciencemag.org/content/338/6113/1458.abstract.

[56] Joerg Schnitzbauer, Maximilian T. Strauss, Thomas Schlichthaerle, Florian Schueder, and Ralf Jungmann. "Super-resolution microscopy with DNA-PAINT." In: *Nature Protocols* 12 (2017), p. 1198. DOI: 10.1038/nprot.2017.024https://www.nature.com/articles/nprot.2017.024#supplementary-information. URL: http://dx.doi.org/10.1038/nprot.2017.024.

[57] Maximilian T. Strauss, Florian Schueder, Daniel Haas, Philipp C. Nickels, and Ralf Jungmann. "Quantifying absolute addressability in DNA origami with molecular resolution." In: *Nature Communications* 9.1 (2018), p. 1600. ISSN: 2041-1723. DOI: 10.1038/s41467-018-04031-z. URL: https://doi.org/10.1038/s41467-018-04031-z.

[58] Zhao Zhao, Jinglin Fu, Soma Dhakal, Alexander Johnson-Buck, Minghui Liu, Ting Zhang, Neal W. Woodbury, Yan Liu, Nils G. Walter, and Hao Yan. "Nanocaged enzymes with enhanced catalytic activity and increased stability against protease digestion." In: *Nature Communications* 7 (2016), p. 10619. DOI: 10.1038/ncomms10619https://www.nature.com/articles/ncomms10619#supplementary-information. URL: http://dx.doi.org/10.1038/ncomms10619.

[59] Shawn M. Douglas, Ido Bachelet, and George M. Church. "A Logic-Gated Nanorobot for Targeted Transport of Molecular Payloads." In: *Science* 335.6070 (2012), p. 831. URL: http://science.sciencemag.org/content/335/6070/831.abstract.

[60] Nicholas A. W. Bell, Christian R. Engst, Marc Ablay, Giorgio Divitini, Caterina Ducati, Tim Liedl, and Ulrich F. Keyser. "DNA Origami Nanopores." In: *Nano Letters* 12.1 (2012), pp. 512–517. ISSN: 1530-6984. DOI: 10.1021/nl204098n. URL: https://doi.org/10.1021/nl204098n.

[61] Swati Krishnan, Daniela Ziegler, Vera Arnaut, Thomas G. Martin, Korbinian Kapsner, Katharina Henneberg, Andreas R. Bausch, Hendrik Dietz, and Friedrich C. Simmel. "Molecular transport through large-diameter DNA nanopores." In: *Nature Communications* 7 (2016), p. 12787. DOI: 10.1038/ncomms12787https://www.nature.com/

articles/ncomms12787#supplementary-information. URL: http://dx.doi.org/10.1038/ncomms12787.

[62] Steven D. Perrault and William M. Shih. "Virus-Inspired Membrane Encapsulation of DNA Nanostructures To Achieve In Vivo Stability." In: *ACS Nano* 8.5 (2014), pp. 5132–5140. ISSN: 1936-0851 1936-086X. DOI: 10.1021/nn5011914. URL: http://www.ncbi.nlm.nih.gov/pmc/articles/PMC4046785/.

[63] Yuki Suzuki, Masayuki Endo, and Hiroshi Sugiyama. "Lipid-bilayer-assisted two-dimensional self-assembly of DNA origami nanostructures." In: *Nature Communications* 6 (2015), p. 8052. DOI: 10.1038/ncomms9052https://www.nature.com/articles/ncomms9052#supplementary-information. URL: http://dx.doi.org/10.1038/ncomms9052.

[64] Thomas G. W. Edwardson, Karina M. M. Carneiro, Christopher K. McLaughlin, Christopher J. Serpell, and Hanadi F. Sleiman. "Site-specific positioning of dendritic alkyl chains on DNA cages enables their geometry-dependent self-assembly." In: *Nature Chemistry* 5 (2013), p. 868. DOI: 10.1038/nchem.1745https://www.nature.com/articles/nchem.1745#supplementary-information. URL: http://dx.doi.org/10.1038/nchem.1745.

[65] Alexander E. Marras, Lifeng Zhou, Hai-Jun Su, and Carlos E. Castro. "Programmable motion of DNA origami mechanisms." In: *Proceedings of the National Academy of Sciences* 112.3 (2015), pp. 713–718. DOI: 10.1073/pnas.1408869112. URL: http://www.pnas.org/content/pnas/112/3/713.full.pdf.

[66] Enzo Kopperger, Jonathan List, Sushi Madhira, Florian Rothfischer, Don C. Lamb, and Friedrich C. Simmel. "A self-assembled nanoscale robotic arm controlled by electric fields." In: *Science* 359.6373 (2018), p. 296. URL: http://science.sciencemag.org/content/359/6373/296.abstract.

[67] Na Wu and Itamar Willner. "pH-Stimulated Reconfiguration and Structural Isomerization of Origami Dimer and Trimer Systems." In: *Nano Letters* 16.10 (2016), pp. 6650–6655. ISSN: 1530-6984. DOI: 10.1021/acs.nanolett.6b03418. URL: https://doi.org/10.1021/acs.nanolett.6b03418.

[68] Yangyang Yang, Masayuki Endo, Kumi Hidaka, and Hiroshi Sugiyama. "Photo-Controllable DNA Origami Nanostructures Assembling into Predesigned Multiorientational Patterns." In: *Journal of the American Chemical Society* 134.51 (2012), pp. 20645–20653. ISSN: 0002-7863. DOI: 10.1021/ja307785r. URL: https://doi.org/10.1021/ja307785r.

[69] Anupama J. Thubagere et al. "A cargo-sorting DNA robot." In: *Science* 357.6356 (2017). URL: http://science.sciencemag.org/content/357/6356/eaan6558.abstract.

[70] Philipp C. Nickels, Bettina Wünsch, Phil Holzmeister, Wooli Bae, Luisa M. Kneer, Dina Grohmann, Philip Tinnefeld, and Tim Liedl. "Molecular force spectroscopy with a DNA origami–based nanoscopic force clamp." In: *Science* 354.6310 (2016), pp. 305–307. DOI: 10.1126/science.aah5974. URL: http://science.sciencemag.org/content/sci/354/6310/305.full.pdf.

[71] Denis Selnihhin, Steffen Møller Sparvath, Søren Preus, Victoria Birkedal, and Ebbe Sloth Andersen. "Multi-Fluorophore DNA Origami Beacon as a Biosensing Platform." In: *ACS Nano* 12.6 (2018), pp. 5699–5708. ISSN: 1936-0851. DOI: 10.1021/acsnano.8b01510. URL: https://doi.org/10.1021/acsnano.8b01510.

[72] Jürgen J. Schmied, Carsten Forthmann, Enrico Pibiri, Birka Lalkens, Philipp Nickels, Tim Liedl, and Philip Tinnefeld. "DNA Origami Nanopillars as Standards for Three-Dimensional Superresolution Microscopy." In: *Nano Letters* 13.2 (2013), pp. 781–785. ISSN: 1530-6984. DOI: 10.1021/nl304492y. URL: https://doi.org/10.1021/nl304492y.

[73] Johannes B. Woehrstein, Maximilian T. Strauss, Luvena L. Ong, Bryan Wei, David Y. Zhang, Ralf Jungmann, and Peng Yin. "Sub–100-nm metafluorophores with digitally tunable optical properties self-assembled from DNA." In: *Science Advances* 3.6 (2017), e1602128. ISSN: 2375-2548. DOI: 10.1126/sciadv.1602128. URL: http://www.ncbi.nlm.nih.gov/pmc/articles/PMC5479647/.

[74] Ingo H. Stein, Christian Steinhauer, and Philip Tinnefeld. "Single-Molecule Four-Color FRET Visualizes Energy-Transfer Paths on DNA Origami." In: *Journal of the American Chemical Society* 133.12 (2011), pp. 4193–4195. ISSN: 0002-7863. DOI: 10.1021/ja1105464. URL: https://doi.org/10.1021/ja1105464.

[75] Sarah J. Hurst, Abigail K. R. Lytton-Jean, and Chad A. Mirkin. "Maximizing DNA Loading on a Range of Gold Nanoparticle Sizes." In: *Analytical Chemistry* 78.24 (2006), pp. 8313–8318. ISSN: 0003-2700. DOI: 10.1021/ac0613582. URL: https://doi.org/10.1021/ac0613582.

[76] Paul Kühler, Eva-Maria Roller, Robert Schreiber, Tim Liedl, Theobald Lohmüller, and Jochen Feldmann. "Plasmonic DNA-Origami Nanoantennas for Surface-Enhanced Raman Spectroscopy." In: *Nano Letters* 14.5 (2014), pp. 2914–2919. ISSN: 1530-6984. DOI: 10.1021/nl5009635. URL: https://doi.org/10.1021/nl5009635.

[77] Anton Kuzyk, Robert Schreiber, Zhiyuan Fan, Gunther Pardatscher, Eva-Maria Roller, Alexander Hogele, Friedrich C. Simmel, Alexander O. Govorov, and Tim Liedl. "DNA-based self-assembly of chiral plasmonic nanostructures with tailored optical response." In: *Nature* 483.7389 (2012), pp. 311–314. ISSN: 0028-0836. DOI: http://www.nature.com/nature/journal/v483/n7389/abs/nature10889.html#supplementary-information. URL: http://dx.doi.org/10.1038/nature10889.

[78] Anton Kuzyk, Robert Schreiber, Hui Zhang, Alexander O. Govorov, Tim Liedl, and Na Liu. "Reconfigurable 3D plasmonic metamolecules." In: *Nat Mater* 13.9 (2014), pp. 862–866. ISSN: 1476-1122. DOI: 10.1038/nmat4031http://www.nature.com/nmat/journal/v13/n9/abs/nmat4031.html#supplementary-information. URL: http://dx.doi.org/10.1038/nmat4031.

[79] S. A. Maier. *Plasmonics: Fundamentals and applications*. 2007. ISBN: 0387331506. DOI: 10.1007/0-387-37825-1. URL: http://dx.doi.org/10.1007/0-387-37825-1.

[80] Mark I. Stockman. "Nanoplasmonics: past, present, and glimpse into future." In: *Optics Express* 19.22 (2011), pp. 22029–22106. DOI: 10.1364/OE.19.022029. URL: http://www.opticsexpress.org/abstract.cfm?URI=oe-19-22-22029.

[81] Matthew Pelton and Garnett W. Bryant. *Introduction to metal-nanoparticle plasmonics*. Hoboken, New Jersey: Wiley : Science Wise Publishing, 2013, xvii, 275 pages. ISBN: 9781118060407 (cloth) 1118060407 (cloth).

[82] Krishnendu Saha, Sarit S. Agasti, Chaekyu Kim, Xiaoning Li, and Vincent M. Rotello. "Gold Nanoparticles in Chemical and Biological Sensing." In: *Chemical Reviews* 112.5 (2012), pp. 2739–2779. ISSN: 0009-2665. DOI: 10.1021/cr2001178. URL: https://doi.org/10.1021/cr2001178.

[83] M. Meier and A. Wokaun. "Enhanced fields on large metal particles: dynamic depolarization." In: *Optics Letters* 8.11 (1983), pp. 581–583. DOI: 10.1364/OL.8.000581. URL: http://ol.osa.org/abstract.cfm?URI=ol-8-11-581.

[84] U. J. Meierhenrich. "Amino Acids and the Asymmetry of Life." In: *European Review* 21.2 (2013), pp. 190–199. ISSN: 1062-7987. DOI: 10.1017/S106279871200035x. URL: <GotoISI>://WOS:000209452300005.

[85] L. Rosenfeld. "Quantenmechanische Theorie der natürlichen optischen Aktivität von Flüssigkeiten und Gasen." In: *Zeitschrift für Physik* 52.3 (1929), pp. 161–174. ISSN: 0044-3328. DOI: 10.1007/BF01342393. URL: https://doi.org/10.1007/BF01342393.

[86] "Circular Dichroism Spectroscopy." In: *Analytical Methods in Supramolecular Chemistry*. DOI: doi:10.1002/9783527610273.ch8. URL: https://onlinelibrary.wiley.com/doi/abs/10.1002/9783527610273.ch8.

[87] Alexander O. Govorov, Yurii K. Gun'ko, Joseph M. Slocik, Valerie A. Gerard, Zhiyuan Fan, and Rajesh R. Naik. "Chiral nanoparticle assemblies: circular dichroism, plasmonic interactions, and exciton effects." In: *Journal of Materials Chemistry* 21.42 (2011), pp. 16806–16818. ISSN: 0959-9428. DOI: 10.1039/C1JM12345A. URL: http://dx.doi.org/10.1039/C1JM12345A.

[88] Justyna K. Gansel, Michael Latzel, Andreas Frölich, Johannes Kaschke, Michael Thiel, and Martin Wegener. "Tapered gold-helix metamaterials as improved circular polarizers." In: *Applied Physics Letters* 100.10 (2012), p. 101109. ISSN: 0003-6951. DOI: 10.1063/1.3693181. URL: https://doi.org/10.1063/1.3693181.

[89] R. Zhao, L. Zhang, J. Zhou, Th Koschny, and C. M. Soukoulis. "Conjugated gammadion chiral metamaterial with uniaxial optical activity and negative refractive index." In: *Physical Review B* 83.3 (2011), p. 035105. DOI: 10.1103/PhysRevB.83.035105. URL: https://link.aps.org/doi/10.1103/PhysRevB.83.035105.

[90] Na Liu and Tim Liedl. "DNA-Assembled Advanced Plasmonic Architectures." In: *Chemical Reviews* 118.6 (2018), pp. 3032–3053. ISSN: 0009-2665. DOI: 10.1021/acs.chemrev.7b00225. URL: https://doi.org/10.1021/acs.chemrev.7b00225.

[91] Mario Hentschel, Martin Schäferling, Xiaoyang Duan, Harald Giessen, and Na Liu. "Chiral plasmonics." In: *Science Advances* 3.5 (2017). URL: http://advances.sciencemag.org/content/3/5/e1602735.abstract.

[92] Sarah E. Ochmann, Carolin Vietz, Kateryna Trofymchuk, Guillermo P. Acuna, Birka Lalkens, and Philip Tinnefeld. "Optical Nanoantenna for Single Molecule-Based Detection of Zika Virus Nucleic Acids without Molecular Multiplication." In: *Analytical Chemistry* 89.23 (2017), pp. 13000–13007. ISSN: 0003-2700. DOI: 10.1021/acs.analchem.7b04082. URL: https://doi.org/10.1021/acs.analchem.7b04082.

[93] Kilian Vogele, Jonathan List, Günther Pardatscher, Nolan B. Holland, Friedrich C. Simmel, and Tobias Pirzer. "Self-Assembled Active Plasmonic Waveguide with a Peptide-Based Thermomechanical Switch." In: *ACS Nano* 10.12 (2016), pp. 11377–11384. ISSN: 1936-0851. DOI: 10.1021/acsnano.6b06635. URL: https://doi.org/10.1021/acsnano.6b06635.

[94] Xibo Shen, Chen Song, Jinye Wang, Dangwei Shi, Zhengang Wang, Na Liu, and Baoquan Ding. "Rolling Up Gold Nanoparticle-Dressed DNA Origami into Three-Dimensional Plasmonic Chiral Nanostructures." In: *Journal of the American Chemical Society* 134.1 (2012), pp. 146–149. ISSN: 0002-7863. DOI: 10.1021/ja209861x. URL: https://doi.org/10.1021/ja209861x.

[95] Wenjing Yan, Liguang Xu, Chuanlai Xu, Wei Ma, Hua Kuang, Libing Wang, and Nicholas A. Kotov. "Self-Assembly of Chiral Nanoparticle Pyramids with Strong R/S Optical Activity." In: *Journal of the American Chemical Society* 134.36 (2012), pp. 15114–15121. ISSN: 0002-7863. DOI: 10.1021/ja3066336. URL: https://doi.org/10.1021/ja3066336.

[96] Wenjing Yan, Liguang Xu, Wei Ma, Liqiang Liu, Libing Wang, Hua Kuang, and Chuanlai Xu. "Pyramidal Sensor Platform with Reversible Chiroptical Signals for DNA Detection." In: *Small* 10.21 (2014), pp. 4293–4297. ISSN: 1613-6810. DOI: 10.1002/smll.201401641. URL: https://doi.org/10.1002/smll.201401641.

[97] Xibo Shen, Pengfei Zhan, Anton Kuzyk, Qing Liu, Ana Asenjo-Garcia, Hui Zhang, F. Javier Garcia de Abajo, Alexander Govorov, Baoquan Ding, and Na Liu. "3D plasmonic chiral colloids." In: *Nanoscale* 6.4 (2014), pp. 2077–2081. ISSN: 2040-3364. DOI: 10.1039/C3NR06006C. URL: http://dx.doi.org/10.1039/C3NR06006C.

[98] Xiang Lan, Xuxing Lu, Chenqi Shen, Yonggang Ke, Weihai Ni, and Qiangbin Wang. "Au Nanorod Helical Superstructures with Designed Chirality." In: *Journal of the American Chemical Society* 137.1 (2015), pp. 457–462. ISSN: 0002-7863. DOI: 10.1021/ja511333q. URL: https://doi.org/10.1021/ja511333q.

[99] Chao Zhou, Xiaoyang Duan, and Na Liu. "A plasmonic nanorod that walks on DNA origami." In: *Nature Communications* 6 (2015), p. 8102. DOI: 10.1038/ncomms9102https://www.nature.com/articles/ncomms9102#supplementary-information. URL: http://dx.doi.org/10.1038/ncomms9102.

[100] M. Knoll and E. Ruska. "Das Elektronenmikroskop." In: *Zeitschrift für Physik* 78.5 (1932), pp. 318–339. ISSN: 0044-3328. DOI: 10.1007/BF01342199. URL: https://doi.org/10.1007/BF01342199.

[101] E. Abbe. "Beiträge zur Theorie des Mikroskops und der mikroskopischen Wahrnehmung." In: *Archiv für mikroskopische Anatomie* 9.1 (1873), pp. 413–418. ISSN: 0176-7364. DOI: 10.1007/bf02956173. URL: https://doi.org/10.1007/BF02956173.

[102] Friedrich Lottspeich and Joachim W. Engels. *Bioanalytik*. 2. Aufl. München ; Heidelberg: Elsevier, Spektrum, Akad. Verl., 2006, XXIV, 1119 s. ISBN: 3827415209.

[103] Chad A. Mirkin, Robert L. Letsinger, Robert C. Mucic, and James J. Storhoff. "A DNA-based method for rationally assembling nanoparticles into macroscopic materials." In: *Nature* 382 (1996), p. 607. DOI: 10.1038/382607a0. URL: http://dx.doi.org/10.1038/382607a0.

[104] A. Paul Alivisatos, Kai P. Johnsson, Xiaogang Peng, Troy E. Wilson, Colin J. Loweth, Marcel P. Bruchez Jr, and Peter G. Schultz. "Organization of nanocrystal molecules using DNA." In: *Nature* 382 (1996), p. 609. DOI: 10.1038/382609a0. URL: http://dx.doi.org/10.1038/382609a0.

[105] Joshua I. Cutler, Evelyn Auyeung, and Chad A. Mirkin. "Spherical Nucleic Acids." In: *Journal of the American Chemical Society* 134.3 (2012), pp. 1376–1391. ISSN: 0002-7863. DOI: 10.1021/ja209351u. URL: https://doi.org/10.1021/ja209351u.

[106] I. Stoeva Savka, Jae-Seung Lee, C. Shad Thaxton, and A. Mirkin Chad. "Multiplexed DNA Detection with Biobarcoded Nanoparticle Probes." In: *Angewandte Chemie International Edition* 45.20 (2006), pp. 3303–3306. ISSN: 1433-7851. DOI: 10.1002/anie.200600124. URL: https://doi.org/10.1002/anie.200600124.

[107] S. Szunerits and Rabah Boukherroub. *Introduction to plasmonics: Advances and applications*. 2015, pp. 1–358.

[108] Xu Zhang, Mark R. Servos, and Juewen Liu. "Instantaneous and Quantitative Functionalization of Gold Nanoparticles with Thiolated DNA Using a pH-Assisted and Surfactant-Free Route." In: *Journal of the American Chemical Society* 134.17 (2012), pp. 7266–7269. ISSN: 0002-7863. DOI: 10.1021/ja3014055. URL: https://doi.org/10.1021/ja3014055.

[109] Biwu Liu and Juewen Liu. "Freezing Directed Construction of Bio/-Nano Interfaces: Reagentless Conjugation, Denser Spherical Nucleic Acids, and Better Nanoflares." In: *Journal of the American Chemical Society* 139.28 (2017), pp. 9471–9474. ISSN: 0002-7863. DOI: 10.1021/jacs.7b04885. URL: https://doi.org/10.1021/jacs.7b04885.

[110] C. R. Goring and Andrew Pritchard. *Micrographia : containing practical essays on reflecting, solar, oxy-hydrogen gas microscopes; micrometers; eye-pieces, etc*. London : Whitaker and Co., 1837.

[111] Richard Zsigmondy. "Nobel Lecture: Properties of Colloids." In: *Nobelprize.org. Nobel Media AB 2014* (). URL: http://www.nobelprize.org/nobel_prizes/chemistry/laureates/1925/zsigmondy-lecture.html.

[112] Jana Olson, Sergio Dominguez-Medina, Anneli Hoggard, Lin-Yung Wang, Wei-Shun Chang, and Stephan Link. "Optical Characterization of Single Plasmonic Nanoparticles." In: *Chemical Society reviews* 44.1 (2015), pp. 40–57. ISSN: 0306-0012 1460-4744. DOI: 10.1039/c4cs00131a. URL: http://www.ncbi.nlm.nih.gov/pmc/articles/PMC4641313/.

[113] Timon Funck, Francesca Nicoli, Anton Kuzyk, and Tim Liedl. "Sensing Picomolar Concentrations of RNA Using Switchable Plasmonic Chirality." In: *Angewandte Chemie* 130.41 (2018), pp. 13683–13686. ISSN: 0044-8249. DOI: 10.1002/ange.201807029. URL: https://doi.org/10.1002/ange.201807029.

[114] Pieter Mestdagh et al. "Evaluation of quantitative miRNA expression platforms in the microRNA quality control (miRQC) study." In: *Nat Meth* 11.8 (2014), pp. 809–815. ISSN: 1548-7091. DOI: 10.1038/nmeth.3014http://www.nature.com/nmeth/journal/v11/n8/abs/nmeth.3014.html#supplementary-information. URL: http://dx.doi.org/10.1038/nmeth.3014.

[115] Clinton H. Hansen, Darren Yang, Mounir A. Koussa, and Wesley P. Wong. "Nanoswitch-linked immunosorbent assay (NLISA) for fast, sensitive, and specific protein detection." In: *Proceedings of the National Academy of Sciences* (2017). DOI: 10.1073/pnas.1708148114. URL: http://www.pnas.org/content/early/2017/09/05/1708148114.abstract.

[116] Heidi-Kristin Walter, Jens Bauer, Jeannine Steinmeyer, Akinori Kuzuya, Christof M. Niemeyer, and Hans-Achim Wagenknecht. ""DNA Origami Traffic Lights" with a Split Aptamer Sensor for a Bicolor Fluorescence Readout." In: *Nano Letters* 17.4 (2017), pp. 2467–2472. ISSN: 1530-6984. DOI: 10.1021/acs.nanolett.7b00159. URL: https://doi.org/10.1021/acs.nanolett.7b00159.

[117] Anastasiya Puchkova, Carolin Vietz, Enrico Pibiri, Bettina Wünsch, María Sanz Paz, Guillermo P. Acuna, and Philip Tinnefeld. "DNA Origami Nanoantennas with over 5000-fold Fluorescence Enhancement and Single-Molecule Detection at 25 uM." In: *Nano Letters* 15.12 (2015), pp. 8354–8359. ISSN: 1530-6984. DOI: 10.1021/acs.nanolett.5b04045. URL: https://doi.org/10.1021/acs.nanolett.5b04045.

[118] Xiang Lan, Zhong Chen, Gaole Dai, Xuxing Lu, Weihai Ni, and Qiangbin Wang. "Bifacial DNA Origami-Directed Discrete, Three-Dimensional, Anisotropic Plasmonic Nanoarchitectures with Tailored Optical Chirality." In: *Journal of the American Chemical Society* 135.31 (2013), pp. 11441–11444. ISSN: 0002-7863. DOI: 10.1021/ja404354c. URL: http://dx.doi.org/10.1021/ja404354c.

[119] Ralf Jungmann, Maier S. Avendaño, Mingjie Dai, Johannes B. Woehrstein, Sarit S. Agasti, Zachary Feiger, Avital Rodal, and Peng Yin. "Quantitative super-resolution imaging with qPAINT." In: *Nature Methods* 13 (2016), p. 439. DOI: 10.1038/nmeth.3804https://www.nature.com/articles/nmeth.3804#supplementary-information. URL: http://dx.doi.org/10.1038/nmeth.3804.

[120] Alexander Johnson-Buck, Xin Su, Maria D. Giraldez, Meiping Zhao, Muneesh Tewari, and Nils G. Walter. "Kinetic fingerprinting to identify and count single nucleic acids." In: *Nature Biotechnology* 33 (2015), p. 730. DOI: 10.1038/nbt.3246https://www.nature.com/articles/nbt.3246#supplementary-information. URL: http://dx.doi.org/10.1038/nbt.3246.

[121] Xiaoling Wu, Changlong Hao, Jatish Kumar, Hua Kuang, Nicholas A. Kotov, Luis M. Liz-Marzan, and Chuanlai Xu. "Environmentally responsive plasmonic nanoassemblies for biosensing." In: *Chemical Society Reviews* (2018). ISSN: 0306-0012. DOI: 10.1039/C7CS00894E. URL: http://dx.doi.org/10.1039/C7CS00894E.

[122] Shawn M. Douglas, Ido Bachelet, and George M. Church. "A Logic-Gated Nanorobot for Targeted Transport of Molecular Payloads." In: *Science* 335.6070 (2012), pp. 831–834. DOI: 10.1126/science.1214081.

URL: http://science.sciencemag.org/content/sci/335/6070/831.full.pdf.

[123] Thomas Gerling, Klaus F. Wagenbauer, Andrea M. Neuner, and Hendrik Dietz. "Dynamic DNA devices and assemblies formed by shape-complementary, non–base pairing 3D components." In: *Science* 347.6229 (2015), pp. 1446–1452. DOI: 10.1126/science.aaa5372. URL: http://science.sciencemag.org/content/sci/347/6229/1446.full.pdf.

[124] Klaus F. Wagenbauer, Christian Sigl, and Hendrik Dietz. "Gigadalton-scale shape-programmable DNA assemblies." In: *Nature* 552 (2017), p. 78. DOI: 10.1038/nature24651https://www.nature.com/articles/nature24651#supplementary-information. URL: http://dx.doi.org/10.1038/nature24651.

[125] Anupama J. Thubagere et al. "A cargo-sorting DNA robot." In: *Science* 357.6356 (2017), eaan6558. DOI: 10.1126/science.aan6558. URL: http://science.sciencemag.org/content/sci/357/6356/eaan6558.full.pdf.

[126] Carlos Ernesto Castro, Fabian Kilchherr, Do-Nyun Kim, Enrique Lin Shiao, Tobias Wauer, Philipp Wortmann, Mark Bathe, and Hendrik Dietz. "A primer to scaffolded DNA origami." In: *Nat Meth* 8.3 (2011), pp. 221–229. ISSN: 1548-7091. DOI: http://www.nature.com/nmeth/journal/v8/n3/abs/nmeth.1570.html#supplementary-information. URL: http://dx.doi.org/10.1038/nmeth.1570.

[127] Sabine Sellner, Samet Kocabey, Katharina Nekolla, Fritz Krombach, Tim Liedl, and Markus Rehberg. "DNA nanotubes as intracellular delivery vehicles in vivo." In: *Biomaterials* 53 (2015), pp. 453–463. ISSN: 0142-9612. DOI: https://doi.org/10.1016/j.biomaterials.2015.02.099. URL: http://www.sciencedirect.com/science/article/pii/S0142961215002379.

[128] Naomi J. Halas, Surbhi Lal, Wei-Shun Chang, Stephan Link, and Peter Nordlander. "Plasmons in Strongly Coupled Metallic Nanostructures." In: *Chemical Reviews* 111.6 (2011), pp. 3913–3961. ISSN: 0009-2665. DOI: 10.1021/cr200061k. URL: http://dx.doi.org/10.1021/cr200061k.

[129] Eva-Maria Roller, Larousse Khosravi Khorashad, Michael Fedoruk, Robert Schreiber, Alexander O. Govorov, and Tim Liedl. "DNA-Assembled Nanoparticle Rings Exhibit Electric and Magnetic Resonances at Visible Frequencies." In: *Nano Letters* 15.2 (2015), pp. 1368–1373. ISSN: 1530-6984. DOI: 10.1021/nl5046473. URL: https://doi.org/10.1021/nl5046473.

[130] Mario Hentschel, Martin Schäferling, Xiaoyang Duan, Harald Giessen, and Na Liu. "Chiral plasmonics." In: *Science Advances* 3.5 (2017). DOI: 10.1126/sciadv.1602735. URL: http://advances.sciencemag.org/content/advances/3/5/e1602735.full.pdf.

[131] Nina Jiang, Xiaolu Zhuo, and Jianfang Wang. "Active Plasmonics: Principles, Structures, and Applications." In: *Chemical Reviews* 118.6 (2018), pp. 3054–3099. ISSN: 0009-2665. DOI: 10.1021/acs.chemrev.7b00252. URL: https://doi.org/10.1021/acs.chemrev.7b00252.

[132] Amendola Vincenzo, Pilot Roberto, Frasconi Marco, M. Maragò Onofrio, and Iatì Maria Antonia. "Surface plasmon resonance in gold nanoparticles: a review." In: *Journal of Physics: Condensed Matter* 29.20 (2017), p. 203002. ISSN: 0953-8984. URL: http://stacks.iop.org/0953-8984/29/i=20/a=203002.

[133] P. Nordlander, C. Oubre, E. Prodan, K. Li, and M. I. Stockman. "Plasmon Hybridization in Nanoparticle Dimers." In: *Nano Letters* 4.5 (2004), pp. 899–903. ISSN: 1530-6984. DOI: 10.1021/nl049681c. URL: https://doi.org/10.1021/nl049681c.

[134] Na Liu, Ming L. Tang, Mario Hentschel, Harald Giessen, and A. Paul Alivisatos. "Nanoantenna-enhanced gas sensing in a single tailored nanofocus." In: *Nature Materials* 10 (2011), p. 631. DOI: 10.1038/nmat3029. URL: http://dx.doi.org/10.1038/nmat3029.

[135] Jeffrey N. Anker, W. Paige Hall, Olga Lyandres, Nilam C. Shah, Jing Zhao, and Richard P. Van Duyne. "Biosensing with plasmonic nanosensors." In: *Nature Materials* 7 (2008), p. 442. DOI: 10.1038/nmat2162. URL: http://dx.doi.org/10.1038/nmat2162.

[136] Xibo Shen, Chen Song, Jinye Wang, Dangwei Shi, Zhengang Wang, Na Liu, and Baoquan Ding. "Rolling Up Gold Nanoparticle-Dressed DNA Origami into Three-Dimensional Plasmonic Chiral Nanostructures." In: *Journal of the American Chemical Society* 134.1 (2012), pp. 146–149. ISSN: 0002-7863. DOI: 10.1021/ja209861x. URL: https://doi.org/10.1021/ja209861x.

[137] Alessandro Cecconello, Lucas V. Besteiro, Alexander O. Govorov, and Itamar Willner. "Chiroplasmonic DNA-based nanostructures." In: *Nature Reviews Materials* 2 (2017), p. 17039. DOI: 10.1038/natrevmats.2017.39. URL: http://dx.doi.org/10.1038/natrevmats.2017.39.

[138] Zhiyuan Fan and Alexander O. Govorov. "Plasmonic Circular Dichroism of Chiral Metal Nanoparticle Assemblies." In: *Nano Letters* 10.7 (2010), pp. 2580–2587. ISSN: 1530-6984. DOI: 10.1021/nl101231b. URL: http://dx.doi.org/10.1021/nl101231b.

[139] Wei Ma, Hua Kuang, Liguang Xu, Li Ding, Chuanlai Xu, Libing Wang, and Nicholas A. Kotov. "Attomolar DNA detection with chiral nanorod assemblies." In: *Nature Communications* 4 (2013), p. 2689. DOI: 10.1038/ncomms3689https://www.nature.com/articles/ncomms3689#supplementary-information. URL: http://dx.doi.org/10.1038/ncomms3689.

[140] Xibo Shen, Pengfei Zhan, Anton Kuzyk, Qing Liu, Ana Asenjo-Garcia, Hui Zhang, F. Javier Garcia de Abajo, Alexander Govorov, Baoquan Ding, and Na Liu. "3D plasmonic chiral colloids." In: *Nanoscale* 6.4 (2014), pp. 2077–2081. ISSN: 2040-3364. DOI: 10.1039/C3NR06006C. URL: http://dx.doi.org/10.1039/C3NR06006C.

[141] Wu Xiaoling, Xu Liguang, Ma Wei, Liu Liqiang, Kuang Hua, Kotov Nicholas A., and Xu Chuanlai. "Propeller-Like Nanorod-Upconversion Nanoparticle Assemblies with Intense Chiroptical Activity and Luminescence Enhancement in Aqueous Phase." In: *Advanced Materials* 28.28 (2016), pp. 5907–5915. DOI: doi:10.1002/adma.201601261. URL: https://onlinelibrary.wiley.com/doi/abs/10.1002/adma.201601261.

[142] David Yu Zhang and Georg Seelig. "Dynamic DNA nanotechnology using strand-displacement reactions." In: *Nature Chemistry* 3 (2011), p. 103. DOI: 10.1038/nchem.957. URL: http://dx.doi.org/10.1038/nchem.957.

[143] Chao Zhou, Xiaoyang Duan, and Na Liu. "DNA-Nanotechnology-Enabled Chiral Plasmonics: From Static to Dynamic." In: *Accounts of Chemical Research* 50.12 (2017), pp. 2906–2914. ISSN: 0001-4842. DOI: 10.1021/acs.accounts.7b00389. URL: https://doi.org/10.1021/acs.accounts.7b00389.

[144] Anton Kuzyk, Maximilian J. Urban, Andrea Idili, Francesco Ricci, and Na Liu. "Selective control of reconfigurable chiral plasmonic metamolecules." In: *Science Advances* 3.4 (2017), e1602803. DOI: 10.1126/sciadv.1602803.

[145] Na Wu and Itamar Willner. "pH-Stimulated Reconfiguration and Structural Isomerization of Origami Dimer and Trimer Systems." In: *Nano Letters* 16.10 (2016), pp. 6650–6655. ISSN: 1530-6984. DOI: 10.1021/acs.nanolett.6b03418. URL: https://doi.org/10.1021/acs.nanolett.6b03418.

[146] Andrea Idili, Alexis Vallée-Bélisle, and Francesco Ricci. "Programmable pH-Triggered DNA Nanoswitches." In: *Journal of the American Chemical Society* 136.16 (2014), pp. 5836–5839. ISSN: 0002-7863. DOI: 10.1021/ja500619w. URL: https://doi.org/10.1021/ja500619w.

[147] Yuwei Hu, Jiangtao Ren, Chun-Hua Lu, and Itamar Willner. "Programmed pH-Driven Reversible Association and Dissociation of Interconnected Circular DNA Dimer Nanostructures." In: *Nano Letters* 16.7 (2016), pp. 4590–4594. ISSN: 1530-6984. DOI: 10.1021/acs.nanolett.6b01891. URL: https://doi.org/10.1021/acs.nanolett.6b01891.

[148] Alessia Amodio, Bin Zhao, Alessandro Porchetta, Andrea Idili, Matteo Castronovo, Chunhai Fan, and Francesco Ricci. "Rational Design of pH-Controlled DNA Strand Displacement." In: *Journal of the*

American Chemical Society 136.47 (2014), pp. 16469–16472. ISSN: 0002-7863. DOI: 10.1021/ja508213d. URL: https://doi.org/10.1021/ja508213d.

[149] Yuwei Hu, Alessandro Cecconello, Andrea Idili, Francesco Ricci, and Itamar Willner. "Triplex DNA Nanostructures: From Basic Properties to Applications." In: *Angewandte Chemie International Edition* 56.48 (2017), pp. 15210–15233. ISSN: 1433-7851. DOI: 10.1002/anie.201701868. URL: https://doi.org/10.1002/anie.201701868.

[150] Anton Kuzyk, Yangyang Yang, Xiaoyang Duan, Simon Stoll, Alexander O. Govorov, Hiroshi Sugiyama, Masayuki Endo, and Na Liu. "A light-driven three-dimensional plasmonic nanosystem that translates molecular motion into reversible chiroptical function." In: *Nature Communications* 7 (2016), p. 10591. DOI: 10.1038/ncomms10591http://dharmasastra.live.cf.private.springer.com/articles/ncomms10591#supplementary-information. URL: http://dx.doi.org/10.1038/ncomms10591.

[151] Yangyang Yang, Masayuki Endo, Kumi Hidaka, and Hiroshi Sugiyama. "Photo-Controllable DNA Origami Nanostructures Assembling into Predesigned Multiorientational Patterns." In: *Journal of the American Chemical Society* 134.51 (2012), pp. 20645–20653. ISSN: 0002-7863. DOI: 10.1021/ja307785r. URL: https://doi.org/10.1021/ja307785r.

[152] Yukiko Kamiya and Hiroyuki Asanuma. "Light-Driven DNA Nanomachine with a Photoresponsive Molecular Engine." In: *Accounts of Chemical Research* 47.6 (2014), pp. 1663–1672. ISSN: 0001-4842. DOI: 10.1021/ar400308f. URL: https://doi.org/10.1021/ar400308f.

[153] Robert Elghanian, James J. Storhoff, Robert C. Mucic, Robert L. Letsinger, and Chad A. Mirkin. "Selective Colorimetric Detection of Polynucleotides Based on the Distance-Dependent Optical Properties of Gold Nanoparticles." In: *Science* 277.5329 (1997), pp. 1078–1081. DOI: 10.1126/science.277.5329.1078. URL: http://science.sciencemag.org/content/sci/277/5329/1078.full.pdf.

[154] Jennifer I. L. Chen, Yeechi Chen, and David S. Ginger. "Plasmonic Nanoparticle Dimers for Optical Sensing of DNA in Complex Media." In: *Journal of the American Chemical Society* 132.28 (2010), pp. 9600–9601. ISSN: 0002-7863. DOI: 10.1021/ja103240g. URL: https://doi.org/10.1021/ja103240g.

[155] Liguang Xu, Wenjing Yan, Wei Ma, Hua Kuang, Xiaoling Wu, Liqaing Liu, Yuan Zhao, Libing Wang, and Chuanlai Xu. "SERS Encoded Silver Pyramids for Attomolar Detection of Multiplexed Disease Biomarkers." In: *Advanced Materials* 27.10 (2015), pp. 1706–1711. DOI: doi:10.1002/adma.201402244. URL: https://onlinelibrary.wiley.com/doi/abs/10.1002/adma.201402244.

[156] Carsten Sönnichsen, Björn M. Reinhard, Jan Liphardt, and A. Paul Alivisatos. "A molecular ruler based on plasmon coupling of single gold and silver nanoparticles." In: *Nature Biotechnology* 23 (2005), p. 741. DOI: 10.1038/nbt1100https://www.nature.com/articles/nbt1100#supplementary-information. URL: http://dx.doi.org/10.1038/nbt1100.

[157] Peter Friebe and Ralf Bartenschlager. "Role of RNA Structures in Genome Terminal Sequences of the Hepatitis C Virus for Replication and Assembly." In: *Journal of Virology* 83.22 (2009), pp. 11989–11995. ISSN: 0022-538X 1098-5514. DOI: 10.1128/JVI.01508-09. URL: http://www.ncbi.nlm.nih.gov/pmc/articles/PMC2772684/.

[158] Wei Ma et al. "Chiral plasmonics of self-assembled nanorod dimers." In: *Scientific Reports* 3 (2013), p. 1934. DOI: 10.1038/srep01934http://dharmasastra.live.cf.private.springer.com/articles/srep01934#supplementary-information. URL: http://dx.doi.org/10.1038/srep01934.

[159] Elena A. Lesnik and Susan M. Freier. "Relative Thermodynamic Stability of DNA, RNA, and DNA:RNA Hybrid Duplexes: Relationship with Base Composition and Structure." In: *Biochemistry* 34.34 (1995), pp. 10807–10815. ISSN: 0006-2960. DOI: 10.1021/bi00034a013. URL: https://doi.org/10.1021/bi00034a013.

[160] F. Huber, H. P. Lang, N. Backmann, D. Rimoldi, and Ch Gerber. "Direct detection of a BRAF mutation in total RNA from melanoma cells using cantilever arrays." In: *Nature Nanotechnology* 8 (2013), p. 125. DOI: 10.1038/nnano.2012.263https://www.nature.com/articles/nnano.2012.263#supplementary-information. URL: http://dx.doi.org/10.1038/nnano.2012.263.

[161] J. D. Scott and D. R. Gretch. "Molecular diagnostics of hepatitis c virus infection: A systematic review." In: *JAMA* 297.7 (2007), pp. 724–732. ISSN: 0098-7484. DOI: 10.1001/jama.297.7.724. URL: http://dx.doi.org/10.1001/jama.297.7.724.

[162] P. Agarwal Nayan, Michael Matthies, N. Gür Fatih, Kensuke Osada, and L. Schmidt Thorsten. "Block Copolymer Micellization as a Protection Strategy for DNA Origami." In: *Angewandte Chemie International Edition* 56.20 (2017), pp. 5460–5464. ISSN: 1433-7851. DOI: 10.1002/anie.201608873. URL: https://doi.org/10.1002/anie.201608873.

[163] Evelyn Auyeung, J. Macfarlane Robert, J. Choi Chung Hang, I. Cutler Joshua, and A. Mirkin Chad. "Transitioning DNA-Engineered Nanoparticle Superlattices from Solution to the Solid State." In: *Advanced Materials* 24.38 (2012), pp. 5181–5186. ISSN: 0935-9648. DOI: 10.1002/adma.201202069. URL: https://doi.org/10.1002/adma.201202069.

[164] Xingchen Ye et al. "Improved Size-Tunable Synthesis of Monodisperse Gold Nanorods through the Use of Aromatic Additives." In: *ACS Nano* 6.3 (2012), pp. 2804–2817. ISSN: 1936-0851. DOI: 10.1021/nn300315j. URL: http://dx.doi.org/10.1021/nn300315j.

[165] Wei Chen, Ai Bian, Ashish Agarwal, Liqiang Liu, Hebai Shen, Libing Wang, Chuanlai Xu, and Nicholas A. Kotov. "Nanoparticle Superstructures Made by Polymerase Chain Reaction: Collective Interactions of Nanoparticles and a New Principle for Chiral Materials." In: *Nano Letters* 9.5 (2009), pp. 2153–2159. ISSN: 1530-6984. DOI: 10.1021/nl900726s. URL: https://doi.org/10.1021/nl900726s.

[166] Alexander J. Mastroianni, Shelley A. Claridge, and A. Paul Alivisatos. "Pyramidal and Chiral Groupings of Gold Nanocrystals Assembled Using DNA Scaffolds." In: *Journal of the American Chemical Society* 131.24 (2009), pp. 8455–8459. ISSN: 0002-7863. DOI: 10.1021/ja808570g. URL: https://doi.org/10.1021/ja808570g.

[167] Zhiyuan Fan and Alexander O. Govorov. "Helical Metal Nanoparticle Assemblies with Defects: Plasmonic Chirality and Circular Dichroism." In: *The Journal of Physical Chemistry C* 115.27 (2011), pp. 13254–13261. ISSN: 1932-7447. DOI: 10.1021/jp204265x. URL: https://doi.org/10.1021/jp204265x.

[168] Jatish Kumar, K. George Thomas, and Luis M. Liz-Marzán. "Nanoscale chirality in metal and semiconductor nanoparticles." In: *Chemical Communications (Cambridge, England)* 52.85 (2016), pp. 12555–12569. ISSN: 1359-7345 1364-548X. DOI: 10.1039/c6cc05613j. URL: http://www.ncbi.nlm.nih.gov/pmc/articles/PMC5317218/.

[169] Masamitsu Wakabayashi, Satoshi Yokojima, Tuyoshi Fukaminato, Kenichi Shiino, Masahiro Irie, and Shinichiro Nakamura. "Anisotropic Dissymmetry Factor, g: Theoretical Investigation on Single Molecule Chiroptical Spectroscopy." In: *The Journal of Physical Chemistry A* 118.27 (2014), pp. 5046–5057. ISSN: 1089-5639. DOI: 10.1021/jp409559t. URL: https://doi.org/10.1021/jp409559t.

[170] Miao Li, Theobald Lohmüller, and Jochen Feldmann. "Optical Injection of Gold Nanoparticles into Living Cells." In: *Nano Letters* 15.1 (2015), pp. 770–775. ISSN: 1530-6984. DOI: 10.1021/nl504497m. URL: https://doi.org/10.1021/nl504497m.

[171] D. Patrick O'Neal, Leon R. Hirsch, Naomi J. Halas, J. Donald Payne, and Jennifer L. West. "Photo-thermal tumor ablation in mice using near infrared-absorbing nanoparticles." In: *Cancer Letters* 209.2 (2004), pp. 171–176. ISSN: 0304-3835. DOI: https://doi.org/10.1016/j.canlet.2004.02.004. URL: http://www.sciencedirect.com/science/article/pii/S0304383504001442.

[172] Gobin Andre M., O'Neal D. Patrick, Watkins Daniel M., Halas Naomi J., Drezek Rebekah A., and West Jennifer L. "Near infrared laser-tissue welding using nanoshells as an exogenous absorber." In: *Lasers in Surgery and Medicine* 37.2 (2005), pp. 123–129. DOI: doi:10.1002/lsm.20206. URL: https://onlinelibrary.wiley.com/doi/abs/10.1002/lsm.20206.

[173] Jingjing Qiu and Wei David Wei. "Surface Plasmon-Mediated Photothermal Chemistry." In: *The Journal of Physical Chemistry C* 118.36 (2014), pp. 20735–20749. ISSN: 1932-7447. DOI: 10.1021/jp5042553. URL: https://doi.org/10.1021/jp5042553.

[174] Svetlana V. Boriskina, Hadi Ghasemi, and Gang Chen. "Plasmonic materials for energy: From physics to applications." In: *Materials Today* 16.10 (2013), pp. 375–386. ISSN: 1369-7021. DOI: https://doi.org/10.1016/j.mattod.2013.09.003. URL: http://www.sciencedirect.com/science/article/pii/S1369702113003003.

[175] Zheyu Fang, Yu-Rong Zhen, Oara Neumann, Albert Polman, F. Javier García de Abajo, Peter Nordlander, and Naomi J. Halas. "Evolution of Light-Induced Vapor Generation at a Liquid-Immersed Metallic Nanoparticle." In: *Nano Letters* 13.4 (2013), pp. 1736–1742. ISSN: 1530-6984. DOI: 10.1021/nl4003238. URL: https://doi.org/10.1021/nl4003238.

[176] Baffou Guillaume and Quidant Romain. "Thermo-plasmonics: using metallic nanostructures as nano-sources of heat." In: *Laser and Photonics Reviews* 7.2 (2013), pp. 171–187. DOI: doi:10.1002/lpor.201200003. URL: https://onlinelibrary.wiley.com/doi/abs/10.1002/lpor.201200003.

[177] G. Baffou, R. Quidant, and C. Girard. "Heat generation in plasmonic nanostructures: Influence of morphology." In: *Applied Physics Letters* 94.15 (2009), p. 153109. DOI: 10.1063/1.3116645. URL: https://aip.scitation.org/doi/abs/10.1063/1.3116645.

[178] Alexander O. Govorov, Wei Zhang, Timur Skeini, Hugh Richardson, Jaebeom Lee, and Nicholas A. Kotov. "Gold nanoparticle ensembles as heaters and actuators: melting and collective plasmon resonances." In: *Nanoscale Research Letters* 1.1 (2006), pp. 84–90. ISSN: 1931-7573 1556-276X. DOI: 10.1007/s11671-006-9015-7. URL: http://www.ncbi.nlm.nih.gov/pmc/articles/PMC3246627/.

[179] Guillaume Baffou, Romain Quidant, and Christian Girard. "Thermoplasmonics modeling: A Green's function approach." In: *Physical Review B* 82.16 (2010), p. 165424. DOI: 10.1103/PhysRevB.82.165424. URL: https://link.aps.org/doi/10.1103/PhysRevB.82.165424.

[180] Calum Jack et al. "Spatial control of chemical processes on nanostructures through nano-localized water heating." In: *Nature Communications* 7 (2016), p. 10946. DOI: 10.1038/ncomms10946https://www.

nature.com/articles/ncomms10946#supplementary-information. URL: http://dx.doi.org/10.1038/ncomms10946.

[181] Ugo Fano, Guido Pupillo, Alberto Zannoni, and Charles W. Clark. "On the Absorption Spectrum of Noble Gases at the Arc Spectrum Limit." In: *Journal of Research of the National Institute of Standards and Technology* 110.6 (2005), pp. 583–587. ISSN: 1044-677X 2165-7254. DOI: 10.6028/jres.110.083. URL: http://www.ncbi.nlm.nih.gov/pmc/articles/PMC4846228/.

[182] Jonathan A. Fan, Chihhui Wu, Kui Bao, Jiming Bao, Rizia Bardhan, Naomi J. Halas, Vinothan N. Manoharan, Peter Nordlander, Gennady Shvets, and Federico Capasso. "Self-Assembled Plasmonic Nanoparticle Clusters." In: *Science* 328.5982 (2010), pp. 1135–1138. DOI: 10.1126/science.1187949. URL: http://science.sciencemag.org/content/sci/328/5982/1135.full.pdf.

[183] Boris Luk'yanchuk, Nikolay I. Zheludev, Stefan A. Maier, Naomi J. Halas, Peter Nordlander, Harald Giessen, and Chong Tow Chong. "The Fano resonance in plasmonic nanostructures and metamaterials." In: *Nature Materials* 9 (2010), p. 707. DOI: 10.1038/nmat2810. URL: http://dx.doi.org/10.1038/nmat2810.

[184] Shuang Zhang, Dentcho A. Genov, Yuan Wang, Ming Liu, and Xiang Zhang. "Plasmon-Induced Transparency in Metamaterials." In: *Physical Review Letters* 101.4 (2008), p. 047401. DOI: 10.1103/PhysRevLett.101.047401. URL: https://link.aps.org/doi/10.1103/PhysRevLett.101.047401.

[185] Feng Hao, Peter Nordlander, Yannick Sonnefraud, Pol Van Dorpe, and Stefan A. Maier. "Tunability of Subradiant Dipolar and Fano-Type Plasmon Resonances in Metallic Ring/Disk Cavities: Implications for Nanoscale Optical Sensing." In: *ACS Nano* 3.3 (2009), pp. 643–652. ISSN: 1936-0851. DOI: 10.1021/nn900012r. URL: https://doi.org/10.1021/nn900012r.

[186] Nikolay A. Mirin, Kui Bao, and Peter Nordlander. "Fano Resonances in Plasmonic Nanoparticle Aggregates." In: *The Journal of Physical Chemistry A* 113.16 (2009), pp. 4028–4034. ISSN: 1089-5639. DOI: 10.1021/jp810411q. URL: https://doi.org/10.1021/jp810411q.

[187] J. Britt Lassiter, Heidar Sobhani, Jonathan A. Fan, Janardan Kundu, Federico Capasso, Peter Nordlander, and Naomi J. Halas. "Fano Resonances in Plasmonic Nanoclusters: Geometrical and Chemical Tunability." In: *Nano Letters* 10.8 (2010), pp. 3184–3189. ISSN: 1530-6984. DOI: 10.1021/nl102108u. URL: https://doi.org/10.1021/nl102108u.

[188] Larousse Khosravi Khorashad, Lucas V. Besteiro, Zhiming Wang, Jason Valentine, and Alexander O. Govorov. "Localization of Excess Temperature Using Plasmonic Hot Spots in Metal Nanostructures: Combining Nano-Optical Antennas with the Fano Effect." In: *The*

Journal of Physical Chemistry C 120.24 (2016), pp. 13215–13226. ISSN: 1932-7447. DOI: 10.1021/acs.jpcc.6b03644. URL: https://doi.org/10.1021/acs.jpcc.6b03644.

[189] Liguang Xu, Hua Kuang, Chuanlai Xu, Wei Ma, Libing Wang, and Nicholas A. Kotov. "Regiospecific Plasmonic Assemblies for in Situ Raman Spectroscopy in Live Cells." In: *Journal of the American Chemical Society* 134.3 (2012), pp. 1699–1709. ISSN: 0002-7863. DOI: 10.1021/ja2088713. URL: https://doi.org/10.1021/ja2088713.

[190] Eva-Maria Roller, Lucas V. Besteiro, Claudia Pupp, Larousse Khosravi Khorashad, Alexander O. Govorov, and Tim Liedl. "Hot spot-mediated non-dissipative and ultrafast plasmon passage." In: *Nature physics* 13.8 (2017), pp. 761–765. ISSN: 1745-2473. DOI: 10.1038/nphys4120. URL: http://www.ncbi.nlm.nih.gov/pmc/articles/PMC5540180/.

[191] Chenqi Shen, Xiang Lan, Xuxing Lu, Travis A. Meyer, Weihai Ni, Yonggang Ke, and Qiangbin Wang. "Site-Specific Surface Functionalization of Gold Nanorods Using DNA Origami Clamps." In: *Journal of the American Chemical Society* 138.6 (2016), pp. 1764–1767. ISSN: 0002-7863. DOI: 10.1021/jacs.5b11566. URL: https://doi.org/10.1021/jacs.5b11566.

[192] Linglu Yang, Bo Yan, and Björn M. Reinhard. "Correlated Optical Spectroscopy and Transmission Electron Microscopy of Individual Hollow Nanoparticles and their Dimers." In: *The journal of physical chemistry. C, Nanomaterials and interfaces* 112.41 (2008), pp. 15989–15996. ISSN: 1932-7447 1932-7455. DOI: 10.1021/jp804790p. URL: http://www.ncbi.nlm.nih.gov/pmc/articles/PMC2685363/.